

Titel der Arbeit: Essays on Option Pricing

Schriftliche Promotionsleistung
zur Erlangung des akademischen Grades
Doctor rerum politicarum

vorgelegt und angenommen
an der Fakultät für Wirtschaftswissenschaft
der Otto-von-Guericke-Universität Magdeburg

Verfasserin: Anastasiia Zbandut
Geburtsdatum und -ort: 14.08.1991, Donezk (Ukraine)
Arbeit eingereicht am: 28.10.2024

Gutachter der schriftlichen Promotionsleistung:
Prof. Dr. Peter Reichling
Prof. Dr. Dr. Bodo Vogt

Datum der Disputation: 19.05.2025

Table of Contents

1. Preface	Page 3
2. Research Paper 1	Page 5
3. Research Paper 2	Page 33
4. Research Paper 3	Page 62
5. Research Paper 4	Page 85

Preface

Derivative contracts play a fundamental role in the financial system since they provide unique flexibility and precision in financial strategies, which are not possible with other instruments. Among these contracts, options are the most traded derivative contracts worldwide, with a volume of 108.2 billion contracts in 2023 and, in the first four months of 2024, their trading volume increased by 104 percent.¹ The use of options has driven major innovations in financial markets, enabling the development of instruments such as contingent claims, structured and volatility derivatives. By replicating the pay-off of other financial assets, options contribute to market efficiency through synthetic positions that take advantage of price inefficiencies across different assets and markets. Furthermore, synthetic positions enhance market liquidity. For investors, options are essential tools in risk and portfolio management, allowing them to hedge against asset volatility and leverage their positions. Option pricing facilitates future estimates of the underlying asset volatility and reflects market expectations. The concept of implied volatility² which captures market uncertainty, serves as a robust measure for future volatility forecasting. To sum up, options are a critical component of modern finance, and their role in the financial markets is crucial for maintaining stability. The [Black and Scholes \(1973\)](#) model revolutionized options pricing by providing a closed-form solution to value options. Since then, extensive research has built on the theoretical framework of option pricing, price and return dynamics, empirical analysis, and forecasting. This cumulative dissertation comprises four papers that contribute to this ongoing research by applying option pricing to company valuation, exploring options rates of return dynamics from multiple perspectives, and analyzing options in the rapidly evolving decentralized finance ecosystem.

The [Merton \(1973\)](#) model significantly transformed company valuation by representing equity and debt as options on company's assets. The first paper extends the computation of the cost of capital within the [Merton \(1973\)](#) and [Modigliani and Miller \(1958\)](#) frameworks incorporating credit risk. This framework also enables the calculation of the value of the tax shield under credit risk. The paper critically discusses the debt beta approach where, under the Capital Asset Pricing Model, the debt beta is calculated with respect to a combined market portfolio of stocks and corporate bonds, which does not exist. Therefore, the first paper proposes an option-based and combined option-factor sensitivities approach that integrates credit risk into the Weighted Average Cost of Capital computations. The paper also compares the data requirements of the discussed approach and conducts a peer-group valuation of Apple Inc. assuming it were not a publicly traded company.

Since the major research on options has been conducted for the US market, in the second and third papers, this dissertation empirically analyzes options rates of return dynamics and compares the results on the US and the EU markets. The second paper builds on [Aretz et al. \(2023\)](#) study and explores the relationship between equity option rates of return and underlying volatility. The empirical study employs the Fama-French-Carhart and exponential GARCH models to decompose the underlying volatility into systematic and idiosyncratic components and examines their impact on option rates of return across different moneyness levels, including nonlinear relationship. The paper provides detail discussion of systematic and idiosyncratic volatility slopes conditional on moneyness. The results contribute to the literature by disclosing the nuanced impact of underlying systematic volatility on option rates of return. The third paper extends the second by investigating the cross-section of index option rates of return again on both the US and EU markets. It employs the ARIMA-GJR-GARCH model to estimate the underlying index volatility and deploys two mixed effect panel regressions. The regression analysis focuses, first, on the cross-section of option rates of return with respect to underlying volatility, volatility of volatility, leverage, moneyness, and elasticity. Second, the analysis compares the elasticity sensitivities to its components, i.e., delta and leverage, and discusses the elasticity dynamics across options and markets with respect to volatility and moneyness bins. These papers contribute to the literature by providing empirical evidence on options market dynamics and highlighting differences that should be taken into consideration for region-specific risk management.

Concluding this dissertation and with regard to a relatively new but rapidly growing financial market, the fourth paper explores the pricing of cryptocurrency options on-chain as a part of a decentralized finance ecosystem. This is the first empirical study in its field and investigates the pricing of wrapped Bitcoin and Ethereum options in the Hegic protocol. It utilizes the two regimes Markov Switching Autoregression (GJR) GARCH model to estimate the underlying volatility and the feasible GLS regression to examine the discrepancies between the Hegic and the benchmark prices. The regression analysis includes the rate of return, volume, and volatility of the underlying and options' amount, strike, and moneyness. The paper also discusses the difference between implied and market volatility, indicating potential mispricing exploitation. This paper contributes to volatility forecasting and opens a discussion on a sophisticated automated market maker for pricing options in decentralized finance ecosystem.

Overall, this dissertation shows a manifold contribution to scientific research on option pricing. It covers both the theoretical and empirical perspectives of option pricing, and the traditional and decentralized financial markets. The results are practically relevant for risk assessment and management, investment strategies optimization, and financial modeling.

¹See [FIA Global Futures and Options Volume 2023](#) and [FIA ETD Volume - April 2024](#).

²In the [Black and Scholes \(1973\)](#) framework.

References

- Aretz, K., Lin, M. T., and Poon, S. H. (2023). Moneyness, total, systematic, and idiosyncratic volatility, and the cross-section of european option returns. *Review of Finance*, 27(1):289–323.
- Black, F. and Scholes, M. (1973). The pricing of options and corporate liabilities. *Journal of Political Economy*, 81(3):637–654.
- Merton, R. C. (1973). Theory of rational option pricing. *Bell Journal of Economics and Management Science*, 4:141–183.
- Modigliani, F. and Miller, M. H. (1958). The cost of capital, corporation finance and the theory of investment. *American Economic Review*, 48(3):261–297.



Copyright Infopro Digital Limited 2019. All rights reserved. You may share using our article tools. This article may be printed for the sole use of the Authorised User (named subscriber), as outlined in our terms and conditions. <https://www.infopro-insight.com/termsconditions/insight-subscriptions>

Research Paper

Costs of capital under credit risk

Peter Reichling and Anastasiia Zbandut

Department of Banking and Finance, Faculty of Economics and Management,
Otto von Guericke University Magdeburg, Postbox 4120, 39016 Magdeburg,
Germany; emails: peter.reichling@ovgu.de, anastasiia.zbandut@ovgu.de

(Received October 10, 2017; revised March 15, 2019; accepted June 3, 2019)

ABSTRACT

In cost-of-capital computations, credit risk is only taken into consideration at the level of the debt beta approach. We show that applications of the debt beta approach in company valuation suffer from unrealistic assumptions about the market index and the cost of debt. As an advantageous approach, we present (quasi-) analytic formulas for costs of equity and debt based on Merton's model in different settings. In our approach, we integrate credit risk in cost-of-equity and debt calculations to receive the credit risk-adjusted weighted average cost of capital. In addition, we compare both the quantity and the quality of the required data in a peer group analysis of our approach with the data requirements of the debt beta approach. Further, we discuss the valuation errors that result from the debt beta approach's assumptions regarding the cost of debt. A valuation of Apple Inc as if it were not publicly traded illustrates the procedures of our approach.

Keywords: company valuation; debt beta; debt-to-equity ratio; Merton's model; weighted average cost of capital (WACC).

1 INTRODUCTION

The discounted cashflow method of company valuation applies the present value method under risk, where expected future cashflows are discounted by risk-adjusted rates of return. In the classical approach based on the capital asset pricing model (CAPM), the required rate of return on equity is set equal to the beta-adjusted expected rate of return of a portfolio that consists of the stock market index and the risk-free asset. A peer group analysis – based on Hamada (1972) – is applied in practice because the beta of a nonpublicly traded company is unknown. As the classical CAPM-based approach does not consider credit risk, the required rate of return on debt is set equal to the risk-free rate. We analyze costs of equity and debt to compute the weighted average cost of capital (WACC) in different frameworks under credit risk.

Under credit risk, ie, limited liability of the equity holders, part of the risk is shifted from the equity holders onto the debt holders. Therefore, the cost of debt is higher and the cost of equity is lower compared with the classical framework. In the CAPM framework under credit risk, the equity beta is reduced and the debt beta is introduced. The debt beta approach has been under development since the 1970s (Haugen and Pappas 1971; Conine 1980; Harris and Pringle 1985; Kaplan and Stein 1990). While Haugen and Pappas (1971) and Harris and Pringle (1985) at least mention that a combined stock–corporate bond index is needed to compute the debt beta, more recent literature focuses mainly on tax shield analysis under credit risk (Ruback 2002; Fernández 2004; Arzac and Glosten 2005). Other authors suggest employing the implied debt beta (Cohen 2008), which is consistent with the company's debt interest rate.

We clarify that the debt beta approach is not feasible in company valuation unless a (preferably return-risk efficient) index of stocks and corporate bonds is used to compute the betas. However, historical data for a combined stock–corporate bond index is not available. This prevents the application of the debt beta approach in practice. In addition, we show that the implied debt beta approach based on the company's interest rate leads to ambiguous cost-of-capital computations in applications.

Besides the debt beta approach, Merton's model is widely used in credit risk evaluation. Merton (1974) represents the origin of structural credit risk models for valuing equity and debt, inducing an enormous amount of research on this topic. Our main contribution to this field is the development of corresponding cost-of-capital formulas. To our knowledge, only Galai and Masulis (1976) deal with the expected rate of return on equity in a combined option theory–CAPM approach. Cooper and Davydenko (2007) address the expected return on risky debt in a discrete-time setting. We provide formulas for both expected return on equity and debt in the continuous setting as well as in the discrete setting. Since costs of capital in Merton's framework

correspond to expected option returns, we follow the technique of Hillegeist *et al* (2004), Vassalou and Xing (2004), Duffie *et al* (2007), Bharath and Shumway (2008) and Campbell *et al* (2008) to determine expected option returns and transfer the results to cost-of-capital computations.

We derive (quasi-) analytic formulas for instantaneous, continuously compounded and simple per-period costs of equity and debt. In contrast to some approaches on expected option returns (see, for example, Cox and Rubinstein 1985, pp. 189–190, 210; Coval and Shumway 2001), which at least partially use CAPM betas, we stay initially within the Black–Scholes–Merton framework. Thus, beta is absent in our option-based formulas at first. However, if the expected return on equity in a peer group analysis is estimated via a multifactor asset pricing model, factor sensitivities are required. This can be avoided by using the iterative procedure of Vassalou and Xing (2004) and Duffie *et al* (2007).

In addition, we show that without capital structure effects – in the absence of discriminatory taxation in particular – proposition I of Modigliani and Miller (1958) holds; this states that the WACC in the levered company equals the expected equity return in the (otherwise) identical unlevered company. To our knowledge, there is no literature that computes the tax shield in an option-based company valuation approach. Cooper and Nyborg (2008) and Koziol (2014) analyze the tax shield in the presence of credit risk. Cooper and Nyborg (2008) follow the debt beta approach, and Koziol (2014) analyzes the WACC under credit risk, bankruptcy costs and taxes in a one-period binomial setting, with a given probability of default but without decomposition at the level of costs of equity and debt. Our approach allows valuing the interest payment under credit risk as a (money-or-nothing) option. As a result, we are able to compute the tax shield.

Our paper is organized as follows. Section 2 repeats the classical Modigliani–Miller CAPM approach. It serves to introduce the notation and illustrate the steps of computing costs of capital. Section 3 describes the debt beta approach, where credit risk is taken into consideration within the CAPM framework. We emphasize the assumptions of the debt beta approach with respect to the market portfolio and show that serious distortions occur if betas are computed with respect to a stock index. In addition, we argue that the implied debt beta approach based on the company's debt interest rate does not fully reflect credit risk, since the debt interest rate is higher than the expected return on debt; this is because of credit risk.

Sections 4 and 5 contain our main findings. Section 4 uses the classical Black–Scholes–Merton stochastic calculus to price derivative contracts. Since equity mirrors a call option and debt parallels a risk-free bond minus a put option in Merton's model, the expected rates of return on equity and debt can be determined via the expected rates of return of the corresponding replicating portfolios. This enables us to compute costs of equity and debt and the WACC in terms of instantaneous expected

rates of return. Moreover, we are able to value the tax shield. Subsequently, we contrast the data requirements in a peer group analysis of our option-based approach with those of the CAPM-based frameworks.

Instantaneous rates of return are relevant for continuous-time portfolio decisions. However, a discrete-time framework is predominantly employed in company valuation. Therefore, we determine per-period costs of capital in terms of continuously and discretely compounded expected rates of return in Section 5. Here, we also illustrate the magnitude of mispricing that occurs if the implied debt beta approach is employed instead of our approach. In Section 6, we merge the option-based framework and a multifactor asset pricing approach. Here, we analyze whether a combination of both frameworks is able to overcome the shortcomings of the debt beta approach. Our analysis is completed by valuing Apple Inc in different frameworks. We discover similar costs of capital for Apple when using the option-based approach and the combined multifactor approach. Section 7 concludes our paper.

2 THE CLASSICAL MODIGLIANI–MILLER CAPITAL ASSET PRICING MODEL APPROACH

The entity approach of company valuation, particularly for nonpublicly traded companies, starts by valuing the corresponding as-if pure equity (unlevered) company to eliminate capital structure effects. These effects result from, among other things, a different taxation of cost of equity and debt. Tax effects are taken into consideration in a later step of the company valuation procedure. If there are no capital structure effects, the cost of equity in the as-if unlevered company – which is unknown – is equal to the WACC as a result of the famous Modigliani–Miller theorem (Modigliani and Miller 1958, proposition I):

$$\text{WACC} = \mathbb{E}(R_E^u) = \mathbb{E}(R_E^l) \frac{E}{E + D} + \underbrace{\mathbb{E}(R_D)}_{=r} \frac{D}{E + D}, \quad (2.1)$$

where $\mathbb{E}(R_E^u)$ is the required rate of return (of equity holders) in the as-if unlevered company; $\mathbb{E}(R_E^l)$ is the required rate of return of equity holders in the levered company; $\mathbb{E}(R_D)$ is the required rate of return of debt holders; r is the risk-free rate; E is the market value of equity; and D is the market value of debt.

Using the risk-free rate as the required rate of return of debt holders implies that there is no credit risk, ie, the liability of equity holders is not limited to the amount invested in the company. The market value of debt amounts to its nominal value if the debt interest rate equals the risk-free rate. Hence, the market value of debt equates to its book value in this situation. We refer to this situation as the classical Modigliani–Miller framework.

For nonpublicly traded companies, the required equity return $\mathbb{E}(R_E^1)$ in (2.1) is unknown. To estimate $\mathbb{E}(R_E^1)$ based on market data (fair value accounting), the well-known CAPM is used in the basic company valuation approach:¹

$$\mathbb{E}(R_E^1) = r + \beta_E(\mathbb{E}(R_M) - r), \quad (2.2)$$

where $\mathbb{E}(R_M)$ is the expected rate of return of the stock market index M and β_E is the equity beta in the levered company.

If the company to be valued is not publicly traded, an unlevering–relevering routine via the betas of publicly traded peer group companies is applied in practice. Starting from the basic leverage formula,

$$R_E^1 = R_A + (R_A - r)\frac{D}{E}, \quad (2.3)$$

where $A = E + D$ is the market value of assets and R_A is the rate of return on assets, the equity beta reads

$$\beta_E = \frac{\text{Cov}(R_E^1, R_M)}{\text{Var}(R_M)} = \underbrace{\frac{\text{Cov}(R_A, R_M)}{\text{Var}(R_M)}}_{=\beta_A} \left(1 + \frac{D}{E}\right), \quad (2.4)$$

where the assets beta of the particular company is set equal to the assets beta of the peer group. Formula (2.4) represents the equation of Hamada (1972) without taxes.

By construction, the WACC equals the required return in the as-if unlevered company within the classical Modigliani–Miller CAPM framework only if the debt interest rate equals the risk-free rate. If there is credit risk, the debt interest rate i_D of the company to be valued includes a credit spread and, therefore, is higher than the risk-free rate. The debt beta approach discussed in the following section was developed to overcome this difficulty.

3 THE DEBT BETA APPROACH

In the case of credit risk, the return to debt holders is risky. Hence, the leverage formula (2.3) changes to

$$R_E^1 = R_A + (R_A - R_D)\frac{D}{E}, \quad (3.1)$$

¹ The CAPM only holds if the market index used to compute the beta is return-risk efficient (Roll's critique). We neither advocate applying the CAPM in company valuation nor ignore the criticism brought forward by, among others, Fernández (2015); we use the CAPM-based approach as a benchmark for our option-based approach in Sections 4 and 5.

where R_D is the risky rate of return on debt. Thus, the equity beta differs from (2.4) and reads as follows under credit risk:

$$\beta_E = \beta_A \left(1 + \frac{D}{E} \right) - \beta_D \frac{D}{E}, \quad \text{where } \beta_D = \frac{\text{Cov}(R_D, R_M)}{\text{Var}(R_M)} = \text{debt beta.} \quad (3.2)$$

Formula (3.2) represents Conine's equation (Conine 1980), also referred to as the extended Hamada (1972) equation or the Fernández equation (Fernández 2004), without taxes. This formula was developed earlier by Haugen and Pappas (1971). Compared with the classical Modigliani–Miller CAPM framework, the equity beta is adjusted because, under credit risk, part of the risk (ie, the risk of additional cover by the equity holders in the case of over-indebtedness) is transferred to the debt holders.

Formulas (3.1) and (3.2) are valid by definition. However, expected returns on assets and debt depending on the respective betas are required to determine the costs of capital. Therefore, we need theoretical support for the following formula:

$$\mathbb{E}(R_D) = r + \beta_D(\mathbb{E}(R_M) - r) \quad \text{and} \quad \mathbb{E}(R_A) = r + \beta_A(\mathbb{E}(R_M) - r). \quad (3.3)$$

If (3.3) holds, the WACC in this situation fulfills the Modigliani–Miller property as well. As we assume that neither the equity nor the debt of the company to be valued is publicly traded, (3.3) is used for the unlevering–relevering peer group procedure. To estimate the peer group debt beta, Haugen and Pappas (1971), Bierman and Oldfield (1979) and Harris and Pringle (1985) suggest measuring the sensitivity of debt returns to a generalized market portfolio that consists of both stocks and corporate bonds. This approach requires that the equity beta must also be calculated with respect to this stock–corporate bond market portfolio to obtain the assets beta. In addition, the market value of debt of the company to be valued is needed in the relevering step of a peer group analysis.

However, exchanges do not provide price data for a (preferably return-risk efficient) stock–corporate bond market portfolio. A time series of historical price data does not exist. The approach of Cornell and Green (1991), which is often cited in the debt beta literature, does not remedy this problem because the authors run regressions of corporate bond returns on stock index returns and Treasury bill returns. However, Treasury bill returns do not reflect (systematic) corporate credit risk.

As a result, the WACC cannot be calculated via stock index betas. This is the reason why Kaplan and Stein (1990) and Damodaran (2012, p. 411), among others, have to make assumptions about the systematic risk of corporate bonds in terms of stock market risk. In either case, this method implies an inconsistent debt-to-equity ratio. To overcome this difficulty, Cohen (2008) and Benninga (2014, p. 599), for

instance, suggest applying the implied debt beta

$$\beta_D^{\text{implied}} = \frac{\mathbb{E}(R_D) - r}{\mathbb{E}(R_M) - r}. \quad (3.4)$$

If (3.4) is used, the costs of equity and debt are consistent with proposition I of Modigliani and Miller (1958). However, (3.4) requires knowing the cost of debt for which we are looking. Therefore, practitioners suggest using the debt interest rate i_D of the company to be valued as a proxy for the expected return to debt holders in applications. Inserting (3.4) into (3.3), where $\mathbb{E}(R_D)$ is substituted by i_D , will lead to a WACC at the level of the required equity return in the as-if unlevered company,

$$\begin{aligned} \text{WACC}^{\text{debt beta}} &= \underbrace{\left(r + \underbrace{\left(\beta_A \left(1 + \frac{D}{E} \right) - \underbrace{\frac{i_D - r}{\mathbb{E}(R_M) - r}}_{\beta_D} \frac{D}{E} \right)}_{\beta_E} (\mathbb{E}(R_M) - r) \right)}_{\mathbb{E}(R_E^l)} \frac{E}{E + D} \\ &\quad + \underbrace{\left(r + \underbrace{\frac{i_D - r}{\mathbb{E}(R_M) - r}}_{\beta_D} (\mathbb{E}(R_M) - r) \right)}_{\mathbb{E}(R_D)} \frac{D}{E + D} \\ &= r + \beta_A (\mathbb{E}(R_M) - r) = \mathbb{E}(R_E^u). \end{aligned} \quad (3.5)$$

This is why the debt beta approach is popular in the industry. Formula (3.5) holds for arbitrary i_D because (3.4) represents a definition rather than a result from asset pricing theory. Therefore, (3.5) is tautological but implies a certain debt-to-equity ratio for a given debt interest rate. However, this ratio does not reflect the true capital structure for either the peer group companies or the company to be valued, since the debt interest rate differs from the expected return of debt holders. This is why some arbitrary adjustments occur in practice.

The debt interest rate must cover credit risk. Therefore, the debt holders do not expect to receive interest payments at the level of i_D in the case of credit risk (Cooper and Nyborg 2008). They at least have to take the probability of default into consideration. Simply adjusting i_D for the probability of default would lead to a lower bound of the expected debt holders' return because, should a default occur, there may be a positive recovery rate. The loss given default would not be 100% in this case.

Therefore, the expected loss that combines the probability of default and the loss given default should be taken into consideration.²

Even if we could determine the expected return on debt, the assets beta must still be determined with respect to the combined market portfolio of stocks and corporate bonds. Thus, the debt beta approach suffers from a circularity problem. These considerations motivate applying an option-based approach to determine costs of capital.

4 INSTANTANEOUS COSTS OF CAPITAL IN THE OPTION-BASED APPROACH

Option pricing theory was originally developed to value corporate liabilities. In the basic option-based approach of company valuation (Merton's model), debt is represented simply using a single zero-coupon bond with face value K and time to maturity T . If the value of assets A_T at maturity exceeds the face value of the bond, the debt holders receive the redemption amount K . If the value of assets at maturity falls below K , the debt holders receive the remaining assets. Thus, the debt holders' position includes a short position in a put option on the assets, and the debtholders' payoff D_T shows option-like characteristics.

The equity payoff E_T at bond maturity is the residual between assets and debt. Thus, equity also possesses an option-style payoff. Since the position of equity holders includes a long put position, the value of equity depends on the time to maturity of debt, although equity does not show a finite expiration date. Figure 1(b) illustrates the well-known property that equity represents a call option on the company's assets in Merton's model, whereas debt under credit risk equals a risk-free zero-coupon bond minus a put option on the assets. This put option values the expected loss of the debt holders and reflects credit risk, which can be seen by comparing both parts of the figure.

In Merton's model, the values of equity and debt are calculated using the famous Black–Scholes formula for a vanilla call option:

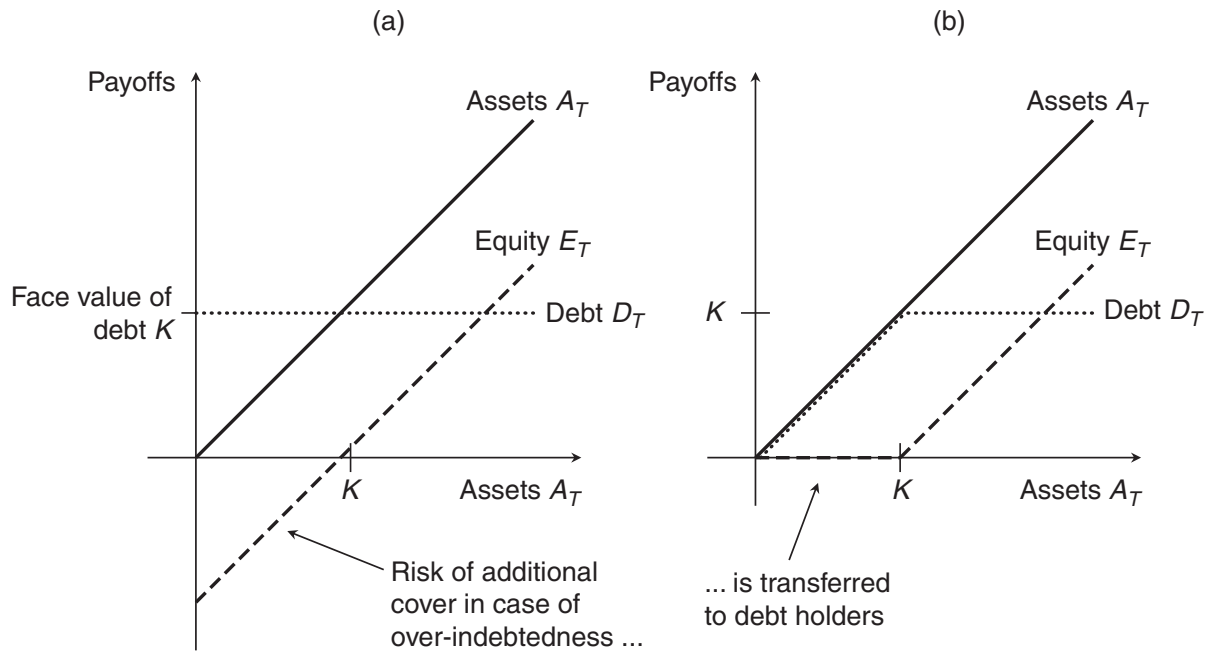
$$\begin{aligned} E &= A\mathbb{N}(d_1) - Ke^{-rT}\mathbb{N}(d_2), \\ D &= A - E = A\mathbb{N}(-d_1) + Ke^{-rT}\mathbb{N}(d_2), \end{aligned} \quad (4.1)$$

where

$$d_1 = \frac{\ln(A/K) + (r + (\sigma^2/2))T}{\sigma\sqrt{T}} \quad \text{and} \quad d_2 = d_1 - \sigma\sqrt{T},$$

Here, $\mathbb{N}(\cdot)$ is the cumulative standard normal distribution function.

² The expected loss can be computed within the option-based approach presented in Sections 4 and 5.

FIGURE 1 Equity and debt payoffs in the option-based approach of company valuation.


(a) Without credit risk. (b) With credit risk.

The corresponding volatilities read as follows (Gheno 2007):³

$$\sigma_E = \frac{N(d_1)\sigma A}{E} \quad \text{and} \quad \sigma_D = \frac{N(-d_1)\sigma A}{D} \quad \Rightarrow \quad \sigma_E \frac{E}{A} + \sigma_D \frac{D}{A} = \sigma. \quad (4.2)$$

As the payoff of assets equals the sum of the payoffs of equity and debt, according to put–call parity, this relation also holds in terms of current values. Therefore, the value of assets is independent of K , ie, capital structure. This implies that the Modigliani–Miller property is also valid under credit risk (if there are no additional costs in the case of default).⁴

In the Black–Scholes framework, derivative contracts are priced according to the value of the replicating portfolio consisting of the underlying and a risk-free bond. Therefore, the expected return of the derivative contract equals the expected return of the corresponding replicating portfolio. Thus, the instantaneous expected return on

³ The Black–Scholes formula for E and the corresponding volatility formula are used to simultaneously determine A and σ (Cooper and Davydenko 2007; Bharath and Shumway 2008). We will apply this idea in a peer group analysis.

⁴ Stiglitz (1969) was the first to prove this characteristic without using put–call parity, which was published by Stoll (1969) in the same year.

equity $\mu_E E$ equals the instantaneous expected return of the replicating portfolio that consists of $N(d_1)$ assets and $-N(d_2)$ risk-free zero-coupon bonds with face value K and time to maturity T . An analogous interpretation holds for the instantaneous expected return on debt $\mu_D D$. Besides the expected rate of return on assets, their volatility, the risk-free rate and the lent term of debt, the costs of equity and debt are determined by the ratio of assets value A and the debt redemption amount K :

$$\begin{aligned}\mu_E E &= \mu A N(d_1) - r K e^{-rT} N(d_2) \\ \Rightarrow \mu_E &= \frac{\mu A N(d_1) - r K e^{-rT} N(d_2)}{A N(d_1) - K e^{-rT} N(d_2)},\end{aligned}$$

and

$$\begin{aligned}\mu_D D &= \mu A N(-d_1) + r K e^{-rT} N(d_2) \\ \Rightarrow \mu_D &= \frac{\mu A N(-d_1) + r K e^{-rT} N(d_2)}{A N(-d_1) + K e^{-rT} N(d_2)},\end{aligned}\quad (4.3)$$

where μ is the expected continuously compounded rate of return on assets.

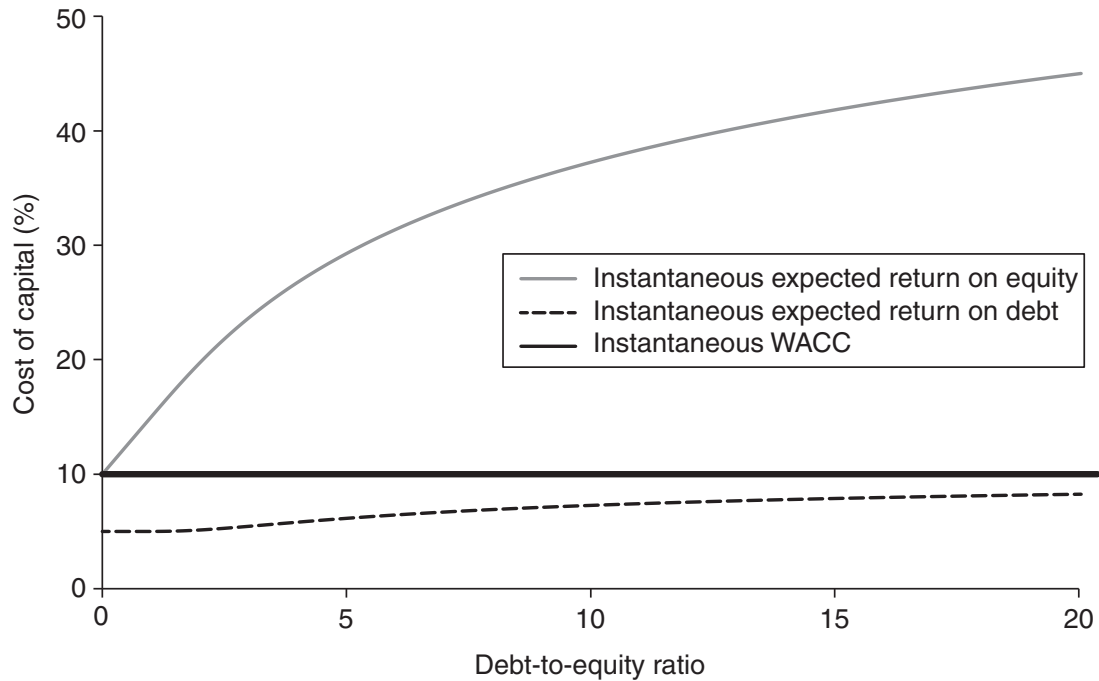
Inserting the instantaneous expected rates of return of (4.3) into (2.1) proves that the WACC equals the instantaneous expected rate of return on assets:⁵

$$\text{WACC}^{\text{instant}} = \mu_E \frac{E}{A} + \mu_D \frac{D}{A} = \mu. \quad (4.4)$$

To illustrate the shapes of cost-of-capital curves depending on the debt-to-equity ratio, we assume the following example data to generate Figure 2. The value of assets equals one monetary unit, their instantaneous expected rate of return amounts to 10%, and their instantaneous volatility is 20%. The risk-free rate equals 5% and the lent term of debt is one period. To show the influence of the debt-to-equity ratio on costs of capital, we vary the face value of debt so the debt-to-equity ratios are between 0 and 20. We use (4.3) to calculate the expected costs of equity and debt. For this, the value of equity is computed using the Black–Scholes formula (4.1). The value of debt is obtained as the difference between the assets value and the equity value.

Figure 2 plots costs of capital against the debt-to-equity ratio. As proposition I of Modigliani and Miller (1958) holds, the WACC is constant. However, the cost of equity and the cost of debt increase nonlinearly. Figure 2 substantiates the only

⁵ Since the assets follow a geometric Brownian motion in the Black–Scholes world, the drift rate (instantaneous expected rate of return) equals the expected continuously compounded rate of return. However, a derivative contract follows a different stochastic process in this framework. This leads to different terms for μ and $\mu_{E,D}$.

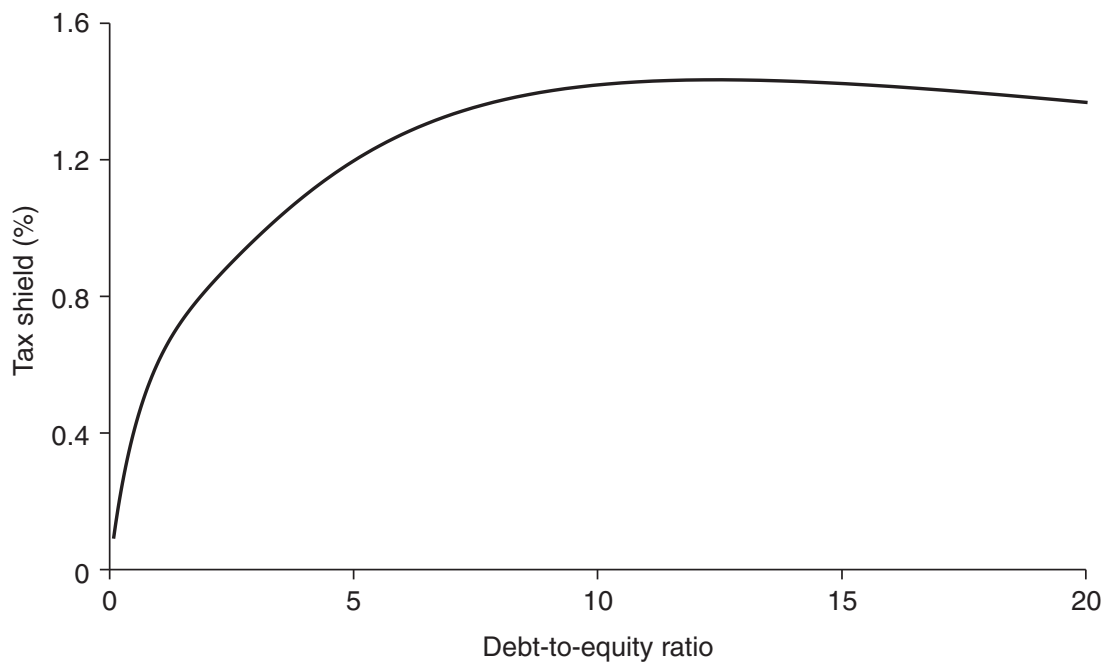
FIGURE 2 Costs of capital depending on the debt-to-equity ratio.

sketched courses of costs of capital in Merton (1974, Figure 9) that found entry in financial textbooks.⁶ With a given volatility of assets, the cost of debt increases with the debt-to-equity ratio as the debt holders bear higher default risk. The cost of debt is limited upward by the WACC, because with an infinitely high debt-to-equity ratio, the debt holders bear all the assets risk and act like equity holders in an unlevered company from an economic point of view. If we compare this with the situation without credit risk, the risk of equity holders is lower. Therefore, the cost of equity is reduced under credit risk.

Equation (4.4) does not hold in cases of discriminatory taxation of equity and debt financing. If the interest payment $(K - D)$ reduces the tax base, the tax reduction amounts to $(K - D)s$, where s denotes the tax rate. We assume the tax reduction only becomes effective if the company stays solvent, ie, $A_T \geq K$. Thus, the tax reduction payoff at maturity reads as follows:

$$\text{tax reduction}_T = \begin{cases} (K - D)s & \text{if } A_T \geq K, \\ 0 & \text{if } A_T < K. \end{cases} \quad (4.5)$$

⁶ In Appendix A, which is available online, we prove the characteristics of the cost-of-capital curves shown in Figure 2.

FIGURE 3 Tax shield (as a percentage of assets value) depending on the debt-to-equity ratio.

Since (4.5) represents the payoff of a money-or-nothing call option, its value – ie, the value of the tax shield – amounts to⁷

$$\text{tax shield} = (K - D)s\mathbb{N}(d_2)e^{-rT}. \quad (4.6)$$

Figure 3 depicts the tax shield depending on the debt-to-equity ratio based on the example data described above and a tax rate of 25%. It shows a concave relationship, where the tax shield initially increases because the debt portion grows. This effect diminishes if the debt-to-equity ratio is high, as the probability of default also becomes high in this situation. Here, the probability that the tax shield becomes effective is low.

To apply our proposed instantaneous expected return approach to a nonpublicly traded company, the WACC of a particular company is determined via a peer group analysis, $\mu = \mu^{\text{peer}}$. According to the first equation in (4.3), μ^{peer} implicitly depends on the expected return on equity μ_E^{peer} , the assets value A^{peer} , the equity value E^{peer}

⁷ The value of the tax shield equals the expected tax reduction payoff under risk-neutral probabilities discounted with the risk-free rate. We address risk-neutral and real-world probabilities in Section 5.

and the assets volatility σ^{peer} . The face value of peer group companies' debt K^{peer} can be collected from financial statements. The risk-free rate r can be obtained from government bond yields. Because a real company's debt does not consist only of a single zero-coupon bond, we suggest using the Macaulay duration of peer group companies' liabilities as a proxy for T^{peer} (Damodaran 2012, p. 833).⁸

The market capitalization of peer group equity E^{peer} is known, and peer group values for μ_E^{peer} and σ_E^{peer} can be estimated based on historical price data. We can infer A^{peer} and σ^{peer} from E^{peer} and σ_E^{peer} by simultaneously solving the Black–Scholes equity formula (4.1) and its corresponding volatility formula (4.2). Thereby, the required data set is complete. Thus, our approach allows for differences in the market value of equity, the book value of debt, the cost of equity and the volatility of equity in peer group companies. However, it is required that both the expected rate of return on assets and the assets volatility of peer group companies and the company to be valued coincide. As long as the distributions of the assets' rates of return are similar, our approach does not require similar company sizes. Note that for relevering, the debt market value of the company to be valued is not needed to compute costs of equity and debt, since μ_E and μ_D (according to (4.3)) do not depend on D .

Table 1 compares data requirements for peer group analyses according to the CAPM approaches and our option-based approach. This table confirms that the data requirements for our approach are on a level with the classical CAPM approach without credit risk. In contrast, the debt beta approach additionally requires a debt risk measure and the market value of debt of the company to be valued. Both are endogenous in the option-based approach due to the put–call parity.

Peer group analysis in the option-based approach is based on μ_E^{peer} and σ_E^{peer} to compute μ and σ of the assets, respectively. However, if assets volatility can be split up into systematic and idiosyncratic risk, an increase in systematic risk leads not only to a higher assets volatility with decreasing μ_E as a consequence, but also to a higher expected assets return with increasing μ_E (Hu and Jacobs 2016; Chaudhury 2017).

Fama and French (1993, 2015), Carhart (1997) and Hou *et al* (2015) show that multifactor models possess explanatory power for cross-sectional equity returns. Assuming a multifactor model, both equity return and risk depend on factor sensitivities. As a result, μ_E and μ (implied by (4.3)) include a risk premium for bearing systematic risk. Section 6 merges the option-based approach and a multifactor asset pricing model as an alternative approach to determine costs of equity and debt.

⁸ We are aware that employing the Macaulay duration as a proxy for T does not reflect that loans with periodic interest payments parallel straight bonds and, therefore, correspond to compound options (Geske 1977).

TABLE 1 Required data for peer group analysis.

	CAPM approach without credit risk	Debt beta approach	Option-based approach
Risk-free rate	+	+	+
Value of equity	Market value	Market value	Market value
Value of debt	Book value	Market value	—
<i>Comment</i>	<i>By assumption of no credit risk</i>	<i>Unknown debt market value of the company to be valued is needed for relevering</i>	<i>Endogenous; only debt face value and time to maturity are required</i>
Equity risk measure	Equity beta	Equity beta	Equity volatility
<i>Comment</i>	<i>Regression on stock market index</i>	<i>Regression on stock–corporate bond market index (data not available)</i>	—
Debt risk measure	—	Debt beta	—
<i>Comment</i>	<i>By assumption of no credit risk</i>	<i>Regression on stock–corporate bond market index (data not available)</i>	<i>Debt volatility is endogenous</i>
Risk premium	Equity premium	Stock–bond market premium	Expected equity excess return
<i>Comment</i>	<i>By assumption of no credit risk</i>	Data not available	<i>Rearranging (4.3) yields $\mu_E - r = \mathbb{N}(d_1)(A/E)(\mu - r)$</i>

Vassalou and Xing (2004) and Avramov *et al* (2009) provide evidence that default risk is systematic, but the systematic default risk factor cannot be explained by Fama–French–Carhart factors. Therefore, Vassalou and Xing (2004) suggest the following procedure: simultaneously solving (4.1) and (4.2), based on an estimation of the value of equity E and its volatility σ_E , leads to the initial values σ_{initial} and A_{initial} . Based on σ_{initial} , (4.1) can be employed to create an assets value time series (A_t) using historical equity price data (E_t). The assets value time series can be used to estimate μ and σ . Setting $\sigma_{\text{initial}} = \sigma$ and iterating leads to the final estimation of μ .

5 PER-PERIOD COSTS OF CAPITAL IN THE OPTION-BASED APPROACH

Instantaneous expected returns are important in continuous-time finance. However, it is usually assumed in practical applications of company valuation that end-of-period cashflows must be discounted. Expected costs of capital per period must be determined in this situation. We (implicitly) define continuously compounded expected rates of return per period on equity μ_E^{periodic} and debt μ_D^{periodic} using the following equations:⁹

$$Ee^{\mu_E^{\text{periodic}}T} = \mathbb{E}(E_T) \quad \text{and} \quad De^{\mu_D^{\text{periodic}}T} = \mathbb{E}(D_T). \quad (5.1)$$

In Appendix B (available online), we show that expected costs of equity and debt per period can be computed as follows:

$$\begin{aligned} e^{\mu_E^{\text{periodic}}T} &= \frac{Ae^{\mu T}\mathbb{N}(\tilde{d}_1) - K\mathbb{N}(\tilde{d}_2)}{A\mathbb{N}(d_1) - Ke^{-rT}\mathbb{N}(d_2)} \\ \Rightarrow \mu_E^{\text{periodic}} &= \frac{1}{T} \ln \left(\frac{Ae^{\mu T}}{E} \mathbb{N}(\tilde{d}_1) - \frac{K}{E} \mathbb{N}(\tilde{d}_2) \right), \end{aligned}$$

and

$$\begin{aligned} e^{\mu_D^{\text{periodic}}T} &= \frac{Ae^{\mu T}\mathbb{N}(-\tilde{d}_1) + K\mathbb{N}(\tilde{d}_2)}{A\mathbb{N}(-d_1) - Ke^{-rT}\mathbb{N}(d_2)} \\ \Rightarrow \mu_D^{\text{periodic}} &= \frac{1}{T} \ln \left(\frac{Ae^{\mu T}}{D} \mathbb{N}(-\tilde{d}_1) + \frac{K}{D} \mathbb{N}(\tilde{d}_2) \right), \end{aligned} \quad (5.2)$$

where \tilde{d}_1 and \tilde{d}_2 are based on the real-world distribution of the value of assets; they differ from the risk-neutral quantities d_1 and d_2 of the Black–Scholes formula in that the expected rate of return on assets μ replaces the risk-free rate r . The quantities d_1 and d_2 are expressed in terms of present values, whereas \tilde{d}_1 and \tilde{d}_2 are expressed in terms of expected future values,

$$d_1 = \frac{\ln(A/(Ke^{-rT})) + (\sigma^2/2)T}{\sigma\sqrt{T}} \quad \text{and} \quad \tilde{d}_1 = \frac{\ln(\mathbb{E}(A_T)/K) + (\sigma^2/2)T}{\sigma\sqrt{T}},$$

since $\mathbb{E}(A_T) = Ae^{\mu T}$.

⁹ The main difference in modeling costs of capital in discrete time is the requirement of expected option payoff formulas, which are rare in the literature (Smith 1976; Rubinstein 1984; Hu and Jacobs 2016). In addition, (5.1) requires equity and debt values. Employing Black–Scholes values in (5.2) below presupposes that the Black–Scholes formula developed in the framework of a complete (continuous-time) capital market is also valid on an incomplete (discrete-time) market.

Hence, $\mathbb{N}(\tilde{d}_1)$ and $-\mathbb{N}(\tilde{d}_2)$ can be interpreted as the expected amounts of assets and risk-free zero-coupon bonds in the equity replicating portfolio. Analogously to our interpretation of the expected instantaneous return on equity in the previous section (see (4.3)), the expected value of equity $\mathbb{E}(E_T) = \mathbb{E}(A_T)\mathbb{N}(\tilde{d}_1) - K\mathbb{N}(\tilde{d}_2)$, which is in line with Rubinstein (1984), corresponds to the expected composition of the replicating portfolio. In this context, $\mathbb{N}(-\tilde{d}_2)$ equals the real-world probability that the put option inherent in debt ends in-the-money. Thus, this term represents the company's probability of default (see, for example, Sundaresan 2013, p. 24).¹⁰

The total period expected WACC, in the form of a discount factor, results from weighting and adding up expected costs of equity and debt. The per-period expected rates of return on equity and debt according to (5.2) fulfill proposition I of Modigliani and Miller (1958):

$$e^{\text{WACC}_T^{\text{periodic}}} = e^{\mu_E^{\text{periodic}} T} \frac{E}{A} + e^{\mu_D^{\text{periodic}} T} \frac{D}{A} = \frac{\mathbb{E}(E_T)}{A} + \frac{\mathbb{E}(D_T)}{A} = e^{\mu T}. \quad (5.3)$$

To illustrate the curves of the company's default probability $\mathbb{N}(-\tilde{d}_2)$ and the corresponding expected loss of the debt holders ($K - \mathbb{E}(D_T)$) depending on the debt-to-equity ratio, we revisit our numerical example of the previous section. Figure 4 shows that, of course, both measures of credit risk increase with the debt-to-equity ratio. In our sample setting, a debt-to-equity ratio of 20 induces a probability of default of 60%. At the same time, the expected loss amounts to nearly 10% so that the recovery rate is slightly above 90%. This supports our reasoning in Section 3 that the expected loss is meaningful for the implied debt beta.

In order to measure the valuation error in terms of wrongly applying the debt beta approach instead of our option-based approach, following Koziol (2014), we analyze the relative differences of expected equity and the debt rates of return based on both the implied debt beta approach and the option-based approach:

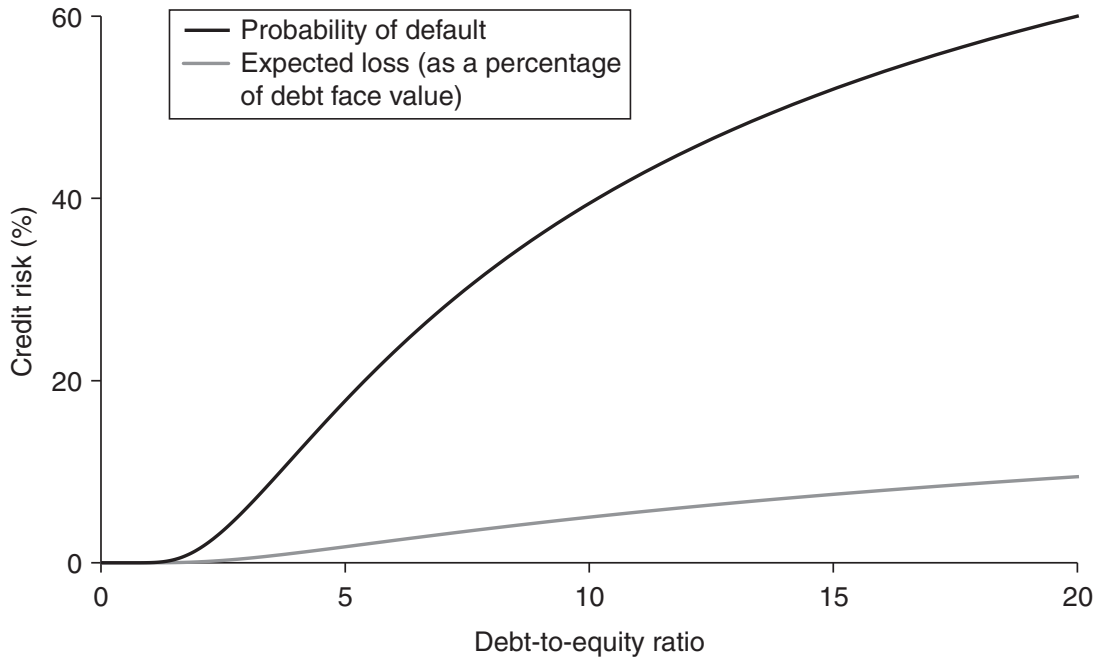
$$\text{valuation error}_E^{\text{debt beta}} = \frac{\mu_E^{\text{debt beta}}}{\mu_E^{\text{periodic}}} - 1$$

and

$$\text{valuation error}_D^{\text{debt beta}} = \frac{\mu_D^{\text{debt beta}}}{\mu_D^{\text{periodic}}} - 1. \quad (5.4)$$

Figure 5 plots the valuation errors of costs of equity and debt based on our example data. In addition, we set the expected market rate of return equal to 12%. Assuming

¹⁰ Since the tax shield possesses an option-style characteristic, its expected value reads $(K - D)\mathbb{N}(\tilde{d}_2)$, where $\mathbb{N}(\tilde{d}_2)$ represents the real-world probability that the company stays solvent.

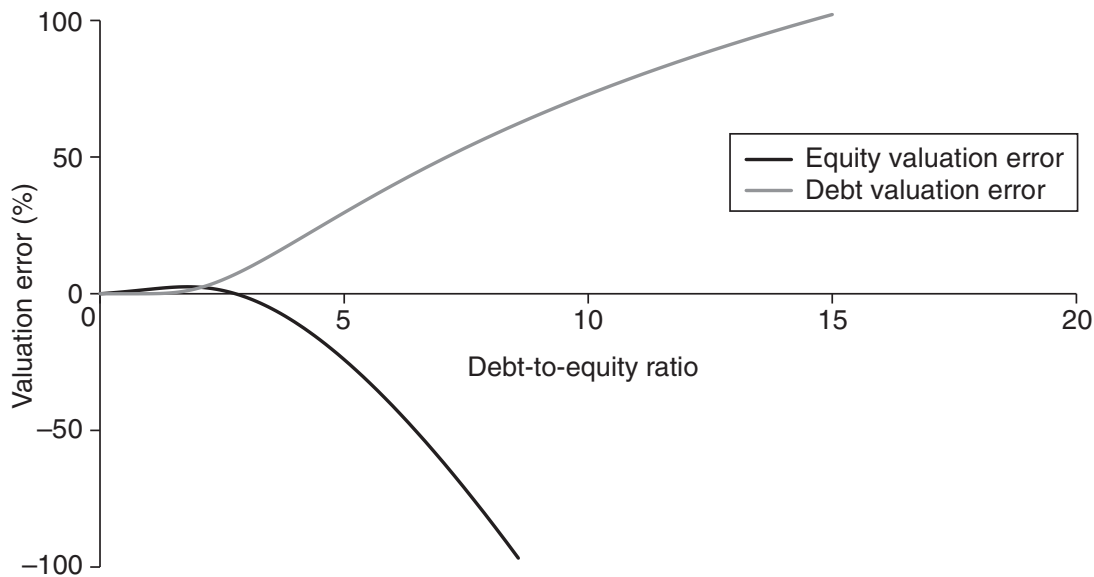
FIGURE 4 Probability of default and expected loss depending on the debt-to-equity ratio.

a constant WACC at a level of 10% implies that the assets beta equals 0.71. Periodic expected costs of equity and debt are computed according to (5.2). The debt interest rate i_D amounts to (Merton 1974, p. 454)

$$De^{i_D T} = K \Rightarrow i_D = \frac{1}{T} \ln \frac{K}{D}. \quad (5.5)$$

Subsequently, we insert i_D in the costs of capital equations used in (3.5). Then, $\mu_{E,D}^{\text{debt beta}}$ and $\mu_{E,D}^{\text{periodic}}$ depend on the debt-to-equity ratio, where the WACC is constant and amounts to 10% by construction. With this example data, all parameters are correct, only the debt beta approach wrongly assumes the cost of debt at the level of the interest rate instead of the expected rate of return on debt. Figure 5 shows that the valuation error may be high even for an equity portion of 20%, ie, a debt-to-equity ratio of 4.

Dramatic valuation errors occur when the debt interest rate exceeds the expected market rate of return. In this situation, the debt beta is larger than 1 (see (3.4)), which leads to an assets beta below the equity beta, on average, of the market. As a result, $\mu_E^{\text{debt beta}}$ is smaller than $\mu_D^{\text{debt beta}}$, which contradicts the risk-sharing rule of equity holders and debt holders. In extreme cases, the expected cost of equity becomes negative in the debt beta approach.

FIGURE 5 Valuation error of the implied debt beta approach.

Completing our discussion of per-period expected returns, we turn to discretely compounded (simple) rates of return as an alternative way of computing costs of capital. Clearly, the use of simple returns instead of continuously compounded returns will not change our general results. Nevertheless, the definition of simple returns must be consistent. Let μ_T^{discrete} denote the expected simple total period rate of return on assets,

$$\mu_T^{\text{discrete}} = (1 + \mu^{\text{discrete}})^T - 1 \quad \text{with} \quad \mu^{\text{discrete}} = e^{\mu} - 1, \quad (5.6)$$

where μ^{discrete} denotes the expected periodic rate of return on assets. Thereby, $(1 + \mu_T^{\text{discrete}})$ represents the appropriate factor to discount $\mathbb{E}(A_T)$. Now, define μ_E^{discrete} and μ_D^{discrete} as the corresponding expected periodic rates of return on equity and debt, respectively:

$$(1 + \mu_E^{\text{discrete}})^T = \frac{\mathbb{E}(E_T)}{E} \quad \text{and} \quad (1 + \mu_D^{\text{discrete}})^T = \frac{\mathbb{E}(D_T)}{D}. \quad (5.7)$$

Then, the total period simple returns

$$\mu_{E,T}^{\text{discrete}} = (1 + \mu_E^{\text{discrete}})^T - 1 \quad \text{and} \quad \mu_{D,T}^{\text{discrete}} = (1 + \mu_D^{\text{discrete}})^T - 1$$

fulfill proposition I of Modigliani and Miller (1958):

$$\text{WACC}_T^{\text{discrete}} = \mu_{E,T}^{\text{discrete}} \frac{E}{A} + \mu_{D,T}^{\text{discrete}} \frac{D}{A} = \frac{\mathbb{E}(E_T)}{A} + \frac{\mathbb{E}(D_T)}{A} - 1 = \mu_T^{\text{discrete}}. \quad (5.8)$$

5.1 Example: stylized valuation of Apple Inc

To prove the feasibility of our option-based approach, we conduct an analysis to value Apple Inc as if it were not publicly traded. The valuation is done by the end of 2017 and the procedure is split into two steps. The first step (unlevering) is to determine the WACC based on a peer group analysis. Using market data for peer group companies, we collect the values of equity and estimate equity volatilities. With these two parameters, we simultaneously solve (4.1) and (4.2) to find the values of assets and their volatilities. To compute peer group WACCs, ie, μ in (4.3), we estimate the expected equity rates of return via the Fama–French–Carhart model. Subsequently, the averages of peer group WACCs and volatilities are assumed to represent Apple’s WACC and volatility, respectively.

In the second step (relevering), we determine Apple’s value of assets based on discounted free cashflow analysis,

$$A = \frac{\mathbb{E}(\text{FCF})}{\mu^{\text{peer}} - g}, \quad (5.9)$$

where $\mathbb{E}(\text{FCF})$ is the expected first-year free cashflow and g is the growth rate, in order to apply (4.3) again.

We choose Alphabet Inc (Google), Amazon.com, Inc and Microsoft Corporation as peer group companies. Here, the market capitalizations at the end of 2017 represent the market values of equity. Their volatilities are estimated based on daily stock returns for 2017. To solve (4.1) and (4.2) for A and σ_A , further data is required. The face values of debt are set equal to their book values and obtained from the annual financial reports for 2017. We assume a time to maturity of three years. The risk-free rate of return is approximated by the one-year rate of return of Treasury bills, which amounted to 1.75% at the end of 2017.

To estimate peer group companies’ equity returns, we proceed as follows. First, we estimate equity factor sensitivities (betas) in the framework of the Fama–French–Carhart model, again based on daily stock price data from 2017. These sensitivities are multiplied with long-term average factor excess returns, which can be found in Kenneth R. French’s data library.¹¹ Table 2 shows the results for the peer group companies.

To apply (5.9), we transform the instantaneous assets rate of return into the corresponding discretely computed rate, which amounts to 12.7%. Our expectation on

¹¹ See <https://bit.ly/2VJeGG7>.

TABLE 2 Peer group parameters in the option-based approach.

Peer group company	MC (E)	Book value of debt (K)	EER (μ_E)	Equity volatility (σ_E)	Value of assets (A)	Assets volatility (σ)	EAR (μ)
Amazon	480	104	13.9	22.5	578	18.6	11.3
Google	613	45	13.5	17.3	656	16.2	12.8
Microsoft	551	169	14.1	16.8	711	13.1	11.9
Average						15.9	12.0

Values E , K and A are measured in US\$ billions. μ_E , σ_E , σ and μ are percentages. "MC" denotes market capitalization, "EER" denotes expected equity return and "EAR" denotes expected assets return.

Apple's future free cashflows is based on Apple's free cashflow in 2018. This can be justified by the fact that Apple's financial year ends in September; so, at the end of 2017, the results of the 2018 financial year were already partly determined. In addition, we assume the growth rate of Apple's free cashflow to be equal to the revenue growth rate for 2017, which amounts to 6.3%. Apple's book value of debt was US\$241 billion. With this data, (5.9) yields an estimated market value of Apple's assets of US\$1025 billion. Via (4.3), costs of equity and debt for Apple amount to 15.9% and 1.75%, respectively. Based on the Black–Scholes formula (4.1), Apple's market values of equity and debt amount to US\$796 billion and US\$229 billion, respectively, which leads to a debt-to-equity ratio of 0.29. The low debt-to-equity ratio causes a marginal credit spread of 0.00006 basis points. The corresponding probability of default and expected loss are negligible.

To contrast the results of the option-based approach with the debt beta approach, we must estimate peer group assets betas in the unlevering part. For this, we initially collect debt interest rates from annual financial reports and apply (3.4) to compute the peer group debt betas. The corresponding equity betas are estimated based on the data of the option-based approach but applied using the single-index model. Subsequently, we solve (3.3) for β_A^{peer} , where market capitalizations and book values of debt are used to determine the debt-to-equity ratios. Table 3 summarizes the peer group parameters of the debt beta approach.

In the relevering part, the average peer group assets beta is set equal to Apple's asset beta. From the last equation of (3.5), we obtain Apple's expected rate of return on assets, ie, Apple's WACC, at a level of 10.5%. To determine Apple's costs of equity and debt, we calculate its debt-to-equity ratio, where we apply (5.9) once again. The estimated market value of Apple's assets amounts to US\$1563 billion, and using the book value of debt leads to a debt-to-equity ratio of 0.18. We refer to (3.5) to find Apple's costs of equity and debt at the levels of 11.7% and 4.0%,

TABLE 3 Peer group parameters of the debt beta approach.

Peer group company	Expected return on debt, $\mathbb{E}(R_D) = i_D$ (%)	Debt beta (β_D)	Equity beta (β_E)	Assets beta (β_A)
Amazon	3.0	0.15	1.24	1.05
Google	2.9	0.14	1.19	1.12
Microsoft	3.2	0.18	1.29	1.03
Average				1.07

respectively. Here, similar to the peer group companies, Apple's cost of debt is set equal to its debt interest rate.

To complete our example, we compute valuation errors according to (5.4). For the debt beta approach compared with the option-based approach, these amount to -26.3% for equity and 130.9% for debt. This peculiarly large debt valuation error results from two assumptions. First, we applied different factor models when using the option-based approach and the debt beta approach to estimate the peer group companies' costs of equity. Second, assuming Apple's debt interest rate to be equal to its cost of debt induces the following contradiction. The difference between debt interest rate and expected debt rate of return represents the expected loss premium of debt holders. Here, it amounts to 4.0% minus 1.75% . Contrarily, the expected loss premium within the option-based approach is almost zero, as Apple's cost of debt almost equals the risk-free rate. This effect may occur in periods when the term structure of interest rates shifts down, since the debt interest rate from the annual statement is related to the past and based on the book value, whereas the expected debt return is related to the future and based on the market value.

6 COMBINING THE OPTION-BASED APPROACH AND A FACTOR SENSITIVITIES APPROACH

Since there is evidence in the literature that credit risk is systematic, in this section, we combine the option-based approach with a multifactor asset pricing model. A multifactor asset pricing model is usually represented by the following formula:

$$\mu = r + \beta'_F \mathbb{E}(\mathbf{r}_F), \quad (6.1)$$

where β'_F denotes the row vector of factor sensitivities and $\mathbb{E}(\mathbf{r}_F)$ is the vector of expected excess factor returns. Based on Black and Scholes (1973, formula (15)), Smith (1976, formula (89)) and Coval and Shumway (2001, formula (11)), the

single-factor sensitivities of derivative contracts f read as follows:

$$\begin{aligned}\beta_{f,F} &= \frac{\text{Cov}((df/f), (dF/F))}{\text{Var}(dF/F)} = \frac{\text{Cov}((1/f)\Delta_f dA, (dF/F))}{\text{Var}(dF/F)} \\ &= \Delta_f \frac{A}{f} \frac{\text{Cov}((dA/A), (dF/F))}{\text{Var}(dF/F)} = \Delta_f \frac{A}{f} \beta_{A,F},\end{aligned}\quad (6.2)$$

where dF/F is the instantaneous factor rate of return, $\Delta_f = \partial f / \partial A$ (delta) and $\beta_{.,F}$ is the instantaneous factor sensitivity.

Following Galai and Masulis (1976), we insert the delta of equity Δ_E and the delta of debt Δ_D , respectively, into (6.2). The resulting instantaneous single-factor sensitivities of equity and debt are

$$\beta_{E,F} = \Delta_E \frac{A}{E} \beta_{A,F} = \mathbb{N}(d_1) \left(1 + \frac{D}{E}\right) \beta_{A,F}$$

and

$$\beta_{D,F} = \Delta_D \frac{A}{D} \beta_{A,F} = \mathbb{N}(-d_1) \left(1 + \frac{E}{D}\right) \beta_{A,F}.\quad (6.3)$$

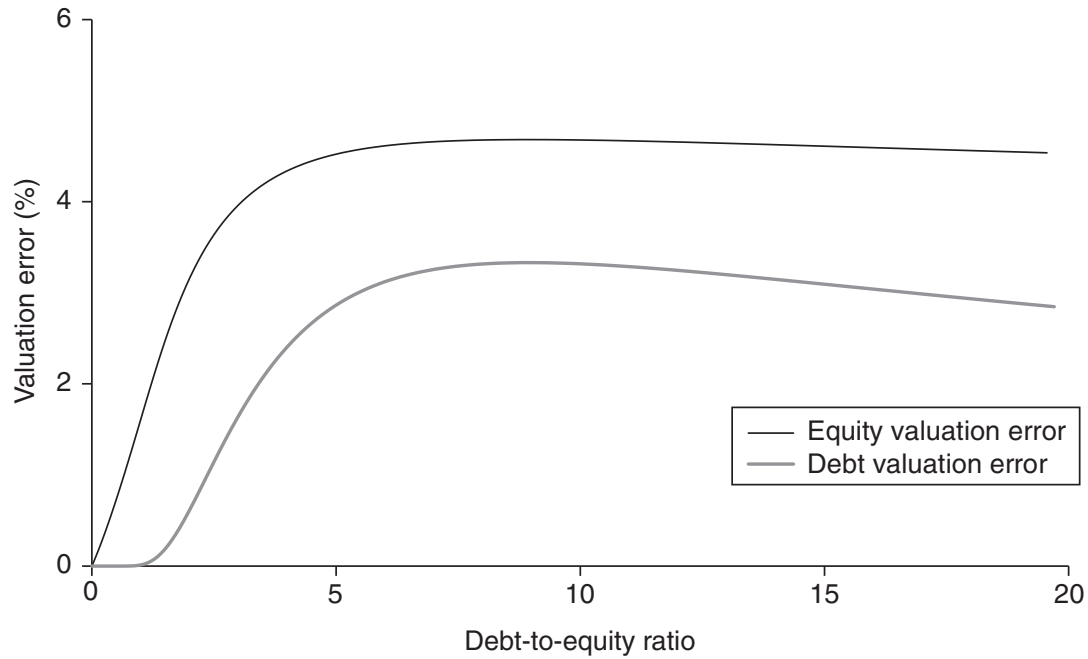
Inserting the single-factor sensitivities of (6.3) into (6.1) leads to expected rates of return on equity and debt. Weighting costs of equity and debt by the corresponding equity and debt ratios proves that proposition I of Modigliani and Miller (1958) is also valid in this approach:

$$\begin{aligned}\text{WACC}^{\text{multifactor}} &= \underbrace{\left(r + \mathbb{N}(d_1) \left(1 + \frac{D}{E}\right) \beta'_{A,F} \mathbb{E}(r_F)\right)}_{=\mathbb{E}(R_E^1)} \frac{E}{E+D} \\ &\quad + \underbrace{\left(r + (1 - \mathbb{N}(d_1)) \left(1 + \frac{E}{D}\right) \beta'_{A,F} \mathbb{E}(r_F)\right)}_{=\mathbb{E}(R_D)} \frac{D}{E+D} \\ &= r + \beta'_{A,F} \mathbb{E}(r_F) = \mu.\end{aligned}\quad (6.4)$$

In order to calculate the expected return on assets, assets factor sensitivities must be determined according to (6.3). Again, A and σ can be obtained using the procedure described in Section 4. Note that the value of debt is endogenous here because $D = A - E$.

Since in (6.4) the instantaneous approach and the per-period approach are combined, one can expect valuation errors

$$\text{valuation error}_E^{\text{multifactor}} = \frac{\mathbb{E}(R_E^1)}{\mu_E^{\text{periodic}}} - 1$$

FIGURE 6 Valuation error of the combined option-based multifactor approach.

and

$$\text{valuation error}_D^{\text{multifactor}} = \frac{\mathbb{E}(R_D)}{\mu_D^{\text{periodic}}} - 1. \quad (6.5)$$

Figure 6 shows the valuation errors of a one-factor model with the example data of Section 4. Compared with the error magnitude of the implied debt beta approach (see Figure 5), the combined option-based multifactor approach appears to be a reasonable alternative in peer group analyses. In our example, the equity valuation error stays below 5% of the expected equity rate of return.

6.1 Valuation of Apple Inc (continued)

We continue our example from Section 4 and apply the combined option-based approach to value Apple, again using the Fama–French–Carhart model. In the unlevering part, we must estimate factor sensitivities and solve (6.3) for $\beta_{A,F}^{\text{peer}}$ for every factor. Here, we take the peer group values for A and E from Table 2 to determine the debt-to-equity ratios. In addition, we use the assets volatilities to compute the $\mathbb{N}(d_1)$. Table 4 shows the peer group parameters of the combined option-based approach, where we use standard notation for the Fama–French–Carhart factors.

Besides different approaches to determine costs of equity and debt ((4.3) versus (6.4)), one more difference between the pure and the combined option-based

TABLE 4 Peer group parameters (unlevered) in the combined option-based approach.

Asset sensitivities $\beta_{A,F}$	$\mathbb{E}(R_M) - r$	SMB	HML	WML
Amazon	1.06	−0.53	−0.80	0.44
Google	1.08	−0.44	−0.63	0.48
Microsoft	0.97	−0.29	−0.40	0.35
Average	1.04	−0.42	−0.61	0.44
Factor excess returns	8.2%	0.5%	1.9%	7.3%
Apple's excess return	10.2%			
Apple's WACC	12.0%			

SMB denotes small minus big; HML denotes high minus low; WML denotes winners minus losers.

approaches lies in the estimation of WACC in peer group analysis. In the pure option-based approach, the average of the expected assets returns of the peer group companies represents the WACC, where the costs of equity of the single peer group companies are determined by the factor sensitivities. Contrarily, in the combined option-based approach single-equity sensitivities are used to determine the assets sensitivities for every peer group company. Subsequently, the averages of these peer group assets sensitivities determine the WACC.

Apple's WACC amounts to 12.0% in the combined approach, which is considerably lower than in the pure option-based approach. Therefore, (5.9) yields a higher value of Apple's assets at the level of US\$1160 billion. In the relevering part, we apply the Black–Scholes formula to determine Apple's debt-to-equity ratio. The corresponding values are $E_{\text{Apple}} = \text{US\$931 billion}$ and $D_{\text{Apple}} = \text{US\$229 billion}$; the debt-to-equity ratio amounts to 0.25. With the definitions in (6.4), Apple's cost of equity is 14.5% and its cost of debt is still 1.75%. Consequently, the valuation error based on (6.5) for debt is almost zero and the equity valuation error amounts to −8.7%.

Finally, Table 5 compares the results of our example with the estimation of Apple's expected equity return based on its stock price data, again using the Fama–French–Carhart model. It shows that the market-based estimation of Apple's cost of equity is very close to our estimated equity return if the pure option-based approach is applied.

7 CONCLUSIONS

We develop and discuss (quasi-) analytic formulas of costs of capital in two different frameworks under credit risk. We show that the debt beta approach – state-of-the-art in CAPM-style cost-of-capital computations – leads to distorted results even if betas are computed with respect to a return-risk efficient index in the stock universe.

TABLE 5 Apple's estimated costs of capital.

	Cost of assets μ	Cost of equity μ_E	Cost of debt μ_D
Pure option-based approach	12.5	15.9	1.75
Combined approach	12.0	14.5	1.75
Debt beta approach	10.5	11.7	4.00
Market data-based estimation	—	15.8	—

All values shown are percentages.

Instead, an appropriate index must consist of both stocks and corporate bonds to represent (systematic) equity and debt risk. Since historical data of a combined stock–corporate bond index is not available, a time series analysis to estimate valid betas is not feasible.

Our results show that the implied debt beta approach is not able to overcome this difficulty, as this method leads to a consistent overall WACC – in terms of fulfilling proposition I of Modigliani and Miller (1958) – but implies an inconsistent debt-to-equity ratio, with distorted costs of equity and debt as a result. We attribute this to the difference between the debt interest rate – which is used in the implied debt beta approach – and the required rate of return of debt holders. In sum, the debt beta approach suffers from both theoretical shortcomings and application barriers.

To overcome these difficulties, we apply the classical Black–Scholes–Merton model of credit valuation to determine costs of equity and debt. In a continuous-time setting, we are able to analyze the shapes of costs of capital with varying debt-to-equity ratios. Moreover, our approach facilitates the computation of the tax shield and proves to be superior to CAPM-based frameworks regarding the quantity and quality of required data in a peer group analysis.

Company valuation usually assumes a discrete-time setting. Therefore, we also provide per-period cost-of-capital formulas in terms of continuously and discretely compounded required rates of return of the capital holders. Our results are based on expected option payoffs, assuming a lognormal distribution of the value of assets that is consistent with the Black–Scholes framework. In this setting, we are able to analyze the influence of the debt-to-equity ratio on the probability of default of the particular company and the expected loss of the company's debt holders. In addition, we compute the valuation error if the implied debt beta approach is used instead of the option-based approach. Moreover, we prove that our results for instantaneous and per-period costs of capital are consistent with proposition I of Modigliani and Miller (1958). Finally, a valuation of Apple Inc as if it were not

publicly traded provides evidence that our option-based approach is able to reflect market expectations.

DECLARATION OF INTEREST

The authors report no conflicts of interest. The authors alone are responsible for the content and writing of the paper.

REFERENCES

- Arzac, E. R., and Glosten, L. R. (2005). A reconsideration of tax shield valuation. *European Financial Management* **11**, 453–461 (<https://doi.org/10.1111/j.1354-7798.2005.00292.x>).
- Avramov, D., Chordia, T., Jostova, G., and Philipov, A. (2009). Credit ratings and the cross-section of stock returns. *Journal of Financial Markets* **12**, 469–499 (<https://doi.org/10.1016/j.finmar.2009.01.005>).
- Benninga, S. (2014). *Financial Modeling*, 4th edn. MIT Press, London.
- Bharath, S. T., and Shumway, T. (2008). Forecasting default with the Merton distance to default model. *Review of Financial Studies* **21**, 1339–1369 (<https://doi.org/10.1093/rfs/hhn044>).
- Bierman, H., and Oldfield, G. S. (1979). Corporate debt and corporate taxes. *Journal of Finance* **34**, 951–956 (<https://doi.org/10.1111/j.1540-6261.1979.tb03447.x>).
- Black, F., and Scholes, M. (1973). The pricing of options and corporate liabilities. *Journal of Political Economy* **81**, 637–654 (<https://doi.org/10.1086/260062>).
- Branger, N., and Schlag, C. (2007). Option betas: risk measures for options. *International Journal of Theoretical and Applied Finance* **10**, 1137–1157 (<https://doi.org/10.1142/S0219024907004585>).
- Campbell, J. Y., Hilscher, J., and Szilagyi, J. (2008). In search of distress risk. *Journal of Finance* **63**, 2899–2939 (<https://doi.org/10.1111/j.1540-6261.2008.01416.x>).
- Carhart, M. M. (1997). On persistence in mutual fund performance. *Journal of Finance* **52**, 57–82 (<https://doi.org/10.1111/j.1540-6261.1997.tb03808.x>).
- Chaudhury, M. (2017). Volatility and expected option returns: a note. *Economics Letters* **152**, 1–4 (<https://doi.org/10.1016/j.econlet.2016.12.014>).
- Cohen, R. D. (2008). Incorporating default risk into Hamada's equation for application to capital structure. *Wilmott Magazine*, March/April, pp. 62–68. URL: <http://rdcohen.50megs.com/IDRHEq.pdf>.
- Conine, T. E. (1980). Corporate debt and corporate taxes: an extension. *Journal of Finance* **35**, 1033–1037 (<https://doi.org/10.1111/j.1540-6261.1980.tb03519.x>).
- Cooper, I. A., and Davydenko, S. A. (2007). Estimating the cost of risky debt. *Journal of Applied Corporate Finance* **19**(3), 90–95 (<https://doi.org/10.1111/j.1745-6622.2007.00150.x>).
- Cooper, I. A., and Nyborg, K. G. (2008). Tax-adjusted discount rates with investor taxes and risky debt. *Financial Management* **37**, 365–379 (<https://doi.org/10.1111/j.1755-053X.2008.00016.x>).

- Cornell, B., and Green, K. (1991). The investment performance of low-grade bond funds. *Journal of Finance* **46**, 29–48 (<https://doi.org/10.1111/j.1540-6261.1991.tb03744.x>).
- Coval, J. D., and Shumway, T. (2001). Expected option returns. *Journal of Finance* **56**, 983–1009 (<https://doi.org/10.1111/0022-1082.00352>).
- Cox, J. C., and Rubinstein, M. (1985). *Options Markets*. Prentice Hall, Englewood Cliffs, NJ.
- Damodaran, A. (2012). *Investment Valuation: Tools and Techniques for Determining the Value of Any Asset*, 3rd edn. Wiley.
- Duffie, D., Saita, L., and Wang, K. (2007). Multi-period corporate default prediction with stochastic covariates. *Journal of Financial Economics* **83**, 635–665 (<https://doi.org/10.1016/j.jfineco.2005.10.011>).
- Fama, E. F., and French, K. R. (1993). Common risk factors in the returns on stocks and bonds. *Journal of Financial Economics* **33**, 3–56 ([https://doi.org/10.1016/0304-405X\(93\)90023-5](https://doi.org/10.1016/0304-405X(93)90023-5)).
- Fama, E. F., and French, K. R. (2015). A five-factor asset pricing model. *Journal of Financial Economics* **116**, 1–22 (<https://doi.org/10.1016/j.jfineco.2014.10.010>).
- Fernández, P. (2004). The value of tax shields is NOT equal to the present value of tax shields. *Journal of Financial Economics* **73**, 145–165 (<https://doi.org/10.1016/j.jfineco.2002.10.001>).
- Fernández, P. (2015). CAPM: an absurd model. *Business Valuation Review* **34**(1), 4–23 (<https://doi.org/10.5791/0882-2875-34.1.4>).
- Galai, D., and Masulis, R. W. (1976). The option pricing model and the risk factor of stock. *Journal of Financial Economics* **3**, 53–81 ([https://doi.org/10.1016/0304-405X\(76\)90020-9](https://doi.org/10.1016/0304-405X(76)90020-9)).
- Geske, R. (1977). The valuation of corporate liabilities as compound options. *Journal of Financial and Quantitative Analysis* **12**, 541–552 (<https://doi.org/10.2307/2330330>).
- Gheno, A. (2007). Corporate valuations and the Merton model. *Applied Financial Economics Letters* **3**, 47–50 (<https://doi.org/10.1080/17446540600706858>).
- Hamada, R. S. (1972). The effect of the firm's capital structure on the systematic risk of common stocks. *Journal of Finance* **27**, 435–452 (<https://doi.org/10.1111/j.1540-6261.1972.tb00971.x>).
- Harris, R. S., and Pringle, J. J. (1985). Risk-adjusted discount rates – extensions from the average-risk case. *Journal of Financial Research* **8**(3), 237–244 (<https://doi.org/10.1111/j.1475-6803.1985.tb00406.x>).
- Haugen, R. A., and Pappas, J. L. (1971). Equilibrium in the pricing of capital assets, risk-bearing debt instruments, and the question of optimal capital structure. *Journal of Financial and Quantitative Analysis* **6**, 943–953 (<https://doi.org/10.2307/2329913>).
- Hillegeist, S. A., Keating, E. K., Cram, D. P., and Lundstedt, K. G. (2004). Assessing the probability of bankruptcy. *Review of Accounting Studies* **9**, 5–34 (<https://doi.org/10.1023/B:RAST.0000013627.90884.b7>).
- Hou, K., Xue, C., and Zhang, L. (2015). Digesting anomalies: an investment approach. *Review of Financial Studies* **28**(3), 650–705 (<https://doi.org/10.1093/rfs/hhu068>).
- Hu, G., and Jacobs, K. (2016). Volatility and expected option returns. Working Paper, Social Science Research Network (<https://doi.org/10.2139/ssrn.2695569>).

- Kaplan, S. N., and Stein, J. C. (1990). How risky is the debt in highly leveraged transactions? *Journal of Financial Economics* **27**, 215–245 (<https://doi.org/10.3386/w3390>).
- Koziol, C. (2014). A simple correction of the WACC discount rate for default risk and bankruptcy costs. *Review of Quantitative Finance and Accounting* **42**(4), 653–666 (<https://doi.org/10.1007/s11156-013-0356-x>).
- Merton, R. C. (1974). On the pricing of corporate debt: the risk structure of interest rates. *Journal of Finance* **29**(2), 449–470 (<https://doi.org/10.1111/j.1540-6261.1974.tb03058.x>).
- Modigliani, F., and Miller, M. H. (1958). The cost of capital, corporation finance and the theory of investment. *American Economic Review* **48**(3), 261–297.
- Roll, R., and Ross, S. A. (1994). On the cross-sectional relation between expected returns and betas. *Journal of Finance* **49**, 101–121 (<https://doi.org/10.1111/j.1540-6261.1994.tb04422.x>).
- Ruback, R. S. (2002). Capital cash flows: a simple approach to valuing risky cash flows. *Financial Management* **32**(2), 85–103 (<https://doi.org/10.2307/3666224>).
- Rubinstein, M. (1984). A simple formula for the expected rate of return of an option over a finite holding period. *Journal of Finance* **39**, 1503–1509 (<https://doi.org/10.1111/j.1540-6261.1984.tb04920.x>).
- Smith, C. W. (1976). Option pricing: a review. *Journal of Financial Economics* **3**, 3–51 ([https://doi.org/10.1016/0304-405X\(76\)90019-2](https://doi.org/10.1016/0304-405X(76)90019-2)).
- Stiglitz, J. E. (1969). A re-examination of the Modigliani–Miller theorem. *American Economic Review* **59**, 784–793.
- Stoll, H. R. (1969). The relationship between put and call option prices. *Journal of Finance* **24**, 801–824 (<https://doi.org/10.1111/j.1540-6261.1969.tb01694.x>).
- Sundaresan, S. (2013). A review of Merton’s model of the firm’s capital structure with its wide applications. *Annual Review of Financial Economics* **5**, 21–41 (<https://doi.org/10.1146/annurev-financial-110112-120923>).
- Vasicek, O. A. (1984). Credit valuation. Working Paper, KMV Corporation. URL: <https://bit.ly/2z6Ygzs>.
- Vassalou, M., and Xing, Y. (2004). Default risk in equity returns. *Journal of Finance* **59**, 831–868 (<https://doi.org/10.1111/j.1540-6261.2004.00650.x>).

The influence of volatility and moneyness on equity option returns - An empirical analysis

Peter Reichling* Juliane Selle† Anastasiia Zbandut*‡

This draft: September 29, 2024

Abstract

This paper contributes to the literature by analyzing the dynamic relationship between equity options and the volatility of the underlying. We determine the sensitivity of equity option returns to changes in systematic and idiosyncratic volatility (SVOL and IVOL) of the underlying conditional on moneyness on the EU and US markets. Total volatility is split into two components by applying the Fama-French-Carhart model, resulting in an average SVOL of about 20 percent and an average IVOL of about 30 percent. Alternatively, we implement an exponential GARCH model that shows average IVOL estimates between 30 percent and 45 percent. We also examine the relationship between expected option rate of return and volatility with respect to elasticity and drift effect. The results show that for call (put) options, there is statistically significant evidence for a positive (negative) but decreasing (increasing) effect of moneyness on option rates of return. We contribute to the literature by disclosing the intriguing nature of the SVOL effect on option rates of return. For call options on the US market, SVOL shows a negative effect on at-the-money options; however, the slope increases with moneyness, so SVOL becomes positive for deep in-the-money options. On the EU market, SVOL shows a positive effect for out-of-the-money options with moneyness below 0.85 and a negative effect on at-the-money call options; however, the slope decreases with moneyness, so SVOL becomes more negative with higher moneyness. For put options, we observe the same pattern. Additionally, we analyze the risk premia over time, i.e., the relation between risk sensitivities and individual option rates of return. Our findings suggest a clearly positive SVOL premium and show mixed results for the IVOL premium, which becomes negative when the regression is applied to single options and positive when applied to portfolios.

JEL Classification: G13, G15, G31, G32

Keywords: option risk premia, option return factors, SVOL, IVOL

*Faculty of Economics and Management, Otto von Guericke University Magdeburg, Germany.

†Audit and Assurance Department, Deloitte, Germany.

‡Corresponding author, email anastasiia.zbandut@ovgu.de, phone +49 391 67 52302, mailing address Universitätsplatz 2, 39106, Magdeburg.

1 Introduction and literature review

A vast strand of scientific research has been devoted to analyzing option price dynamics. Since Black and Scholes (1973) and Merton (1973) (BSM from here), the validity of theoretically predicted prices and the sensitivity to its determinants, such as stock and strike prices or volatility of the underlying, has been extensively examined with empirically observed data. A major criticism of the BSM model is its assumption of constant volatility of the underlying. This issue was addressed by Heston (1993), who derived a closed-form solution for the price of European call options that incorporates stochastic volatility.

A far less extensive portion of the scientific literature is focused on analyzing option returns. Rubinstein (1984) is among the first to calculate the expected return of a European-style call option, assuming a log-normally distributed price of the underlying and that the market participants agree upon a constant interest rate. Coval and Shumway (2001) provide empirical evidence about the dynamics of index option returns by analyzing two separate forms of option risk. Firstly, they consider the leverage effect¹ embedded in option values, which, according to the BSM model, is reflected in option betas that, in turn, are commonly represented by option elasticities. Their analysis shows that call options, on average, earn higher returns than the respective underlying securities. Secondly, they consider the curvature effect, i.e., the nonlinearity of option pay-offs. In contrast to the BSM model, they provide robust evidence that options are not redundant assets and earn a risk premium net of the leverage effect. Moreover, the authors document that the cross-section of option returns is affected by moneyness and maturity levels. Broadie et al. (2009) empirically show that expected option returns are highly sensitive to stock volatility and that this relationship is concave and varies across different strike prices.

Recently, several papers developed a theoretical foundation of how volatility influences option returns.² Hu and Jacobs (2020) are among the first who, based on their empirical finding, argue that the source of the volatility of the underlying serves as a pricing factor in option returns. The authors argue that leverage embedded in option values is a function of moneyness, maturity, and volatility of the underlying and can be understood via the option's elasticity. This result is related to our work since options with high elasticity reflect greater leverage, which would be typical for low-volatility options where small changes in the underlying can lead to a proportionally larger change in the option's price. This characteristic is also present in out-of-the-money (OTM) options, whereas low elasticity is often the case for in-the-money (ITM) options. Hu and Jacobs (2020) analytically show in the BSM framework that the return vega³ is negative for call options and positive for put options, meaning the expected call (put) return is decreasing (increasing) with the underlying volatility. Their predictions are empirically supported by US market data for index and equity options over a sample period from January 1996 to July 2013. The authors alternatively consider the stochastic volatility model of Heston (1993), where the sign of the return vega cannot be derived analytically. However, numerical calculations for various parametrizations still show an inverse (direct) relation between call (put) option returns and volatility.

Chaudhury (2017) contributes to the work of Hu and Jacobs (2020) by deriving a general formula for return vegas. However, compared to their study, he considers both parts of the underlying volatility, i.e., systematic (SVOL) and idiosyncratic (IVOL) volatility. The author demonstrates that an increase in IVOL leads to lower call (higher put) option returns. At the same time, he argues that there exists a

¹Here, leverage refers to the fact that the option price usually changes more strongly in relative terms than the value of the underlying asset.

²In contrast, the literature related to the risk-return trade-off on the stock market is rather extensive. Ang et al. (2006) and Dennis et al. (2006) are just two examples of studies examining the relationship between changes in volatility and the cross-section of stock returns. Both works decompose volatility into its two components, find robust evidence for a negative effect of systematic volatility, and show mixed results for the influence of idiosyncratic volatility.

³The return vega is the first derivative of the expected option rate of return with respect to the volatility of the underlying.

counteracting effect from changes in SVOL due to the drift effect.⁴ This finding is related to our work since the increase in systematic risk implies a greater probability of an option ending in the money, which increases the option price. Simultaneously, a higher systematic risk is associated with lower expected average returns of the underlying (lower drift rate), which serves as a counter effect. Thus, there is an indirect relationship between the drift rate and option elasticity. The expected price of the underlying, impacted by the drift, affects the moneyness of the option at expiration and simultaneously influences the sensitivity of the option price to changes in the price of the underlying, i.e., the option delta. For call options with a higher drift rate, options become more valuable, leading to a higher option delta. On the contrary, put options with a higher drift rate become less sensitive, which leads to a lower option delta. Chaudhury (2017) further elaborates on how the direction and magnitude of the net effect, resulting from those two opposing effects, depend on the underlying asset's beta, option moneyness, and maturity. For example, for call options with a time-to-maturity of more than one year, volatility above 30 percent, and a moneyness level above 106 percent, the return vega turns positive since the SVOL effect is strong enough to offset the negative IVOL effect.

Aretz et al. (2023), although they do not cite Chaudhury (2017), also focus on the components of underlying volatility, i.e., SVOL and IVOL, to measure the influence of volatility on option rates of return. The authors theoretically examine the relation between expected option returns and the underlying volatility by taking the partial derivative of the instantaneous expected excess return based on Cox and Rubinstein (1983) with respect to the underlying volatility.⁵ They confirm that there exist two effects, i.e., the elasticity effect and the drift effect. The source of underlying volatility influences these two effects differently; IVOL affects only option elasticity, while SVOL impacts both elasticity and drift. Moreover, the pay-off structure of options plays an important role which effect dominates. For ITM options, the drift effect dominates since an increase in SVOL decreases the drift rate, which, in turn, reduces the value of ITM options. The change in the expected return of the underlying due to SVOL has a greater impact than the change in elasticity caused by SVOL. For OTM options, the elasticity effect dominates since an increase in IVOL makes OTM options more valuable due to the greater probability of ending up in the money. Here, the impact of increased IVOL on option elasticity overcompensates the drift effect due to SVOL. However, the authors also note that the dominant effect may change; for example, as a call option turns less in the money, the elasticity effect becomes more pronounced. This implies that for options further out of the money, changes in elasticity due to volatility have a greater impact on expected option returns. They confirm their findings empirically with the help of double-sorted portfolios and regression analysis applied to single-stock American-style call option data from January 1996 to August 2014. When splitting total volatility into its two components, they conclude that higher IVOL reduces (raises) the expected return of call (put) options and that the effect of higher SVOL can be positive or negative for both call and put options. In addition, they find that the strike price influences the strengths of these two effects. Therefore, the existing empirical work regarding the sensitivity of equity option rates of return to changes in SVOL and IVOL shows that this relationship is nuanced and not always straightforward.

Our sample data consists of multiple data sets and contains the data for American-style options on the US and the EU markets. The sample period is between January 2011 and March 2021, with a sample size between 10 and 70 million single observations per data set. Our work complements previous studies with more recent, bigger-scaled samples and analysis conducted for both option markets and option types, i.e., call and put options. We further contribute to the existing literature by decomposing total volatility into its two components via the Fama-French-Carhart four-factor (FFC) model and via

⁴The drift effect refers to the tendency for stocks with greater volatility to be linked to higher expected prices, resulting in increased expected option returns.

⁵Kraft (2003) also showed that the relationship between the instantaneous expected rate of return of the derivative contract and its omega, i.e., elasticity, is linear. This also holds for the local volatility of the derivative contract.

an exponential GARCH (EGARCH) model.⁶ While the initial estimates (FFC model) of IVOL range from approximately 29 percent to 33 percent, the alternative estimation (EGARCH model) presents a slightly higher average, between 30 percent to 45 percent.

In our main regressions, we follow the Fama-MacBeth (FM) method so that the cross-sectional and time-series dimensions of the returns are considered separately. We integrate the discussion by Campbell et al. (1997) on an inverted FM approach into our analysis.⁷ In the original FM method, the first step involves the time-series regressions to estimate beta sensitivities and the second step performs the cross-sectional regression to estimate risk premia. However, in the Campbell et al. (1997) discussion, for pre-determined beta sensitivities, the FM approach is inverted and starts with cross-sectional regressions and then includes these findings in time-series regressions. This inverted two-step approach allows us to capture both the cross-sectional and time-series dimensions of the data more effectively. Furthermore, it helps to estimate and draw inferences about the risk premia of the factors, which may not be constant over time. We modify the standard regression to account for varying moneyness levels, nonlinearities, and liquidity controls. After estimating SVOL and IVOL for every underlying stock using the FFC model (and the EGARCH model in our robustness test), we run cross-sectional regressions of option rates of return on SVOL, IVOL, and moneyness (M) for each point in time (first step).

Subsequently (second step), we run time series regressions of option rates of return on risk premia, i.e., the coefficients found in the first step. Therefore, the first step determines each option's exposure to risk components SVOL and IVOL, i.e., risk sensitivities, and the second step determines how much an investor can earn for this exposure. Our approach differs from Aretz et al. (2023), where the authors first group option rates of return based on moneyness and then regress them on SVOL, IVOL, and moneyness. Instead of grouping, we use interaction terms of SVOL and IVOL with moneyness to uncover the non-linear relationship between the risk components and different moneyness levels. This serves in understanding the joint effect of risk and moneyness and their interaction with each other to influence the option return. With respect to IVOL and at-the-money (ATM) options, the first step results presented in the section 3.3 are in accordance with previous findings where IVOL betas are negative for call options⁸ and positive for put options in both the US and the EU markets. The influence of moneyness levels is stronger compared to previous studies,⁹ as IVOL sensitivities for call options are more negative for ITM options and turn positive for OTM options with moneyness below 82 percent to 91 percent. Conversely, IVOL sensitivities for put options are more positive for OTM options and turn negative for ITM options with moneyness below 51 percent to 68 percent, respectively.

Our results clarify some contradictory findings in the literature and show, in the first step, that the sign of the SVOL sensitivity does not only depend on moneyness but also varies across the US and EU option markets. On the EU market, the negative effect of SVOL for ATM call options intensifies for ITM options and turns positive for OTM options with moneyness below 85 percent. However, on the US market, it behaves the opposite way, where it intensifies for OTM options and only turns positive for ITM options with moneyness above 130 percent. We document that put option sensitivities mirror the results for call options so that they are positive for ATM options, increasing (decreasing) with moneyness on the EU (US) market, turning negative for ITM (OTM) options with moneyness below 95 (above 116) percent. The results of the second step support the explanatory power of the first step's sensitivities. Our regressions show a positive SVOL premium and mixed results for the IVOL premium, which is negative when the regression is applied to single options and positive when applied to portfolios grouped by moneyness and IVOL. We conduct robustness tests of our empirical results with respect to liquidity controls and alternative volatility estimates (FFC versus EGARCH).

⁶See Nelson (1991) and Carhart (1997).

⁷See Campbell et al. (1997), pp. 215-217.

⁸See Aretz et al. (2023), p. 304.

⁹See Aretz et al. (2023), p. 309.

The rest of our paper is structured as follows: While section 2 revisits the economic theory behind option rates of return and their sensitivity to the volatility of the underlying, section 3 is devoted to the empirical analysis of our data set. We describe the call and put option samples from the EU and US market in section 3.1, section 3.2 explains the construction of the chosen econometric model, and section 3.3 evaluates the empirical results. Robustness tests follow in section 4 before the paper concludes in section 5.

2 Theory on expected option rates of return

Under the premises of the BSM model, Hu and Jacobs (2020) compute the expected call (put) C (P) option rate of return by considering the expected option pay-off under the physical probability:¹⁰

$$\begin{aligned} E(R_C) &= \frac{E(C_T)}{C} = \frac{e^{\mu \cdot T} [S \cdot N(d_1^*) - K \cdot e^{-\mu \cdot T} \cdot N(d_2^*)]}{S \cdot N(d_1) - K \cdot e^{-r \cdot T} N(d_2)} \\ E(R_P) &= \frac{E(P_T)}{P} = \frac{e^{\mu \cdot T} [K \cdot e^{-\mu \cdot T} \cdot N(-d_2^*) - S \cdot N(-d_1^*)]}{K \cdot e^{-r \cdot T} \cdot N(-d_2) - S \cdot N(-d_1)} \end{aligned} \quad (2.1)$$

where the underlying stock price S follows a geometric Brownian motion with drift rate μ and constant volatility σ , K denotes the option strike price, T denotes the time-to-maturity, r is the risk-free rate and $N(\cdot)$ denotes the standard normal cumulative distribution function with $d_1 = \frac{\ln(\frac{S}{K}) + (r + \frac{1}{2} \cdot \sigma^2)T}{\sigma \cdot \sqrt{T}}$ and $d_2 = d_1 - \sigma \cdot \sqrt{T}$ and with $d_1^* = \frac{\ln(\frac{S}{K}) + (\mu + \frac{1}{2} \cdot \sigma^2)T}{\sigma \cdot \sqrt{T}}$ and $d_2^* = d_1^* - \sigma \cdot \sqrt{T}$, respectively. The sensitivity of the option rate of return to changes in the volatility of the underlying is represented as the return vega $\mathcal{V}^{\text{return}}$. Hu and Jacobs (2020) derive the return vega $\mathcal{V}^{\text{return}}$ where they only consider the idiosyncratic risk of the underlying as follows:¹¹

$$\begin{aligned} \mathcal{V}_C^{\text{return}} &= \frac{\partial E(R_C)}{\partial \sigma} = \frac{e^{\mu \cdot T} \cdot S \cdot \sqrt{T} \cdot EX}{[C]^2} < 0 \text{ with } EX = n(d_1^*) \cdot C - n(d_1) \cdot E(C_T) \cdot e^{-\mu \cdot T} < 0 \\ \mathcal{V}_P^{\text{return}} &= \frac{\partial E(R_P)}{\partial \sigma} = \frac{e^{\mu \cdot T} \cdot S \cdot \sqrt{T} \cdot B}{[P]^2} > 0 \text{ with } B = n(-d_1^*) \cdot P - n(-d_1) \cdot E(P_T) \cdot e^{-\mu \cdot T} > 0 \end{aligned} \quad (2.2)$$

where $n(\cdot)$ denotes the standard normal density function.

Chaudhury (2017) generalizes these results by considering the systematic and the idiosyncratic risk of the underlying. By defining the drift rate as $\mu = r + \lambda \cdot \sigma$ where λ is the (positive) systematic risk premium, he shows:

$$\begin{aligned} \mathcal{V}_C^{\text{return}} &= \frac{\partial E(R_C)}{\partial \sigma} = \frac{X_C \cdot e^{r \cdot T}}{[E^Q(C_T)]^2} \text{ with } X_C = \underbrace{e^{r \cdot T + \mu \cdot T} \cdot S \cdot \sqrt{T}}_{>0} \cdot \left[\underbrace{EX}_{<0} + \underbrace{C \cdot N(d_1^*) \cdot \lambda \cdot \sqrt{T}}_{>0} \right] \\ \mathcal{V}_P^{\text{return}} &= \frac{\partial E(R_P)}{\partial \sigma} = \frac{X_P \cdot e^{r \cdot T}}{[E^Q(P_T)]^2} \text{ with } X_P = \underbrace{e^{r \cdot T + \mu \cdot T} \cdot S \cdot \sqrt{T}}_{>0} \cdot \left[\underbrace{B}_{>0} - \underbrace{P \cdot N(-d_1^*) \cdot \lambda \cdot \sqrt{T}}_{>0} \right] \end{aligned} \quad (2.3)$$

where $E^Q(C_T) = C \cdot e^{r \cdot T}$ and $E^Q(P_T) = P \cdot e^{r \cdot T}$. The signs of X_C and X_P determine the signs of $\mathcal{V}_C^{\text{return}}$ and $\mathcal{V}_P^{\text{return}}$, respectively.¹² The author relates the terms X_C and X_P to the terms EX and B from Hu and Jacobs (2020), for which the signs are known. Hence, the signs of X_C and X_P depend on the relative size of the terms $C \cdot N(d_1^*) \cdot \lambda \cdot \sqrt{T}$ and $P \cdot N(-d_1^*) \cdot \lambda \cdot \sqrt{T}$, which describe the varying drift effect. Only if the drift effect is small, i.e., $|EX| > C \cdot N(d_1^*) \cdot \lambda \cdot \sqrt{T}$ and $|B| > P \cdot N(-d_1^*) \cdot \lambda \cdot \sqrt{T}$, $\mathcal{V}_C^{\text{return}}$ and $\mathcal{V}_P^{\text{return}}$ keep their respective negative and positive sign as in equation 2.2. This suggests that the

¹⁰See Hu and Jacobs (2020), p. 1029.

¹¹See Hu and Jacobs (2020), p. 1030.

¹²See Chaudhury (2017), pp. 1-2.

volatility component determines the effect on option rates of return as discussed in section 1.¹³

Aretz et al. (2023) emphasize the ambiguous nature of the option return vega. They assume a two-period, continuous-pay-off stochastic discount factor model with a log-normally distributed future pay-off of the underlying and of the future realization of the stochastic discount factor. By deriving the return vega in this framework, the authors show that the expected return of a European call option unambiguously increases with the strike price and decreases with the drift rate and IVOL. However, the sign of the return vega can only be determined for certain moneyness levels. It is positive for ATM and ITM call options but remains unclear for OTM options. The authors explain this result by the elasticity effect and the drift effect. They show that the elasticity effect is always negative for changes in SVOL and IVOL. The drift effect influences expected option rates of return via the expected rate of return of the underlying. Whether the effect is positive or negative depends on the derivative sign of the underlying asset's expected rate of return with respect to the corresponding volatility component. It is positive for SVOL; however, it is nearly zero for IVOL. Hence, the total effect, i.e., the sum of elasticity effect and drift effect, is negative for IVOL and depends on the trade-off between the two oppositely-signed effects for SVOL as discussed in section 1.¹⁴

3 Empirical analysis

3.1 Data

Option data is obtained from IVolatility.com. The sample period is from January 2011 to March 2021. Data for the Fama-French factors and the risk-free rate of return are obtained from Kenneth French's website for the corresponding time period. Each individual option in the data set is uniquely identified by the company name of the underlying stock, its strike price and its expiration date. Time-to-maturity, calculated in business days, is the difference between expiration and observation date. The closing stock price of the underlying S is used to compute the daily stock return as $r_t = \frac{S_t}{S_{t-1}} - 1$, which is used in the FFC approach to estimate SVOL and IVOL. To increase data quality, we apply the following filters: (i) only options with positive bid and ask prices, as well as positive trading volume and open interest, are kept in the sample; (ii) only options are considered that have not reached their expiration date yet; (iii) options that have a higher bid price than the ask price are removed from our analysis. Additionally, we leave out observations that lead to low sample sizes for a regression (less than 30 observations per single regression). Our data set contains data for American-style call and put options on the EU and the US market separately.

The option rate of return $R_{i,t}$ for option i at time t is calculated as follows:

$$R_{i,t} = \frac{P_{i,t}}{P_{i,t-1}} - 1 \quad (3.1)$$

where the option price $P_{i,t}$ is the average of bid and ask prices. Moneyness M is defined as the ratio of the underlying stock's closing price S and the option's strike price K at the starting point of the corresponding time series. For moneyness levels $1.025 \geq M \geq 0.975$, we refer to ATM options, call options with $M > 1.025$ represent ITM options, and with $M < 0.975$, they represent OTM options. The opposite holds for put options.

Descriptive statistics for the analyzed samples are depicted in table 3.1. In accordance with previous studies, the mean daily returns of call options are positive, although their lower quartiles are negative. When converted to monthly returns, our samples show values at the level of 15.8 percent to 18.2 percent and are, thereby, at a comparable level to those found by Hu and Jacobs (2020) and Aretz et al. (2023)

¹³See Chaudhury (2017), p. 4.

¹⁴See Aretz et al. (2023), p. 2.

Table 3.1: Descriptive statistics of option samples

	Daily Return	Moneyiness	Maturity	Volume	Open Interest
Call options - EU market ($n = 9,891,360$)					
Mean	0.0069	1.6617	125	115	2504
Std Deviation	0.2375	6.3953	182	729	7985
25 %-Quartile	-0.0858	0.8867	26	4	69
50 %-Quartile	-0.0044	0.9676	64	15	328
75 %-Quartile	0.0668	1.0415	159	50	1689
Put options - EU market ($n = 10,842,793$)					
Mean	-0.0010	1.3064	117	110	2631
Std Deviation	0.2171	3.0266	166	762	7834
25 %-Quartile	-0.0791	0.9456	25	4	67
50 %-Quartile	-0.0087	1.0316	60	12	322
75 %-Quartile	0.0506	1.1347	149	50	1761
Call options - US market ($n = 70,843,968$)					
Mean	0.0080	1.1226	85	144	1792
Std Deviation	0.2965	8.8411	114	181	9151
25 %-Quartile	-0.1080	0.8870	14	3	60
50 %-Quartile	-0.0054	0.9723	36	12	251
75 %-Quartile	0.0801	1.0422	109	51	1039
Put options - US market ($n = 55,239,132$)					
Mean	-0.0105	1.1637	75	107	1558
Std Deviation	0.3034	4.5291	105	831	7188
25 %-Quartile	-0.1264	0.9782	13	3	55
50 %-Quartile	-0.0203	1.0415	30	11	219
75 %-Quartile	0.0580	1.1470	95	44	910

This table reports descriptive statistics for all sub samples with their sample size n . Daily return is defined by equation 3.1, moneyiness is the ratio S/κ , maturity is the time-to-maturity in business days, volume is the daily trading volume as the number of options traded, and open interest as the number of currently active options, i.e., traded but not yet closed by an offsetting trade or an exercise.

with 11.1 percent and 14.6 percent, respectively. The mean daily returns of put options in our sample are negative. Both call and put option samples show average moneyiness levels of above 1.025, corresponding to ITM call and OTM put options. Further, the samples cover a wide range of different options with respect to maturities, trading volume, and open interest.

On average, data for the EU market shows longer time-to-maturities, slightly lower trading volumes and higher open interest than the larger sample for the US market. With 71 million observations for call options and 55 million observations for put options, the US samples size is five to seven times higher than the EU samples with 10 million call and 11 million put observations.

3.2 Model construction

As a preparatory work in our analysis, we apply the FFC approach in time series analyses of daily stock returns r to estimate $SVOL_i$ and $IVOL_i$ for each option's underlying i :

$$r_{i,t} = \alpha_i^{FFC} + \beta_i^{mkt} \cdot (r_{mkt,t} - r_{f,t}) + \beta_i^{smb} \cdot r_{smb,t} + \beta_i^{hml} \cdot r_{hml,t} + \beta_i^{mom} \cdot r_{mom,t} + \varepsilon_{i,t} \quad (3.2)$$

where $r_{mkt,t} - r_{f,t}$ denotes the market excess return, $r_{smb,t}$ is the size factor, $r_{hml,t}$ is the value factor and $r_{mom,t}$ is the monthly momentum factor. We use the factor returns for the US and EU markets, respectively. In accordance with Aretz et al. (2023), we estimate $IVOL_i$ as the annualized standard deviation of the residuals $\varepsilon_{i,t}$ and $SVOL_i$ as the annualized standard deviation of the fitted values $r_{i,t} - \varepsilon_{i,t}$.

Alternatively, we estimate $IVOL_i$ by implementing the EGARCH model to capture the time-varying nature of volatility. Here, $IVOL_i$ equals the one-period-ahead predicted idiosyncratic volatility based on:

$$\begin{aligned} \varepsilon_{i,t} &\sim \mathcal{N}(0, \sigma_{i,t}^2) \\ \ln \sigma_{i,t}^2 &= \alpha_i^{EGARCH} + \sum_{l=1}^p b_{i,l} \cdot \ln \sigma_{i,t-l}^2 + \sum_{k=1}^q c_{i,k} \cdot \left(\theta_i \cdot \frac{\varepsilon_{i,t-k}}{\sigma_{i,t-k}} + \gamma_i \cdot \left(\left| \frac{\varepsilon_{i,t-k}}{\sigma_{i,t-k}} \right| - \sqrt{2/\pi} \right) \right) \end{aligned} \quad (3.3)$$

To account for differences among the underlying stocks, an individual EGARCH model is estimated for nine combinations of the parameters p and q in equation 3.3, whereby p and q can each take the values 1, 2 or 3. Subsequently, the (p, q) -combination with the lowest Akaike Information Criteria (AIC) is selected to estimate the expected IVOL of each individual stock i . This approach is popular in the literature related to stock return analyses.¹⁵

Our goal is to examine the explanatory power of option risk sensitivities. For this, we apply the inverted FM procedure. As the first step of this procedure, we analyze the sensitivity of option rates of return R with respect to SVOL and IVOL, accounting for moneyness M . Here, we employ the following cross-sectional regressions for each t :¹⁶

$$R_{j,i,t} = \alpha_t^{CS} + \beta_t^{SVOL} \cdot SVOL_i + \beta_t^{IVOL} \cdot IVOL_i + \beta_t^M \cdot M_{j,i,t} + \eta_{j,i,t} \quad (3.4)$$

where $R_{j,i,t}$ is the rate of return of option j written on the underlying stock i at point in time t and $\eta_{j,i,t}$ is the corresponding residual. The idea is to identify the time effect of risk sensitivities on option rates of return. Both SVOL and IVOL measure individual risks of the underlying. However, when estimated in a time-series analysis, they are constant over time. Therefore, we estimate time varying option risk sensitivities with respect to SVOL and IVOL in a cross-sectional analysis. To control for nonlinearities, we expand this regression by adding interaction and squared terms to the right-hand side of equation 3.4. This also helps to capture a wide range of market conditions and option characteristics, and allows for a more detailed analysis of how options conditional on moneyness behave under varying market conditions. Thus, the regressions are carried out in three configurations, which represent the base configurations in our analysis:

(i) *pure*, as shown in equation 3.4

(ii) *interacted*, by adding regressors $SVOL_i \cdot M_{j,i,t}$ and $IVOL_i \cdot M_{j,i,t}$

$$R_{j,i,t} = \alpha_t^{CS} + \beta_t^{SVOL} \cdot SVOL_i + \beta_t^{IVOL} \cdot IVOL_i + \beta_t^M \cdot M_{j,i,t} + \beta_t^{M \cdot SVOL} \cdot M_{j,i,t} \cdot SVOL_i + \beta_t^{M \cdot IVOL} \cdot M_{j,i,t} \cdot IVOL_i + \eta_{j,i,t} \quad (3.5)$$

(iii) *squared*, by further adding the regressors $SVOL_i \cdot M_{j,i,t}^2$, $IVOL_i \cdot M_{j,i,t}^2$ and $M_{j,i,t}^2$

$$R_{j,i,t} = \alpha_t^{CS} + \beta_t^{SVOL} \cdot SVOL_i + \beta_t^{IVOL} \cdot IVOL_i + \beta_t^M \cdot M_{j,i,t} + \beta_t^{M \cdot SVOL} \cdot M_{j,i,t} \cdot SVOL_i + \beta_t^{M \cdot IVOL} \cdot M_{j,i,t} \cdot IVOL_i + \beta_t^{M^2} \cdot M_{j,i,t}^2 + \beta_t^{M^2 \cdot SVOL} \cdot M_{j,i,t}^2 \cdot SVOL_i + \beta_t^{M^2 \cdot IVOL} \cdot M_{j,i,t}^2 \cdot IVOL_i + \eta_{j,i,t} \quad (3.6)$$

We mitigate possible heteroscedasticity and autocorrelation in the error terms of our regression model by applying the Newey-West adjusted standard errors method. In their work, Hu and Jacobs (2020) also used this method to account for autocorrelation and heteroscedasticity. We employ the Jarque-Bera test statistic to assess whether our regression residuals conform to a normal distribution. The null hypothesis could not be rejected. Therefore, the time-series average over all t provides feasible estimates of the beta coefficients.

The second step in our analysis is to determine the explanatory power of risk sensitivities from equation 3.4. For this, we run time-series regressions for each individual option j . In the pure configuration,

¹⁵See, e.g., Fu (2009), Guo et al. (2014) and Bergbrant and Kassa (2021).

¹⁶The regressors in equations 3.2 and 3.4 differ (stock rates of returns versus option rates of return). Our samples contain observations for about 2600 days (for the EU and US markets T is equal to 2621 and 2571 days, respectively). This amounts to around 2600 cross-sectional regressions. Examples for the application of the FM regressions in the analysis of stock returns can be found, e.g., in Ang et al. (2009), Malagon et al. (2015) and Bergbrant and Kassa (2021).

these regressions read as follows (analog equations are applied to interacted and squared configurations):

$$R_{j,t} = \omega_j^{TS} + \gamma_j^{SVOL} \cdot \hat{\beta}_t^{SVOL} + \gamma_j^{IVOL} \cdot \hat{\beta}_t^{IVOL} + \gamma_j^M \cdot \hat{\beta}_t^M + \zeta_{j,t} \quad (3.7)$$

where the first step coefficients $\hat{\beta}$ reflect the influence of SVOL, IVOL and M on option rates of return at a particular point in time t . The second step coefficients $\hat{\gamma}$ from equation 3.7 explain the relation between risk sensitivities and individual option rates of return over time and are interpreted as risk premia. A drawback of the FM method is known as the errors-in-variables bias. We account for this bias by applying equation 3.7 to portfolios rather than single assets. For this, the data is sorted into five moneyness groups and ten IVOL groups so that there are up to 50 possible portfolios. The portfolios are equally weighted, which ensures that the analysis is not overly influenced by any single option. The results of portfolio formation are described in table 3.2. All four samples contain a wide range of moneyness and volatility levels. The US data fills all 50 portfolios, and the EU data not less than 45 portfolios, with only the third highest volatility bin being empty. This indicates a robust dataset, enhancing the validity and applicability of our study's conclusions. A much higher number of observations is centered in the OTM bins rather than in the ITM ones.

Table 3.2: Descriptive statistics of option portfolios

		EU market		US market	
		Call options	Put options	Call options	Put options
Total Observations		9,891,360	10,842,793	70,843,968	55,239,132
Number of Portfolios		45	45	50	50
Average Observations per Portfolio		219,808	240,951	1,416,879	1,104,783
Moneyness Bins (number of observations)	$M < 0.9$	2,769,313	1,989,210	19,582,866	6,483,475
	$M < 0.975$	2,471,841	1,393,700	16,596,931	6,795,082
	ATM	1,799,567	1,781,746	13,807,712	10,797,467
	$M > 1.025$	1,213,009	2,280,453	9,524,748	12,705,452
	$M > 1.1$	1,637,630	3,397,684	11,331,711	18,457,656
IVOL Bins	Lower Bound	0.0736	0.0860	0.0450	0.0915
	Upper Bound	0.8876	0.9195	0.9972	0.9936
	Bin Size	0.0814	0.0834	0.0952	0.0902

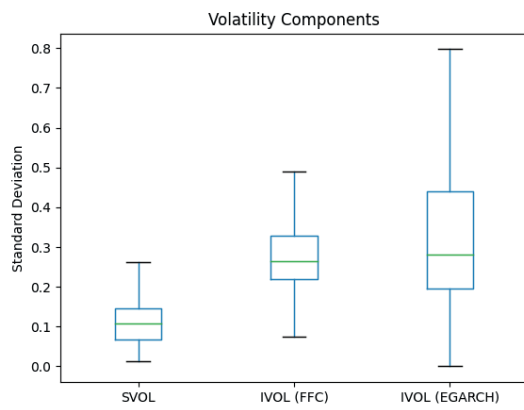
The table reports descriptive statistics for portfolios created by sorting the option data into five moneyness and ten IVOL bins. The boundaries for the moneyness bins are chosen around one ATM group with $0.975 < M < 1.025$ and for the IVOL bins by dividing the range of the minimum and maximum values (lower bound and upper bound) into ten equally spaced intervals.

3.3 Empirical results

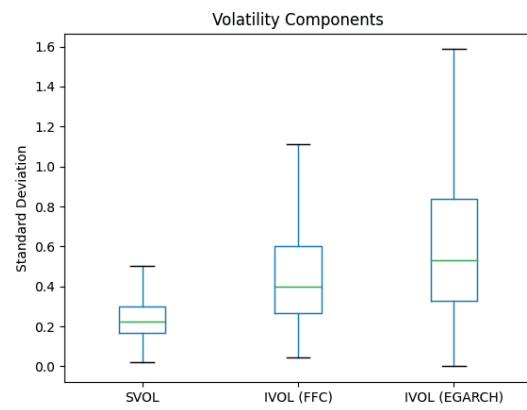
Figure 3.1 visualizes the estimated volatility components SVOL and IVOL according to equation 3.2 (FFC) and the alternative estimation of expected IVOL according to equation 3.3 (EGARCH). Based on equation 3.2 for the EU market, our samples show an annualized mean SVOL of around 15 percent and an annualized mean IVOL of around 29 percent. For the US market, the estimates are slightly higher with 23 percent and 33 percent, respectively. Generally, the boxplots for the US market show a higher dispersion than those for the EU market. Our results for call options on the US market are in line with Aretz et al. (2023). Their mean estimates for SVOL of around 32 percent and for IVOL of around 43 percent are somewhat higher but also more dispersed with standard deviations of 21 percent and 26 percent, respectively. Based on equation 3.3, the estimates for expected IVOL show a mean value of around 30 percent for the EU market and 45 percent for the US market. Thus, the EGARCH model gives higher estimates with a higher degree of dispersion.

The results for the first step in our analysis, where we estimate the sensitivity of option rates of return with respect to SVOL and IVOL, can be found in table 3.3. The reported coefficients represent the average of 2,600 estimates of β_t , and the corresponding t -statistics is computed as the ratio of this average and its standard error. The various regression configurations show adjusted coefficients of determination

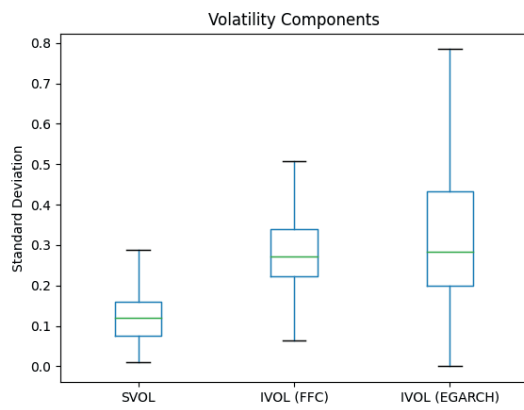
Figure 3.1: Volatility components estimates.



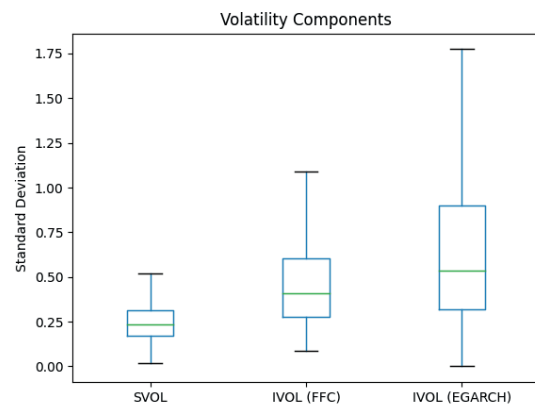
(a) Call options - EU market



(b) Call options - US market



(c) Put options - EU market



(d) Put options - US market

Table 3.3: Cross-sectional regressions - First step

Configuration	Call options - EU market			Call options - US market		
	pure	interacted	squared	pure	interacted	squared
Intercept	0.0031 (0.0025)	-0.0673*** (0.0044)	-0.1509*** (0.0255)	0.0058*** (0.0060)	-0.0155*** (0.0105)	-0.0414*** (0.0151)
<i>SVOL</i>	-0.0246** (0.0133)	0.1692*** (0.0227)	0.2223* (0.1672)	-0.0140* (0.0282)	-0.0454*** (0.0427)	-0.0673*** (0.0592)
<i>IVOL</i>	-0.0109* (0.0067)	0.0489*** (0.0153)	0.1232 (0.1289)	-0.0057 (0.0133)	0.0423*** (0.0186)	0.0795*** (0.0248)
<i>M</i>	0.0083*** (0.0008)	0.0801*** (0.0040)	0.1895*** (0.0526)	0.0032*** (0.0009)	0.0248*** (0.0082)	0.0546*** (0.0144)
<i>M</i> · <i>SVOL</i>		-0.1985*** (0.0184)	-0.2199 (0.3285)		0.0314*** (0.0269)	0.0590*** (0.0514)
<i>M</i> · <i>IVOL</i>		-0.0593*** (0.0152)	-0.1548 (0.2602)		-0.0481*** (0.0110)	-0.0926*** (0.0200)
<i>M</i> ²			-0.0231 (0.0268)			-0.0031*** (0.0011)
<i>M</i> ² · <i>SVOL</i>			-0.0426 (0.1616)			-0.0061*** (0.0045)
<i>M</i> ² · <i>IVOL</i>			0.0219 (0.1301)			-0.0061*** (0.0016)
<i>adjR</i> ²	0.0308	0.0351	0.0414	0.0224	0.0240	0.0261
Configuration	Put options - EU market			Put options - US market		
	pure	interacted	squared	pure	interacted	squared
Intercept	-0.0121*** (0.0025)	0.0538*** (0.0046)	0.1504*** (0.0087)	-0.0198*** (0.0028)	0.0020 (0.0038)	0.0204*** (0.0045)
<i>SVOL</i>	0.0114 (0.0111)	-0.1502*** (0.0157)	-0.4265*** (0.0686)	0.0019 (0.0091)	0.0342*** (0.0106)	0.0809*** (0.0127)
<i>IVOL</i>	0.0383*** (0.0063)	-0.0293*** (0.0103)	-0.0732** (0.0334)	0.0275*** (0.0049)	-0.0227*** (0.0068)	-0.0537*** (0.0077)
<i>M</i>	-0.0072*** (0.0006)	-0.0685*** (0.0028)	-0.2229*** (0.0153)	-0.0033*** (0.0002)	-0.0235*** (0.0014)	-0.0491*** (0.0025)
<i>M</i> · <i>SVOL</i>		0.1580*** (0.0122)	0.6240*** (0.1290)		-0.0279*** (0.0027)	-0.0790*** (0.0063)
<i>M</i> · <i>IVOL</i>		0.0572*** (0.0066)	0.1333* (0.0689)		0.0446*** (0.0026)	0.0893*** (0.0044)
<i>M</i> ²			0.0588*** (0.0072)			0.0073*** (0.0005)
<i>M</i> ² · <i>SVOL</i>			-0.1854*** (0.0595)			0.0083*** (0.0006)
<i>M</i> ² · <i>IVOL</i>			-0.0360 (0.0354)			-0.0137*** (0.0009)
<i>adjR</i> ²	0.0289	0.0337	0.0408	0.0222	0.0245	0.0268

The table reports results for the first step in our analysis (equation 3.4). Volatility components are estimated with the FFC model. The top panel refers to call options on the EU and US market. The bottom panel shows the results for put options. Standard errors are reported in parentheses. Statistical significance at the 1 percent, 5 percent, 10 percent levels are denoted by ***, **, *, respectively.

of 2.9 percent to 4.1 percent for the EU data and 2.2 percent to 2.7 percent for the US data. The pure configuration explains a consistently lower proportion of the variation in option rates of return than the squared configuration. When examining different configurations, we note the contrasting behavior of the linear coefficients for SVOL and IVOL in the pure versus the interacted and squared configurations.

According to the top panel of table 3.3 (results for call options), the linear coefficients for SVOL and IVOL (β^{SVOL} and β^{IVOL} , respectively) in the pure configuration are negative for both markets, significant (except for the IVOL coefficient for the US market) and higher for the EU market. For the interacted and squared configurations, the linear coefficients for SVOL and IVOL are positive (except for the SVOL coefficient for the US market) and significant (except for the IVOL coefficient in the squared configuration for the EU market). This result suggests that the relationship between these volatility measures and option rates of return depends on other factors, i.e., moneyness, which aligns with the theoretical proof by Aretz et al. (2023).

As an extension to previous studies, our approach confirms that this relationship is not linear and depends on the factor's form, i.e., linear versus squared. In interaction with moneyness M , $\beta^{M \cdot SVOL}$ is significantly negative for the EU market and significantly positive for the US market; $\beta^{M \cdot IVOL}$ is negative and highly significant for both markets. In nonlinear interaction with moneyness M^2 , $\beta^{M^2 \cdot SVOL}$ is negative for both markets, however, only significant for the US market; $\beta^{M^2 \cdot IVOL}$ is positive for the EU market and negative for the US market, being again only significant for the US market. Hence, an increase in SVOL leads to a decrease in call option rates of return at a decreasing scale, which is conditional on moneyness. The same holds for the IVOL effect. We note that the influence of SVOL on option rates of return is different between the EU and the US markets. For the EU market, the linear influence is positive, turns negative with interaction with moneyness, and becomes less negative for deep ITM options. However, it is only significant in its linear term. In contrast, for the US market, SVOL negatively influences call option rates of return at a decreasing scale (only $\beta^{M \cdot SVOL}$ is positive), and all coefficients are highly significant. The different influence of SVOL on option rates of return on the EU and on the US markets indicates that the drift effect on those markets varies. Additionally, the Kenneth R. French data library uses a region's value-weighted market portfolio in the estimation of the market return. For the US market, the library uses all CRSP companies incorporated in the US and listed on the NYSE, AMEX, or NASDAQ. For the EU market, it uses all companies listed on the corresponding developed European countries' indices¹⁷. The US market portfolio includes companies in the technological sector with high market capitalization, which leads to higher SVOL due to their sensitivity to broader changes in the market environment. While the EU market portfolio includes companies from different countries, sectors and even currencies, which leads to lower and more diversified SVOL.

The linear coefficients for moneyness M are positive and highly significant. They are lower for the US market and highest for the squared configuration. This result suggests that the deeper in the money a call option is, the higher is its rate of return. We note that this effect is less pronounced in the US than in the EU market, which could be attributed to the aforementioned differences between the two markets. The nonlinear influence of moneyness M^2 is negative for both markets, higher for the EU market and significant only for the US market. Therefore, an increase in moneyness leads to an increase in call option rates of return, but on a decreasing scale, so the effect becomes weaker for ITM call options. The literature did not analyze the relationship between different forms of moneyness (adding interaction and squared terms) and option rates of return before.

The bottom panel of table 3.3 shows corresponding findings for put options. Here, the linear coefficients for SVOL and IVOL in the pure configuration are positive for both markets, where only the IVOL coefficients are significant. The results show an intriguing flip-flop pattern in the SVOL coefficients.

¹⁷Countries included are Austria, Belgium, Switzerland, Germany, Denmark, Spain, Finland, France, Great Britain, Greece, Ireland, Italy, Netherlands, Norway, Portugal, Sweden.

Again, the influence on put option rates of return is different for the EU and US markets. For the US market, the linear SVOL coefficient remains positive in both interacted and squared configurations; however, it turns negative in interaction with moneyness M and then again changes to positive in the nonlinear interaction with moneyness M^2 . For the EU market, this relation is mirrored, so the linear SVOL coefficient is negative, becomes positive in interaction with moneyness M , and changes to negative in nonlinear interaction with moneyness M^2 . All coefficients are highly significant. The linear IVOL coefficients are positive in the pure configuration but become negative in both interacted and squared configurations for both markets. In interaction with moneyness M , the coefficient $\beta^{M \cdot IVOL}$ is positive and highly significant for both markets in both interacted and squared configurations; however, it turns negative in the nonlinear interaction with moneyness M^2 for both markets, but remains significant only for the US market. For put options, linear moneyness coefficients are negative and highly significant, in absolute terms, lower for the US market and the highest for the squared configuration. There is a positive and significant nonlinear influence of moneyness M^2 indicating that the decreasing effect on put option rates of return appears to be weaker for higher moneyness levels, i.e., OTM put options. Hence, IVOL shows a negative effect on rates of return for ATM put options which becomes more negative for higher moneyness levels and turns positive for sufficiently OTM options. This implies a diminishing sensitivity of put option rates of return to changes in moneyness as they become deeper OTM options.

We analyze volatility slopes to investigate the influence of SVOL and IVOL on option rates of return further. We define volatility slopes as the partial derivatives of R with respect to IVOL and SVOL, respectively, based on equation 3.6 (squared configuration):

$$\begin{aligned}\frac{\partial R}{\partial SVOL} &= \beta^{SVOL} + \beta^{M \cdot SVOL} \cdot M + \beta^{M^2 \cdot SVOL} \cdot M^2 \\ \frac{\partial R}{\partial IVOL} &= \beta^{IVOL} + \beta^{M \cdot IVOL} \cdot M + \beta^{M^2 \cdot IVOL} \cdot M^2\end{aligned}\tag{3.8}$$

Figure 3.2 (call options) and figure 3.3 (put options) visualize volatility slopes for our samples. The left-hand sides of figure 3.2 depict systematic volatility slopes for the EU market (upper graph) and the US market (lower graph). The results show a distinct difference between the EU and the US markets. For the EU market, the systematic volatility slope shows a negative effect on ATM call option rates of return, which becomes more negative with higher moneyness and positive for OTM options with moneyness below 0.85. For the US market, the systematic volatility slope also shows a negative effect on ATM call option rates of return; however, the slope increases (for the EU market, the slope decreases) with moneyness. This result suggests that the US market is more sensitive to changes in underlying asset prices and their deviation from the strike price. In the depicted range, the slope is negative, but it becomes positive for ITM calls with $M > 1.3$ (not displayed in figure 3.2) since the interaction term $M \cdot SVOL$ is positive. Here, our findings confirm Aretz et al. (2023) corollary 1, particularly, a positive SVOL effect on OTM options for the EU market and both positive and negative SVOL effect on ITM options for the US market. We also confirm the changing SVOL effect with regard to moneyness levels, which indicates the changing dominance between the elasticity effect and the drift effect. However, previous studies neither theoretically nor empirically discovered a negative SVOL effect on ATM options. In addition, the range of the systematic volatility slope is smaller for the US market than for the EU market. The right-hand side graphs of figure 3.2 depict idiosyncratic volatility slopes. For both markets, the slope is mostly negative, decreasing with moneyness, and positive only for OTM options, where signs switch at moneyness levels between 0.82 (interacted configuration) and 0.91 (squared configuration). This finding is in line with Aretz et al. (2023). The idiosyncratic volatility slopes, which are mostly negative in both markets, reflect that individual company risk affects options rates of return similarly in these markets. It also confirms the dominance of the elasticity effect for OTM options.

Figure 3.2: Volatility Slopes Conditional on Moneyness (call options).

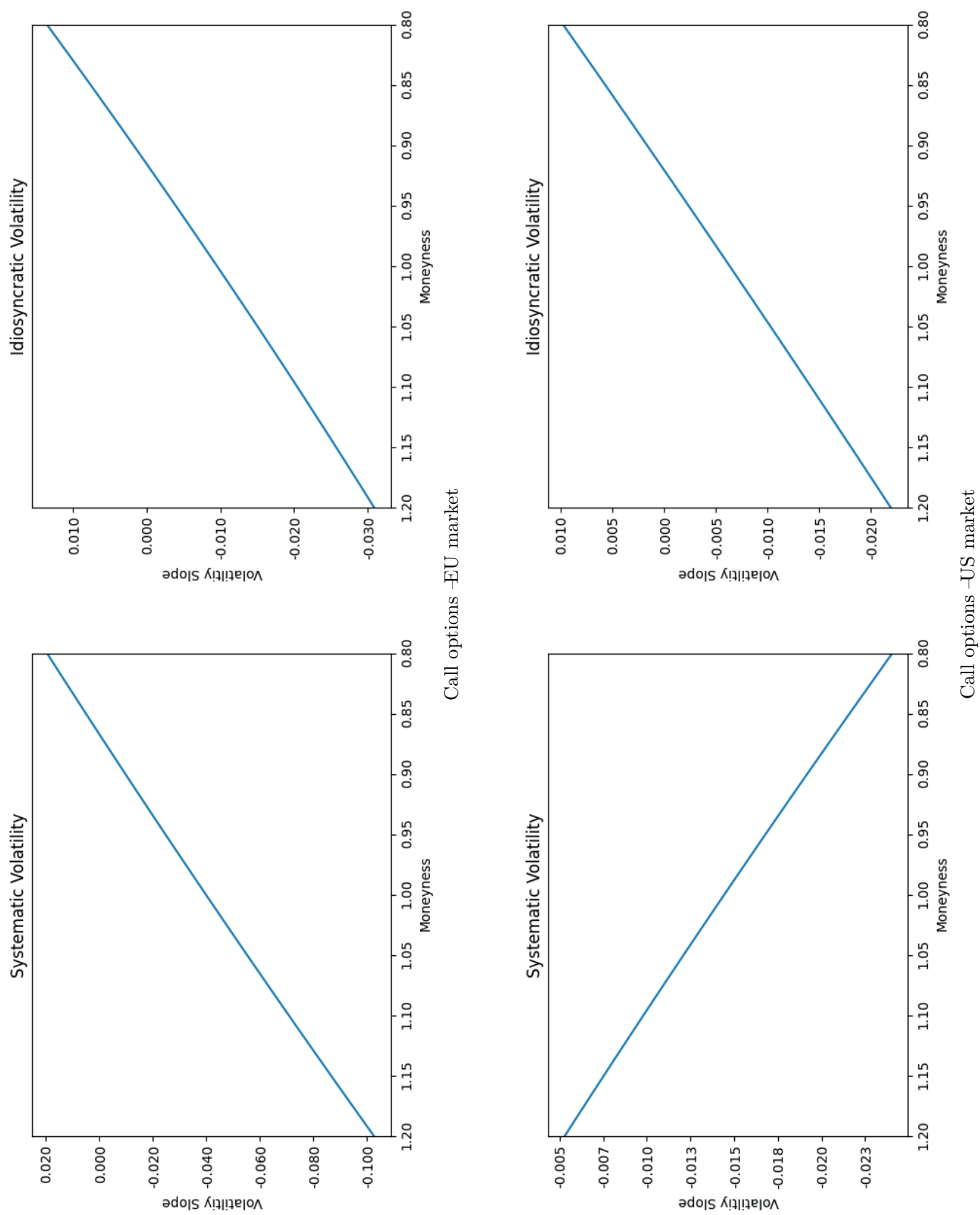


Figure 3.3: Volatility Slopes Conditional on Moneyness (put options).

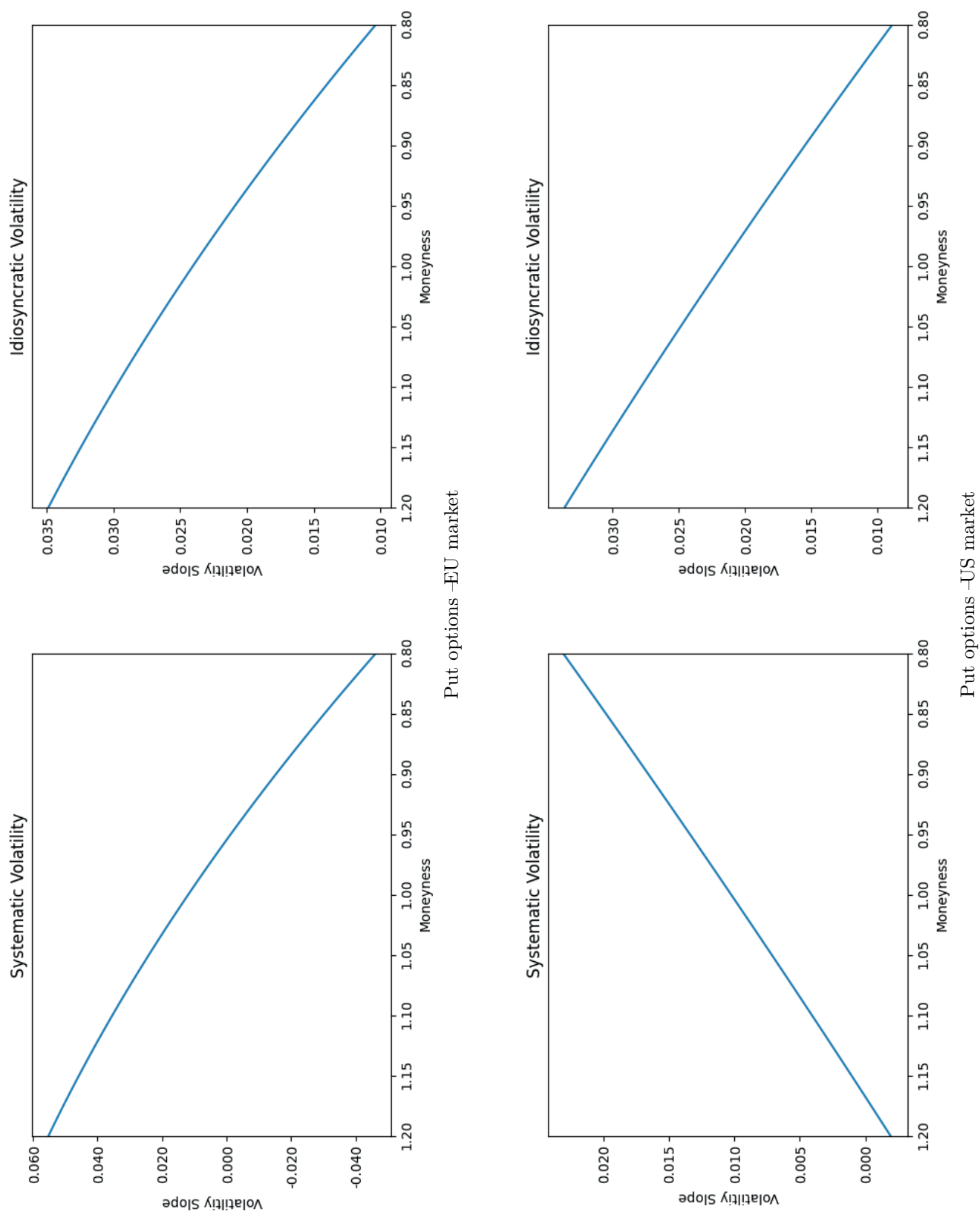


Figure 3.3 displays the corresponding results for put options. In summary, they mirror the call option results but with opposite signs. Again, the influence of moneyness shows different directions of the systematic volatility slope for the EU and the US markets. For the EU market (upper left-hand side graph of figure 3.3), the systematic volatility slope is positive for OTM and ATM put options. It increases with moneyness (positive interaction term $M \cdot \text{SVOL}$) and turns negative for ITM put options with moneyness below 0.95. The latter indicates that the elasticity effect overshadows the drift effect and highlights the argumentation of Chaudhury (2017) regarding the reverse relationship, which depends on the most dominant effect. However, for the US market (lower left-hand side graph of figure 3.3), the systematic volatility slope shows a different pattern; it decreases with moneyness (negative interaction term $M \cdot \text{SVOL}$) and becomes negative for OTM options with moneyness above 1.2. This finding contradicts Hu and Jacobs (2020) reasoning. However, it highlights the dominance of the drift effect over the elasticity effect. This also indicates a significant divergence in the influence of moneyness on systematic volatility and differences in downside risk perception (since put options provide a hedge against downside risk) between the two markets. The right-hand side graphs of figure 3.3 show the corresponding idiosyncratic volatility slopes for the EU and the US market. Both slopes are positive for ATM put options and increase with moneyness. From table 3.3, the interacted and squared configurations show negative coefficients for IVOL, positive in interaction with moneyness M and negative again in interaction with nonlinear moneyness M^2 . Hence, the positive influence of IVOL on put option rates of return becomes more positive with increasing moneyness but at a decreasing scale. It turns negative only for ITM put options with M below 0.51 (interacted configuration) and 0.68 (squared configuration), respectively (not displayed in figure 3.3). Here, we confirm the pronounced elasticity effect in put options. The range of idiosyncratic volatility slopes for put options is larger than for call options.

At this point, we contrast our results to the findings of previous studies. While Hu and Jacobs (2020) did not decompose volatility into SVOL and IVOL components, our findings regarding the negative betas for call options and the positive ones for put options in the pure configurations align with their broader findings on volatility influence. The volatility coefficient for call options in their sample amounts to -0.389 , compared to -0.446 in our sample. For put options, the volatility coefficients are even closer, with 0.590 and 0.584 , respectively. Our study extends their work by breaking down volatility components and focusing on daily instead of monthly returns. This leads to much larger datasets, which allow for a more detailed analysis to capture the dynamics of option rates of return and their relationship to the corresponding volatility components more accurately. Moreover, we consider a broader range of option types across both the EU and the US market. Our findings regarding SVOL and IVOL are also partially in line with the results of Aretz et al. (2023), at least for call options on the US market, as they do not consider put options in their analysis. Their coefficients for the interacted terms $M \cdot \text{SVOL}$ and $M \cdot \text{IVOL}$ are always positive, so that volatility slopes increase with moneyness. However, in our analysis, the $M \cdot \text{IVOL}$ coefficient is negative, leading to an idiosyncratic volatility slope that decreases with moneyness. In particular, Aretz et al. (2023) find a negative effect of SVOL on US call option rates of return for OTM and ATM options and a positive effect only for sufficiently ITM options. We observe the same negative effect of SVOL for ATM options and, at least for the US market, for OTM options. We find a positive effect for ITM options (with moneyness above 1.3) only for the US market, while there is no such evidence for the EU market. Related to the influence of IVOL on call option rates of return, we confirm their results regarding the negative effect for ATM and sufficiently ITM options. However, the positive effect for OTM call options in our sample is not observed by other authors. In summary, our findings partially corroborate previous research. We extend previous findings thereby enriching the understanding of the option rates of return dynamics, volatility, moneyness and their forms across different markets. Our results also highlight the difference in option rates of return dynamics between

the EU and the US market.

Table 3.4: Time-series regressions - Second step

Configuration	Call options - EU market			Call options - US market		
	pure	interacted	squared	pure	interacted	squared
Intercept	0.0054*** (0.0015)	0.0065*** (0.0022)	0.0017 (0.0028)	0.0098*** (0.0022)	0.0144*** (0.0023)	0.0201*** (0.0023)
β^{SVOL}	0.0590*** (0.0041)	0.0563*** (0.0043)	0.0558*** (0.0042)	0.0553*** (0.0058)	0.0540*** (0.0064)	0.0515*** (0.0068)
β^{IVOL}	-0.0407*** (0.0084)	-0.0414*** (0.0079)	-0.0432*** (0.0075)	-0.1294*** (0.0123)	-0.1389*** (0.0149)	-0.1366*** (0.0124)
β^M	0.0798 (0.0591)	-0.0258 (0.0712)	0.0537* (0.0323)	-1.5982*** (0.5855)	-3.3075*** (0.4276)	-2.8500*** (0.2935)
$\beta^{M \cdot SVOL}$		0.0473*** (0.0173)	0.0636*** (0.0081)		-0.7407*** (0.1168)	-0.6303*** (0.0784)
$\beta^{M \cdot IVOL}$		-0.0416* (0.0253)	-0.0223 (0.0149)		-2.1608*** (0.2830)	-1.8152*** (0.1920)
β^{M^2}			0.0143 (0.0632)			-46.0118*** (6.3884)
$\beta^{M^2 \cdot SVOL}$			0.0568*** (0.0143)			-12.3610*** (1.7830)
$\beta^{M^2 \cdot IVOL}$			-0.0296 (0.0257)			-28.9879*** (4.2297)
$adj R^2$	0.3344	0.3381	0.3821	0.3952	0.4464	0.4959
F-statistic	200.97	143.40	113.72	209.52	164.05	169.76
p-value	0.00	0.00	0.00	0.00	0.00	0.00
JB-statistic	217.0180	171.5434	175.9686	99.1569	221.0127	133.1247
p-value	0.0000	0.0000	0.0000	0.0000	0.0000	0.0000

Configuration	Put options - EU market			Put options - US market		
	pure	interacted	squared	pure	interacted	squared
Intercept	-0.0011 (0.0022)	-0.0113*** (0.0031)	-0.0064 (0.0040)	-0.0177*** (0.0037)	-0.0237*** (0.0034)	-0.0239*** (0.0033)
β^{SVOL}	0.0532*** (0.0047)	0.0524*** (0.0044)	0.0549*** (0.0042)	0.0347*** (0.0085)	0.0489*** (0.0098)	0.0549*** (0.0096)
β^{IVOL}	-0.1147*** (0.0105)	-0.0898*** (0.0114)	-0.0725*** (0.0126)	-0.2447*** (0.0240)	-0.2039*** (0.0244)	-0.1804*** (0.0247)
β^M	0.2957*** (0.0934)	0.0606 (0.0737)	-0.0372 (0.0750)	-3.0032*** (0.6065)	-3.6506*** (0.4613)	-3.5755*** (0.3615)
$\beta^{M \cdot SVOL}$		0.0957*** (0.0148)	0.0758*** (0.0144)		-0.7412*** (0.1242)	-0.7993*** (0.1093)
$\beta^{M \cdot IVOL}$		-0.0238 (0.0267)	-0.0548** (0.0230)		-2.3192*** (0.3258)	-2.2695*** (0.2764)
β^{M^2}			-0.3590* (0.1854)			-54.1206*** (7.4574)
$\beta^{M^2 \cdot SVOL}$			0.0732** (0.0331)			-14.9796*** (2.2032)
$\beta^{M^2 \cdot IVOL}$			-0.1089* (0.0559)			-34.7541*** (5.0004)
$adj R^2$	0.4492	0.4939	0.5514	0.5322	0.6210	0.6832
F-statistic	187.24	184.00	151.03	263.64	335.79	280.05
p-value	0.00	0.00	0.00	0.00	0.00	0.00
JB-statistic	847.8958	1640.2716	3554.9860	5359.5675	1545.8430	2606.7931
p-value	0.0000	0.0000	0.0000	0.0000	0.0000	0.0000

The table reports the results for the time-series regressions according to equation 3.7. The top panel refers to call options and the bottom panel refers to put options. In addition to $\hat{\gamma}$, the respective Newey-West adjusted standard errors are reported in parentheses. Statistical significance at the 1 percent, 5 percent, 10 percent level is denoted by ***, **, *. In addition to the R^2 value, the goodness-of-fit of the applied model can be judged by the F-statistic and the JB-statistic with the corresponding p-values.

The results of the second step in our analysis, where we estimate risk premia (time-series regressions according to equation 3.7), are presented in table 3.4. The second step regression results in three, five, or eight $\hat{\gamma}$ s for each individual option j for the pure, the interacted and the squared configurations, respectively. The results in table 3.7 represent the average of each $\hat{\gamma}$ over all individual options. Compared to the first step cross-sectional regressions, the higher adjusted coefficients of determination (between 33.4 percent to 49.6 percent for call options and 44.9 percent to 68.3 percent for put options) and high levels of F-statistics prove a high goodness-of-fit of our model, in particular for the US data. While the focus of this part of our empirical analysis lays on the coefficients of $\hat{\gamma}^{SVOL}$ and $\hat{\gamma}^{IVOL}$, we note that most coefficients for moneyness $\hat{\gamma}^M$ are not significant for the EU market, but significantly negative for

Table 3.5: Portfolio time-series regressions - Second step

Configuration	Call options - EU market			Call options - US market		
	pure	interacted	squared	pure	interacted	squared
Intercept	0.0282 (0.0169)	0.0266*** (0.0059)	0.0595*** (0.0123)	0.0709*** (0.0142)	0.0361 (0.0306)	0.0520 (0.0591)
β^{SVOL}	0.2381** (0.1042)	0.4609*** (0.0630)	0.0896 (0.0907)	2.3506*** (0.2746)	2.7243*** (0.3065)	2.4543*** (0.3489)
β^{IVOL}	0.5935*** (0.1493)	0.3465 (0.2992)	0.9810*** (0.3273)	1.4295*** (0.5104)	1.7129*** (0.5205)	1.2438* (0.6965)
β^M	-0.4702 (0.5664)	3.5780** (1.7156)	-4.7256*** (1.5059)	-10.2363*** (1.8466)	-22.3687*** (3.9924)	-30.9904*** (8.6246)
$\beta^{M \cdot SVOL}$		1.5382*** (0.5566)	-0.7143 (0.4612)		-3.5933*** (0.4139)	-7.7324** (3.2635)
$\beta^{M \cdot IVOL}$		1.6277*** (0.4880)	-1.2832*** (0.3898)		-13.9218*** (2.2244)	-19.6370** (7.6809)
β^{M^2}			-23.8167*** (6.0712)			-518.6952** (208.3030)
$\beta^{M^2 \cdot SVOL}$			-4.5606*** (1.5429)			-149.8041** (63.2507)
$\beta^{M^2 \cdot IVOL}$			-9.5533*** (2.1262)			-325.6015** (145.1200)
R^2	0.1250	0.2584	0.4862	0.6762	0.7510	0.8188
F-statistic	8.08	41.70	58.11	57.08	73.94	236.00
p-value	0.00	0.00	0.00	0.00	0.00	0.00
JB-statistic	0.6514	0.5610	0.2113	0.3179	3.0622	2.8368
p-value	0.7220	0.7554	0.8998	0.8530	0.2163	0.2421

Configuration	Put options - EU market			Put options - US market		
	pure	interacted	squared	pure	interacted	squared
Intercept	-0.1054*** (0.0250)	-0.0546*** (0.0139)	-0.1225*** (0.0137)	-0.0772*** (0.0175)	-0.1197*** (0.0130)	-0.2331*** (0.0316)
β^{SVOL}	0.8972** (0.3508)	0.4901*** (0.0939)	0.8214*** (0.1386)	2.0084*** (0.2407)	1.6967*** (0.3456)	1.4696*** (0.3772)
β^{IVOL}	2.4180*** (0.4969)	0.5029 (0.5544)	1.1365** (0.5043)	-0.0905 (0.4114)	-0.1262 (0.5135)	0.2692 (0.4502)
β^M	-4.0401*** (1.2955)	-0.2119 (0.2108)	-4.0776*** (1.1447)	-11.2948*** (3.1175)	-13.1497 (7.8571)	-12.5397* (7.3237)
$\beta^{M \cdot SVOL}$		0.7700*** (0.0605)	0.7993* (0.4005)		-0.8557 (2.8684)	-1.2712 (2.2551)
$\beta^{M \cdot IVOL}$		0.2092 (0.5212)	-0.1758 (0.9478)		-7.2386 (6.5856)	-5.0245 (4.9400)
β^{M^2}			-13.8008** (5.0764)			29.0629 (144.8184)
$\beta^{M^2 \cdot SVOL}$			0.5949 (1.2644)			20.0618 (39.6543)
$\beta^{M^2 \cdot IVOL}$			-2.5097 (2.5360)			42.3813 (94.5817)
R^2	0.6424	0.8668	0.9219	0.8164	0.8341	0.8855
F-statistic	14.19	1305.02	5990.37	54.61	143.77	292.32
p-value	0.00	0.00	0.00	0.00	0.00	0.00
JB-statistic	1.9768	0.9488	1.6686	5.1084	2.4328	1.0004
p-value	0.3722	0.6223	0.4342	0.0778	0.2963	0.6064

The table reports the results for the time-series regressions applied to portfolios according to equation 3.7. The top panel refers to call options and the bottom panel refers to put options. In addition to $\hat{\gamma}$, the respective Newey-West adjusted standard errors are reported in parentheses. Statistical significance at the 1 percent, 5 percent, 10 percent level is denoted by ***, **, *. In addition to the R^2 value, the goodness-of-fit of the applied model is represented by the F-statistic and the JB-statistic as well as the corresponding p-values.

the US market. Further, the interaction and squared terms are also highly significant for the US data, while we observe a mixed picture for the EU data, where mainly terms related to SVOL are significant.

The call and put options results suggest a significantly positive risk premium for the market sensitivity towards SVOL. The results for the market sensitivity towards IVOL oppose those observed for SVOL and show a significant negative risk premium. The magnitude of this effect varies for the different samples, ranging between -0.04 for call options on the EU market and -0.20 for put options on the US market. The observed negative risk premium for IVOL appears to be a somewhat counterintuitive finding. This can be understood from an insurance or hedging perspective. In this sense, it might be beneficial for an investor to accept a negative risk premium to hold the option to compensate for alternative risk and, thereby, reduce the risk of his portfolio. However, the null hypothesis of normally distributed regression residuals is rejected based on the JB statistic with consistently high values and low p-values. Non-normal residuals might indicate an inadequate model and, as described in section 3.2, this may arise due to a possible errors-in-variables bias and is mitigated by means of portfolio formation.

The results of the regression implemented for portfolios rather than single assets are presented in table 3.5. In contrast to the regressions run for single assets, the JB statistics show lower values and higher p-values, particularly for the EU market. The null hypothesis of normally distributed errors can not be rejected at the five percent significance level, except for the pure configuration for US put options. Further, the F-statistics and their p-values indicate an overall significance of the applied model. The sample for call options on the EU market shows low adjusted coefficients of determination between 12.5 percent to 48.6 percent compared to put samples that reach 60 percent to 90 percent.

Again, both call and put options show a positive, highly significant SVOL premium (except for the squared configuration for EU call options). Contrary to our previous results, we also observe a positive and highly significant IVOL premium for most samples, except for US put options. However, some exceptions to these patterns occur. For instance, the IVOL premium for put options is insignificant in the interacted configurations for the EU market and in all configurations for the US market. The moneyness premium tends to be negative with varying significance levels. For interacted and squared terms, the premium is mostly negative for call options; however, the direction is unclear for put options. In sum, our findings suggest a clearly positive SVOL premium and show mixed results for the IVOL premium, which is negative when the regression is applied to single assets and positive when applied to portfolios.

4 Robustness Tests

In this part we analyse the robustness of the results presented in section 3.3. We consider robustness with respect to (i) adding control variables and (ii) using alternative volatility estimates. The empirical results for these modifications to the base configurations according to equations 3.4, 3.5, and 3.6 can be found in the appendix.

Modification (i) expands equation 3.4 by additionally including option trading volume and open interest as regressors.¹⁸ For the first step regressions, both call and put option samples show an improved goodness-of-fit with higher adjusted coefficients of determination than in the base configurations and the same signs and magnitude for moneyness betas. Table A.1 shows that SVOL and IVOL coefficients remain unchanged for call option rates of return, except for a positive sign with nonlinear interaction with moneyness $\beta^{M^2 \cdot SVOL}$ for the US market. Coefficients are statistically significant throughout all configurations. Moreover, table A.1 shows robust SVOL and IVOL coefficients for put options. The magnitude of all call and put options coefficients for both markets are very similar to those reported in

¹⁸Liquidity controls are often used for robustness purposes in the analysis of both stock and option rates of return. See, e.g., Malagon et al. (2018) and Aretz et al. (2023).

table 3.3. To sum up, including volume and open interest neither changes the main messages outlined in section 3.3 nor provides additional information, so our results are robust to including these control variables.

The results of the second step regressions implemented for single assets are displayed in table A.2. For call options, the results are similar to those reported in section 3.3 for the US market, except for all intercepts being negative. For call options on the EU market, the moneyness premium γ^M in the interacted configuration and the IVOL premium in interaction with nonlinear moneyness $\gamma^{M^2 \cdot IVOL}$ in the squared configuration are positive, however, remain insignificant. For put options on the US market, only the linear SVOL premium in the pure configuration changes to a negative one but is insignificant compared to table 3.3 where it is positive and significant. For put options on the EU market, $\gamma^{M^2 \cdot IVOL}$ in the squared configuration changes the sign to negative but is insignificant compared to positive and significant in table 3.3; the moneyness premium in the pure configuration remains its sign but becomes insignificant. All coefficients are slightly lower in absolute terms except γ^{M^2} , $\gamma^{M^2 \cdot SVOL}$ and $\gamma^{M^2 \cdot IVOL}$ in the squared configuration for the US market; these coefficients become notably lower.

Table A.3 shows a robustness test when including controls in the portfolio setting. Here, for call options on the EU market, the moneyness premium γ^M in the pure configuration becomes positive but stays insignificant. On the US market, SVOL and IVOL premia are also negative in all configurations and highly significant. For put options on the EU market, the SVOL premium is negative (insignificant) in the interacted configuration, coefficients $\gamma^{M \cdot SVOL}$ and $\gamma^{M \cdot IVOL}$ are negative and significant. However, $\gamma^{M \cdot IVOL}$ becomes positive in the squared configuration, although being insignificant. For the US market, the SVOL premium is negative in all configurations, significant only in the interacted configuration. In interaction with both linear and nonlinear moneyness, it keeps the sign but becomes highly significant. In the squared configuration, the IVOL premium becomes negative, and the moneyness premium becomes positive. In general, all coefficients for US put options become highly significant.

Modification (ii) uses EGARCH estimates according to equation 3.3 instead of FFC estimates for idiosyncratic volatility. Modified regression configurations show lower adjusted coefficients of determination for both call and put options for both markets compared to the base configuration. For call options, all linear SVOL coefficients are robust to EGARCH estimates for both markets, except for the SVOL coefficient in the pure configuration for the US market, which becomes insignificant. For the EU market, the coefficient $\beta^{M^2 \cdot SVOL}$ in the squared configuration becomes significantly positive. Linear EGARCH IVOL coefficients for call options are of relatively lower magnitude than in the base configuration; however, they are still almost all highly significant. The coefficient $\beta^{M^2 \cdot IVOL}$ in the squared configuration changes to negative for the EU market and to significantly positive for the US market. For put options on the EU market, linear SVOL coefficients remain unchanged in general; only the coefficient in the pure configuration becomes highly significant. For put options on the US market, linear SVOL coefficients in the pure and interacted configurations are negative, and they are only significant in the pure configuration. The linear EGARCH IVOL coefficients for put options are also lower in magnitude than in the base configuration and are almost all highly significant. All other coefficients remain at their sign and significance level, except the $\beta^{M \cdot SVOL}$ coefficient for the EU market, which becomes insignificant. Signs and magnitude for moneyness betas remain unchanged.

The robustness of the second step results for the single-asset setting is reported in table B.2. As in the base configurations, there is a significantly positive SVOL premium and a significantly negative IVOL premium, both at slightly higher magnitudes in absolute terms. Again, the findings (reported in table B.3) differ when applying regressions to portfolios. For call options, the results show positive and significant SVOL and IVOL premia for both markets. In interaction with linear moneyness M , the SVOL premium is negative (positive) in the interacted configuration for the EU (US) market and positive for both markets in the squared configuration but only significant on the US market in the interacted

configuration. In interaction with nonlinear moneyness M^2 , SVOL and IVOL premia are positive for both markets, however highly significant only for the US market. In contrast to the base configuration, this premium is negative. For put options, the SVOL premium matches our previous results and is positive for both markets, except for the squared configuration for the EU market. The SVOL premium in interaction with nonlinear moneyness becomes significantly negative for the EU market. Compared to the base configuration, the IVOL premium becomes significantly negative for the EU market and significantly positive for the US market in the squared configuration. For the EU market, the IVOL premium in interaction with moneyness becomes significantly negative. For the US market, all coefficients in the squared configuration are positive and become highly significant.

To sum up the robustness of our analysis, we confirm the consistency of a positive SVOL premium across multiple configurations and the negative IVOL premium in the single-asset setting (significant only for the EU market). The interaction terms with moneyness (linear and nonlinear) in the portfolio setting show mixed results, indicating that these relationships are complex and nonlinear. The observed differences in the findings between the EU and the US market again confirm the differences on both markets.

5 Conclusion

Our paper provides an in-depth empirical study of the relationship between equity option rates of return and volatility of the underlying, taking into consideration the sensitivity of option rates of return to systematic volatility (SVOL), idiosyncratic volatility (IVOL), and moneyness at a particular point in time. It also examines the relation between these risk sensitivities and individual option rates of return over time. We utilize large-scale datasets covering call and put options on the EU and US markets from 2011 to 2021, with each sample containing up to 70 million observations. The primary goal of the analysis is to analyze the complex relationship between option rates of return and risk sensitivities conditional on moneyness. With our approach, we also inspect the relationship and its magnitude between expected option rates of return and underlying volatility with respect to the elasticity effect and the drift effect. We examine the theoretical predictions about a negative effect of volatility on call option rates of return and a positive effect on put option rates of return as long as only IVOL is considered. However, we also explore the total volatility effect when simultaneously considering SVOL and IVOL and note that it depends on further option characteristics such as moneyness.

Our data indicates that daily option rates of return are sufficiently close to a normal distribution and show averages at around 15.78 percent to 18.21 percent per month for call options and -0.02 percent to -0.21 percent per month for put options. We apply the Fama-French-Carhart model to the respective underlying stock rates of return and split total volatility into two components. This results in an average SVOL of 15 percent and IVOL of 29 percent on the EU and an average SVOL of 23 percent and IVOL of 33 percent on the US market. The alternatively implemented EGARCH model shows average IVOL estimates of 30 percent and 45 percent on the EU and the US market, respectively. We employ the Fama-McBeth-Campbell procedure to identify the sensitivity of option rates of return to idiosyncratic and systematic volatility, accounting for various moneyness levels and nonlinearities. In the first step of our analysis, one cross-sectional regression is run for each of the approximately 2,600 days in the sample to obtain time series estimates for both volatility components and moneyness betas, i.e., the exposure of option rates of return to volatility and moneyness. Our findings show that for call (put) options, there is statistically significant evidence for a positive (negative) but decreasing (increasing) effect of moneyness on option rates of return. The SVOL and IVOL coefficients for ATM options are negative for call options and positive for put options. Further, the IVOL coefficient decreases with moneyness for call options, and it is even more negative for ITM options. It only gets positive for sufficiently OTM options with

moneyiness below 91 percent. On the EU market, the SVOL coefficients for call options show the same inverse relationship with moneyiness (switching signs at the moneyiness of 85 percent).

On the US market, the coefficients increase with moneyiness; they are negative for OTM options and switch to positive for ITM options with moneyiness above 130 percent. For put options, the signs of the SVOL and IVOL coefficients consistently behave the exact opposite way to those observed for call options; only the tipping points in terms of moneyiness between positive and negative coefficients are slightly different. These findings suggest potential differences in market-specific dynamics and differences in the dominant effect on these markets. Overall, the first step results partially confirm the general trends observed in previous studies. A combined total volatility coefficient with respect to monthly returns of ATM options in the US market of -0.446 for call options and 0.584 for put options is consistent with the results of Hu and Jacobs (2020). Additionally, when comparing the effects on call options with those of Aretz et al. (2023), we confirm a negative IVOL effect for ATM and ITM options on both markets, what previously was observed only for the US market, and our study reveals the same effect for the EU market. We contribute to the literature by disclosing the intriguing nature of the SVOL effect on option rates of return. On the US market, there is a negative SVOL effect for ATM and OTM options and a positive one for ITM options. However, we also find a positive IVOL effect on OTM call options on both markets, a negative SVOL effect on ITM call options, and a positive one for OTM call options on the EU market.

The second step regression is conducted as a time-series analysis, using the risk sensitivities as explanatory variables to determine their explanatory power and estimate their corresponding risk premia. The SVOL risk premium is positive and highly significant for both call and put options. There is also statistically significant evidence for a negative IVOL risk premium. However, the validity of these findings might be debatable since the regression residuals fail the Jarque-Bera test for normality. This may arise due to an errors-in-variables bias. To address this issue, we implement an alternative regression, sorting the data into 50 equally weighted portfolios based on five moneyiness groups and ten IVOL groups. The null hypothesis is not rejected in this setting, and the model is globally significant. Also, here, the data suggests a positive and highly significant SVOL risk premium –conversely, the IVOL risk premium is now also significantly positive.

We run several robustness tests to confirm the main message of our findings, i.e., including liquidity controls and using an alternative volatility estimate. Including liquidity controls improves the predictive power of the regression models. However, the use of alternative EGARCH estimates slightly weakens their performance. Some deviations were observed in a few configurations for the US market. The effect of SVOL on put option rates of return is negative, and the effect of IVOL on call option rates of return switches from negative to positive at higher moneyiness levels. The second step regressions in the single-asset setting are robust with respect to all applied modifications. Some robustness configurations in the portfolio setting show deviations for the IVOL risk premium, which is negative compared to the base configuration.

Appendix: Further empirical results

A Including liquidity controls

The empirical results presented in this section are generated with the same approach as those in the section 3.3. However, the base configurations are expanded by additionally including option trading volume and open interest as liquidity controls.

Table A.1: Cross-sectional regressions – First step

Configuration	Call options - EU market			Call options - US market		
	pure	interacted	squared	pure	interacted	squared
Intercept	0.0022 (0.0025)	-0.0691*** (0.0045)	-0.1555*** (0.0232)	0.0055*** (0.0021)	-0.0158*** (0.0025)	-0.0418*** (0.0029)
<i>SVOL</i>	-0.0265** (0.0132)	0.1624*** (0.0227)	0.1981 (0.1628)	-0.0155* (0.0098)	-0.0470*** (0.0106)	-0.0693*** (0.0113)
<i>IVOL</i>	-0.0093* (0.0066)	0.0552*** (0.0157)	0.1458 (0.1200)	-0.0055 (0.0045)	0.0427*** (0.0053)	0.0799*** (0.0059)
<i>M</i>	0.0085*** (0.0008)	0.0811*** (0.0041)	0.1958*** (0.0475)	0.0032*** (0.0002)	0.0249*** (0.0010)	0.0546*** (0.0018)
<i>M · SVOL</i>		-0.1942*** (0.0184)	-0.1810 (0.3198)		0.0316*** (0.0026)	0.0595*** (0.0049)
<i>M · IVOL</i>		-0.0638*** (0.0158)	-0.1924 (0.2409)		-0.0482*** (0.0018)	-0.0928*** (0.0032)
<i>M</i> ²			-0.0257 (0.0240)			-0.0031*** (0.0002)
<i>M</i> ² · <i>SVOL</i>			-0.0602 (0.1575)			-0.0061*** (0.0008)
<i>M</i> ² · <i>IVOL</i>			0.0393 (0.1196)			0.0067*** (0.0004)
Volume	0.0000*** (0.0000)	0.0000*** (0.0000)	0.0000*** (0.0000)	0.0000*** (0.0000)	0.0000*** (0.0000)	0.0000*** (0.0000)
Open Interest	-0.0000*** (0.0000)	-0.0000*** (0.0000)	-0.0000*** (0.0000)	-0.0000*** (0.0000)	-0.0000*** (0.0000)	-0.0000*** (0.0000)
<i>R</i> ²	0.0354	0.0396	0.0459	0.0265	0.0281	0.0301

Configuration	Put options - EU market			Put options - US market		
	pure	interacted	squared	pure	interacted	squared
Intercept	-0.0131*** (0.0025)	0.0526*** (0.0046)	0.1515*** (0.0085)	-0.0200*** (0.0028)	0.0019 (0.0038)	0.0203*** (0.0045)
<i>SVOL</i>	0.0054 (0.0111)	-0.1551*** (0.0158)	-0.3899*** (0.0568)	-0.0002 (0.0091)	0.0321*** (0.0105)	0.0797*** (0.0126)
<i>IVOL</i>	0.0424*** (0.0062)	-0.0250*** (0.0100)	-0.0954*** (0.0218)	0.0285*** (0.0049)	-0.0219*** (0.0067)	-0.0532*** (0.0077)
<i>M</i>	-0.0072*** (0.0006)	-0.0684*** (0.0028)	-0.2281*** (0.0142)	-0.0033*** (0.0002)	-0.0237*** (0.0014)	-0.0494*** (0.0025)
<i>M · SVOL</i>		0.1572*** (0.0123)	0.5405*** (0.1036)		-0.0279*** (0.0027)	-0.0800*** (0.0062)
<i>M · IVOL</i>		0.0571*** (0.0064)	0.1886*** (0.0386)		0.0448*** (0.0025)	0.0899*** (0.0044)
<i>M</i> ²			0.0616*** (0.0062)			0.0073*** (0.0005)
<i>M</i> ² · <i>SVOL</i>			-0.1448*** (0.0463)			0.0083*** (0.0006)
<i>M</i> ² · <i>IVOL</i>			-0.0643*** (0.0176)			-0.0138*** (0.0009)
Volume	0.0000 (0.0000)	0.0000 (0.0000)	0.0000 (0.0000)	0.0000*** (0.0000)	0.0000*** (0.0000)	0.0000*** (0.0000)
Open Interest	0.0000 (0.0000)	0.0000 (0.0000)	0.0000** (0.0000)	0.0000*** (0.0000)	0.0000*** (0.0000)	0.0000*** (0.0000)
<i>R</i> ²	0.0330	0.0378	0.0448	0.0269	0.0291	0.0314

The table reports results for the first step regression applied to the model described by equation 3.4. The coefficients are derived by regressing daily option returns R on risk factors $SVOL$, $IVOL$ and M (and additional combinations in interacted and squared configurations) as well as on control variables volume and open interest for each individual time step t and then taking the time-series average of the single cross-sectional estimates for $\hat{\beta}$. The top panel refers to call options and the bottom panel to put options. In addition to $\hat{\beta}$, the respective standard errors are reported in parentheses. Statistical significance is judged according to the global t-statistic and the 1 percent, 5 percent, 10 percent levels are denoted by ***, **, *. The goodness-of-fit of the applied model is judged by the average R^2 value.

Table A.2: Time-series regressions – Second step

Configuration	Call options - EU market			Call options - US market		
	pure	interacted	squared	pure	interacted	squared
Intercept	-0.0035 (0.0024)	-0.0021 (0.0025)	-0.0023 (0.0025)	-0.0142*** (0.0013)	-0.0109*** (0.0013)	-0.0063*** (0.0015)
<i>SVOL</i>	0.0464*** (0.0049)	0.0437*** (0.0049)	0.0457*** (0.0044)	0.0213*** (0.0037)	0.0217*** (0.0043)	0.0235*** (0.0045)
<i>IVOL</i>	-0.0326*** (0.0083)	-0.0352*** (0.0073)	-0.0368*** (0.0071)	-0.0983*** (0.0063)	-0.0996*** (0.0062)	-0.0959*** (0.0066)
<i>M</i>	0.1247 (0.0891)	0.0452 (0.0523)	0.0768** (0.0308)	-1.1047*** (0.1984)	-1.5276*** (0.2593)	-1.2939*** (0.2162)
<i>M · SVOL</i>		0.0520*** (0.0132)	0.0709*** (0.0091)		-0.3495*** (0.0573)	-0.2713*** (0.0552)
<i>M · IVOL</i>		-0.0067 (0.0186)	-0.0018 (0.0158)		-1.0117*** (0.1606)	-0.8269*** (0.1431)
<i>M</i> ²			0.0596 (0.0578)			-20.4259*** (4.4503)
<i>M</i> ² · <i>SVOL</i>			0.0826*** (0.0151)			-5.3682*** (1.2496)
<i>M</i> ² · <i>IVOL</i>			0.0057 (0.0264)			-12.7361*** (2.9474)
Volume	834.6633*** (189.2596)	818.6842*** (184.5453)	801.3255*** (115.6767)	1662.7945*** (83.5769)	1644.6688*** (84.3323)	1604.2971*** (84.9871)
Open Interest	-14133.5494*** (1796.8008)	-14974.1553*** (2024.4968)	-11745.4954*** (1998.5205)	-24186.5176*** (1628.3966)	-22674.6436*** (1549.2069)	-21271.7219*** (1495.90)
<i>R</i> ²	0.4640	0.4684	0.4930	0.7095	0.7163	0.7291
F-statistic	149.62	133.49	97.40	331.92	270.48	230.74
<i>p</i> -value	0.0000	0.0000	0.0000	0.0000	0.0000	0.0000
JB-statistic	2702.6373	1953.8342	635.3690	-0.0037	-0.0037	-0.0037
<i>p</i> -value	0.0000	0.0000	0.0000	0.0000	0.0000	0.0000

Configuration	Put options - EU market			Put options - US market		
	pure	interacted	squared	pure	interacted	squared
Intercept	-0.0010 (0.0023)	-0.0103*** (0.0031)	-0.0048 (0.0037)	-0.0107*** (0.0025)	-0.0136*** (0.0024)	-0.0146*** (0.0026)
<i>SVOL</i>	0.0498*** (0.0051)	0.0491*** (0.0047)	0.0397*** (0.0050)	-0.0006 (0.0046)	0.0123** (0.0058)	0.0194*** (0.0060)
<i>IVOL</i>	-0.1108*** (0.0109)	-0.0889*** (0.0112)	-0.0629*** (0.0100)	-0.1598*** (0.0107)	-0.1467*** (0.0123)	-0.1447*** (0.0144)
<i>M</i>	0.1909 (0.1167)	0.0644 (0.0749)	-0.0709 (0.0646)	-0.4037 (0.3580)	-1.1180*** (0.2422)	-1.3898*** (0.1899)
<i>M · SVOL</i>		0.0914*** (0.0152)	0.0463*** (0.0124)		-0.1719*** (0.0660)	-0.2880*** (0.0532)
<i>M · IVOL</i>		-0.0204 (0.0273)	-0.0614*** (0.0193)		-0.7805*** (0.1684)	-0.9734*** (0.1431)
<i>M</i> ²			-0.5487*** (0.1480)			-19.0452*** (3.6792)
<i>M</i> ² · <i>SVOL</i>			-0.0009 (0.0261)			-5.1388*** (1.0897)
<i>M</i> ² · <i>IVOL</i>			-0.1941*** (0.0455)			-12.336*** (2.4531)
Volume	170.8344 (119.3369)	183.7440 (112.0621)	611.8111*** (50.6129)	1573.1215*** (86.6915)	1526.8481*** (86.6578)	1457.2021*** (93.6908)
Open Interest	-4931.5398* (2814.1692)	-4204.4843 (2850.6427)	-18280.8327*** (2146.2212)	-31599.4297*** (2701.2896)	-27452.9441*** (2108.3679)	-24610.9401*** (2006.5701)
<i>R</i> ²	0.4849	0.5292	0.6490	0.8125	0.8259	0.8304
F-statistic	121.33	174.74	214.71	349.42	327.80	283.04
<i>p</i> -value	0.0000	0.0000	0.0000	0.0000	0.0000	0.0000
JB-statistic	2307.8816	3200.7233	2504.5540	3663.2430	2074.9652	2350.4605
<i>p</i> -value	0.0000	0.0000	0.0000	0.0000	0.0000	0.0000

The table reports results for the second step regression according to equation 3.7. The coefficients are derived by regressing average daily option returns \bar{R} on first step betas $\hat{\beta}^{SVOL}$, $\hat{\beta}^{IVOL}$ and $\hat{\beta}^M$ (and additional combinations in the interacted and squared configurations) as well as $\hat{\beta}^{Volume}$ and $\hat{\beta}_t^{Open\ Interest}$ in one global time-series regression. The top panel refers to call options and the bottom panel to put options. In addition to $\hat{\gamma}$, the respective Newey-West adjusted standard errors are reported in parentheses. Statistical significance at the 1 percent, 5 percent, 10 percent level is denoted by ***, **, *. In addition to the R^2 value, the goodness-of-fit of the applied model is judged by the F-statistic and the JB-statistic as well as the corresponding *p*-values.

Table A.3: Portfolio regressions – Second step

	Call options - EU market			Call options - US market		
	pure	interacted	squared	pure	interacted	squared
Intercept	-0.0334 (0.0209)	-0.0166 (0.0251)	0.0605** (0.0269)	-0.2240*** (0.0684)	-0.4638*** (0.1143)	-0.3574*** (0.1211)
<i>SVOL</i>	0.0203 (0.0490)	0.1138 (0.1524)	0.1147 (0.2149)	-1.5106*** (0.3732)	-1.4154*** (0.4854)	-1.0684** (0.4650)
<i>IVOL</i>	0.4166*** (0.0912)	0.2406** (0.1150)	1.1015*** (0.3190)	-0.7754** (0.3284)	-0.4769* (0.2747)	-1.6757*** (0.5013)
<i>M</i>	0.6622 (0.7699)	3.1193** (1.4221)	-3.2396** (1.5145)	-28.7445*** (4.2222)	-21.7675*** (2.3385)	-38.0022*** (6.9901)
<i>M · SVOL</i>		1.1139** (0.4911)	-0.3162 (0.5594)		-11.9017*** (1.6042)	-14.8813*** (2.6606)
<i>M · IVOL</i>		1.6014*** (0.4072)	-0.5403 (0.4149)		-18.6088*** (1.8987)	-30.3760*** (5.8873)
<i>M</i> ²			-17.8807*** (5.8552)			-727.1410*** (190.5812)
<i>M</i> ² · <i>SVOL</i>			-3.0277* (1.6463)			-212.0742*** (53.0659)
<i>M</i> ² · <i>IVOL</i>			-6.9493*** (1.9316)			-485.5693*** (130.8696)
Volume	2029.3460 (4353.7000)	5405.0539 (5575.1706)	-3771.3124 (5745.8268)	9248.5520 (9476.3142)	34169.5503*** (12064.3365)	5160.8048 (11433.2746)
Open Interest	-257132.8511*** (44445.7148)	-208119.8072*** (46060.4359)	-199589.6434*** (45573.3071)	-594110.7481*** (100463.0732)	-417690.7682*** (60129.0049)	-663861.1664*** (127537.1081)
R ²	0.3143	0.3997	0.5264	0.8752	0.9027	0.9052
F-statistic	42.58	43.90	59.69	28.11	57.60	132.25
<i>p</i> -value	0.0000	0.0000	0.0000	0.0000	0.0000	0.0000
JB-statistic	3.1171	11.3297	0.4570	2.5963	2.1608	2.7708
<i>p</i> -value	0.2104	0.0035	0.7957	0.2730	0.3395	0.2502
	Put options - EU market			Put options - US market		
	pure	interacted	squared	pure	interacted	squared
Intercept	-0.1347*** (0.0182)	-0.0276*** (0.0092)	-0.0989*** (0.0223)	-0.0938*** (0.0114)	-0.0989*** (0.0225)	-0.0149 (0.0722)
<i>SVOL</i>	0.0498 (0.1881)	-0.0455 (0.1001)	0.4991*** (0.1824)	-0.0341 (0.5404)	-1.0963*** (0.2390)	-0.3066 (0.2729)
<i>IVOL</i>	1.9392*** (0.5031)	0.5802 (0.4301)	1.1177* (0.5621)	-0.7167* (0.3897)	-1.9019*** (0.3428)	-0.6239* (0.3335)
<i>M</i>	-1.6452* (0.9001)	-2.5117*** (0.5665)	-2.7869*** (0.6101)	-18.2073*** (1.7833)	-43.1702*** (15.2666)	59.7306*** (14.4130)
<i>M · SVOL</i>		-0.1035* (0.0610)	0.7007* (0.3700)		-14.7683*** (4.7912)	14.2962*** (3.1936)
<i>M · IVOL</i>		-0.6503** (0.2709)	0.1427 (0.8501)		-31.9381*** (11.3563)	38.0148*** (8.6328)
<i>M</i> ²			-6.9620* (3.5690)			1411.8989*** (239.0898)
<i>M</i> ² · <i>SVOL</i>			1.3650 (1.1158)			401.4489*** (65.4884)
<i>M</i> ² · <i>IVOL</i>			-0.3930 (2.1850)			937.3408*** (154.3318)
Volume	24707.5495*** (3300.2800)	-7381.4228* (4110.1515)	-887.6768 (2557.6364)	11646.7695** (4905.1425)	26988.1066*** (7652.5190)	1797.5691 (8528.0512)
Open Interest	-204768.4279*** (74794.6658)	-428239.9832*** (54023.8182)	-317632.4010*** (51137.1172)	-75156.6005 (64885.9595)	34697.4750 (105229.9821)	-635365.2707*** (177718.2698)
R ²	0.7844	0.9100	0.9356	0.8489	0.8813	0.9308
F-statistic	63.32	1863.79	84.57	160.22	290.31	760.11
<i>p</i> -value	0.0000	0.0000	0.0000	0.0000	0.0000	0.0000
JB-statistic	2.9232	1.0217	1.6530	1.4429	14.0556	1.5004
<i>p</i> -value	0.2319	0.6000	0.4376	0.4861	0.0009	0.4723

The table reports results for the second step regression according to equation 3.7. The coefficients are derived by regressing equally-weighted portfolio returns R on first step portfolio betas $\hat{\beta}^{SVOL}$, $\hat{\beta}^{IVOL}$ and $\hat{\beta}^M$ (and additional combinations in the interacted and squared configurations) as well as $\hat{\beta}^{Volume}$ and $\hat{\beta}^{Open\ Interest}$. The top panel refers to call options and the bottom panel to put options. In addition to $\hat{\gamma}$, the respective Newey-West adjusted standard errors are reported in parentheses. Statistical significance at the 1 percent, 5 percent, 10 percent level is denoted by ***, **, *. In addition to the R^2 value, the goodness-of-fit of the applied model is judged by the F-statistic and the JB-statistic as well as the corresponding *p*-values.

B Alternative volatility estimates

The empirical results presented in this section are generated with the same approach as those in the section 3.3. However, the base configurations are modified by using volatility estimates based on the EGARCH instead of the FFC model.

Table B.1: Cross-sectional regressions – First step

Configuration	Call options - EU market			Call options - US market		
	pure	interacted	squared	pure	interacted	squared
Intercept	0.0020 (0.0021)	-0.0626*** (0.0038)	-0.1503*** (0.0268)	0.0051*** (0.0020)	-0.0152*** (0.0023)	-0.0435*** (0.0028)
<i>SVOL</i>	-0.0306*** (0.0126)	0.1743*** (0.0192)	0.4128*** (0.0690)	-0.0087 (0.0099)	-0.0414*** (0.0107)	-0.0660*** (0.0117)
<i>IVOL</i>	-0.0032 (0.0036)	0.0447*** (0.0078)	0.0492 (0.0697)	-0.0052** (0.0031)	0.0287*** (0.0035)	0.0629*** (0.0041)
<i>M</i>	0.0082*** (0.0008)	0.0741*** (0.0033)	0.1932*** (0.0562)	0.0033*** (0.0002)	0.0240*** (0.0009)	0.0560*** (0.0017)
<i>M · SVOL</i>		-0.2037*** (0.0148)	-0.5704*** (0.1403)		0.0324*** (0.0027)	0.0638*** (0.0055)
<i>M · IVOL</i>		-0.0505*** (0.0074)	-0.0288 (0.1458)		-0.0341*** (0.0012)	-0.0740*** (0.0024)
<i>M</i> ²			-0.0286 (0.0292)			-0.0028*** (0.0002)
<i>M</i> ² · <i>SVOL</i>			0.1155* (0.0743)			-0.0070*** (0.0009)
<i>M</i> ² · <i>SVOL</i>			-0.0248 (0.0757)			0.0048*** (0.0003)
<i>R</i> ²	0.0281	0.0323	0.0384	0.0180	0.0197	0.0217
Configuration	Put options - EU market			Put options - US market		
	pure	interacted	squared	pure	interacted	squared
Intercept	-0.0073*** (0.0020)	0.0440*** (0.0037)	0.1297*** (0.0090)	-0.0172*** (0.0027)	0.0041 (0.0036)	0.0226*** (0.0044)
<i>SVOL</i>	0.0347*** (0.0101)	-0.1310*** (0.0164)	-0.3787*** (0.0669)	-0.0217*** (0.0093)	-0.0110 (0.0105)	0.0116 (0.0126)
<i>IVOL</i>	0.0087*** (0.0028)	-0.0118* (0.0073)	-0.0221 (0.0307)	0.0257*** (0.0032)	-0.0036 (0.0042)	-0.0197*** (0.0051)
<i>M</i>	-0.0071*** (0.0006)	-0.0553*** (0.0024)	-0.1865*** (0.0155)	-0.0033*** (0.0002)	-0.0232*** (0.0014)	-0.0465*** (0.0024)
<i>M · SVOL</i>		0.1537*** (0.0126)	0.5243*** (0.1249)		-0.0075*** (0.0029)	-0.0307*** (0.0061)
<i>M · IVOL</i>		0.0192*** (0.0060)	0.0476 (0.0506)		0.0261*** (0.0015)	0.0477*** (0.0028)
<i>M</i> ²			0.0462*** (0.0069)			0.0052*** (0.0003)
<i>M</i> ² · <i>SVOL</i>			-0.1223** (0.0585)			0.0031*** (0.0008)
<i>M</i> ² · <i>IVOL</i>			-0.0189 (0.0209)			-0.0058*** (0.0004)
<i>R</i> ²	0.0250	0.0297	0.0365	0.0174	0.0194	0.0216

The table reports results for the first step regression applied to the model described by equation 3.4 and using volatility components estimated with an EGARCH model. The coefficients are derived by regressing daily option returns R on risk factors $SVOL$, $IVOL$ and M (and additional combinations in the interacted and squared configurations) for each individual time step t and then taking the time-series average of the single cross-sectional estimates for $\hat{\beta}$. The top panel refers to call options and the bottom panel to put options. In addition to $\hat{\beta}$, the respective standard errors are reported in parentheses. Statistical significance is judged according to the global t-statistic and the 1 percent, 5 percent, 10 percent levels are denoted by ***, **, *. The goodness-of-fit of the applied model is judged by the average R^2 value.

Table B.2: Time-series regressions – Second step

Configuration	Call options - EU market			Call options - US market		
	pure	interacted	squared	pure	interacted	squared
Intercept	0.0062*** (0.0016)	0.0077*** (0.0021)	0.0012 (0.0028)	0.0096*** (0.0023)	0.0117*** (0.0025)	0.0189*** (0.0027)
<i>SVOL</i>	0.0586*** (0.0037)	0.0578*** (0.0037)	0.0573*** (0.0036)	0.0670*** (0.0059)	0.0665*** (0.0062)	0.0653*** (0.0066)
<i>IVOL</i>	-0.0538*** (0.0141)	-0.0505*** (0.0156)	-0.0648*** (0.0126)	-0.1484*** (0.0181)	-0.1524*** (0.0229)	-0.1437*** (0.0204)
<i>M</i>	0.0578 (0.0507)	-0.0497 (0.0849)	0.0954*** (0.0341)	-1.5997*** (0.5332)	-2.2955*** (0.3088)	-1.8131*** (0.1554)
<i>M · SVOL</i>		0.0476** (0.0185)	0.0708*** (0.0071)		-0.4456*** (0.0700)	-0.3207*** (0.0459)
<i>M · IVOL</i>		-0.0584 (0.0439)	-0.0187 (0.0200)		-2.0398*** (0.2534)	-1.5168*** (0.1516)
<i>M</i> ²			0.1337* (0.0794)			-22.2877*** (3.7115)
<i>M</i> ² · <i>SVOL</i>			0.0760*** (0.0127)			-5.6353*** (1.0533)
<i>M</i> ² · <i>IVOL</i>			0.0077 (0.0357)			-19.3724*** (3.6385)
<i>R</i> ²	0.2588	0.2597	0.2921	0.3942	0.4203	0.4653
F-statistic	116.60	74.12	49.68	197.12	151.01	143.83
<i>p</i> -value	0.0000	0.0000	0.0000	0.0000	0.0000	0.0000
JB-statistic	108.5094	161.5634	138.9543	94.5744	299.5511	116.0610
<i>p</i> -value	0.0000	0.0000	0.0000	0.0000	0.0000	0.0000

Configuration	Put options - EU market			Put options - US market		
	pure	interacted	squared	pure	interacted	squared
Intercept	-0.0059** (0.0027)	-0.0185*** (0.0033)	-0.0107** (0.0046)	-0.0163*** (0.0038)	-0.0224*** (0.0034)	-0.0250*** (0.0034)
<i>SVOL</i>	0.0540*** (0.0046)	0.0555*** (0.0042)	0.0498*** (0.0046)	0.0510*** (0.0084)	0.0673*** (0.0097)	0.0761*** (0.0094)
<i>IVOL</i>	-0.1533*** (0.0224)	-0.1161*** (0.0209)	-0.1071*** (0.0213)	-0.3112*** (0.0386)	-0.2271*** (0.0434)	-0.1933*** (0.0361)
<i>M</i>	0.2263 (0.1791)	-0.1259 (0.1074)	-0.0492 (0.1055)	-3.3064*** (0.5415)	-1.7388*** (0.4807)	-1.7137*** (0.2039)
<i>M · SVOL</i>		0.0819*** (0.0214)	0.0624*** (0.0197)		-0.2206 (0.1383)	-0.2394*** (0.0602)
<i>M · IVOL</i>		-0.1113** (0.0503)	-0.0306 (0.0470)		-1.3069*** (0.4925)	-1.3292*** (0.2314)
<i>M</i> ²			-0.2613 (0.2894)			-21.6441*** (4.2967)
<i>M</i> ² · <i>SVOL</i>			0.0597 (0.0497)			-5.4841*** (1.2364)
<i>M</i> ² · <i>IVOL</i>			0.0422 (0.1173)			-19.2035*** (4.3580)
<i>R</i> ²	0.2249	0.3173	0.3684	0.5343	0.5785	0.6376
F-statistic	85.78	99.47	64.36	274.94	151.76	268.73
<i>p</i> -value	0.0000	0.0000	0.0000	0.0000	0.0000	0.0000
JB-statistic	1244.4931	2259.4430	3252.3616	4689.9031	1821.1360	3134.9067
<i>p</i> -value	0.0000	0.0000	0.0000	0.0000	0.0000	0.0000

The table reports results for the second step regression according to equation 3.7. The coefficients are derived by regressing average daily option returns \bar{R} on first step betas $\hat{\beta}^{SVOL}$, $\hat{\beta}^{IVOL}$ and $\hat{\beta}^M$ (and additional combinations in the interacted and squared configurations) in one global time-series regression. The top panel refers to call options and the bottom panel to put options. In addition to $\hat{\gamma}$, the respective Newey-West adjusted standard errors are reported in parentheses. Statistical significance at the 1 percent, 5 percent, 10 percent level is denoted by ***, **, *. In addition to the R^2 value, the goodness-of-fit of the applied model is judged by the F-statistic and the JB-statistic as well as the corresponding *p*-values.

Table B.3: Portfolio regressions – Second step

Configuration	Call options - EU market			Call options - US market		
	pure	interacted	squared	pure	interacted	squared
Intercept	0.0080 (0.0118)	0.0115 (0.0129)	0.0387*** (0.0080)	0.0250 (0.0203)	0.2586*** (0.0556)	0.0563 (0.0770)
$SVOL$	0.0820* (0.0410)	0.1050*** (0.0380)	0.1824** (0.0732)	1.2391*** (0.3135)	1.1849*** (0.1546)	1.9332*** (0.5410)
$IVOL$	0.3068 (0.4559)	0.3795 (0.3184)	1.5882*** (0.3014)	0.2913 (0.3323)	2.0471*** (0.4591)	1.3367*** (0.3784)
M	0.7573 (0.4835)	-0.4772 (1.2171)	-0.8704 (0.5388)	-2.9072 (2.8682)	-23.6406*** (6.4211)	-0.4334 (1.7525)
$M \cdot SVOL$		-0.0479 (0.3081)	0.1175 (0.0926)		1.1307 (1.4650)	1.1797** (0.5638)
$M \cdot IVOL$		0.2155 (0.6468)	1.3223*** (0.3189)		-8.3601* (4.8465)	5.4629** (2.1249)
M^2			-1.9016 (1.2210)			235.2962** (97.5196)
$M^2 \cdot SVOL$			0.1588 (0.2055)			71.4137** (27.2092)
$M^2 \cdot IVOL$			1.4283** (0.6383)			311.0648*** (97.2006)
R^2	0.0992	0.1015	0.3410	0.3223	0.5464	0.7074
F-statistic	13.96	4.32	814.38	12.12	43.12	182.02
p-value	0.0000	0.0000	0.0000	0.0000	0.0000	0.0000
JB-statistic	1.5190	1.3758	0.0043	61.4686	2.3322	0.9712
p-value	0.4679	0.5026	0.9979	0.0000	0.3116	0.6153

Configuration	Put options - EU market			Put options - US market		
	pure	interacted	squared	pure	interacted	squared
Intercept	-0.0363*** (0.0102)	-0.1021*** (0.0248)	0.0079 (0.0086)	0.0039 (0.0183)	-0.0589** (0.0246)	-0.2364*** (0.0280)
$SVOL$	0.5618*** (0.1724)	0.3387* (0.1774)	-0.2320*** (0.0653)	1.4772*** (0.2345)	1.1367*** (0.2160)	2.1617*** (0.3101)
$IVOL$	-1.7830** (0.8305)	-1.7892** (0.8186)	-0.6750*** (0.1327)	-1.0302 (0.7213)	-1.1258* (0.6378)	1.8480*** (0.6559)
M	-3.1720*** (0.8389)	-2.1985*** (0.3007)	0.2112 (0.9678)	-6.3547*** (1.5706)	-11.1852*** (4.1399)	1.7132 (1.7601)
$M \cdot SVOL$		0.4519 (0.2673)	-0.4610*** (0.1640)		-0.8871 (1.2054)	6.1655*** (0.8179)
$M \cdot IVOL$		-2.6025*** (0.5988)	-0.6798* (0.3695)		-9.4324* (4.8743)	10.6481*** (2.1409)
M^2			-1.1153 (4.1037)			348.7821*** (69.5549)
$M^2 \cdot SVOL$			-1.6132** (0.7670)			124.7138*** (22.8270)
$M^2 \cdot IVOL$			-2.0856 (1.8315)			388.0172*** (75.2387)
R^2	0.6370	0.7624	0.8911	0.7202	0.7496	0.8509
F-statistic	7.91	91.75	541.20	27.16	55.31	196.16
p-value	0.0000	0.0000	0.0000	0.0000	0.0000	0.0000
JB-statistic	7.8030	4.5369	0.0920	1.0802	1.0469	1.0100
p-value	0.0202	0.1035	0.9551	0.5827	0.5925	0.6035

The table reports results for the second step regression according to equation 3.7. The coefficients shown here are derived by regressing equally-weighted portfolio returns R on first step portfolio betas $\hat{\beta}^{SVOL}$, $\hat{\beta}^{IVOL}$ and $\hat{\beta}^M$ (and additional combinations in the interacted and squared configurations). The top panel refers to call options and the bottom panel to Put options. In addition to $\hat{\gamma}$, the respective Newey-West adjusted standard errors are reported in parentheses. Statistical significance at the 1 percent, 5 percent, 10 percent level is denoted by ***, **, *. In addition to the R^2 value, the goodness-of-fit of the applied model is judged by the F-statistic and the JB-statistic as well as the corresponding p -values.

References

- Ang, A., Hodrick, R. J., Xing, Y., and Zhang, X. (2006). The cross-section of volatility and expected returns. *Journal of Finance*, 61(1):259-299.
- Ang, A., Hodrick, R. J., Xing, Y., and Zhang, X. (2009). High idiosyncratic volatility and low returns: International and further u.s. evidence. *Journal of Financial Economics*, 91:123.
- Aretz, K., Lin, M.-T., and Poon, S.-H. (2023). Moneyiness, total, systematic, and idiosyncratic volatility, and the cross-section of european option returns. *Review of Finance*, 27(1):289-323.
- Bergbrant, M. and Kassa, H. (2021). Is idiosyncratic volatility related to returns? evidence from a subset of firms with quality idiosyncratic volatility estimates. *Journal of Banking & Finance*, 127.
- Black, F. and Scholes, M. (1973). The pricing of options and corporate liabilities. *Journal of Political Economy*, 81(3):637-654.
- Broadie, M., Chernov, M., and Johannes, M. (2009). Understanding index option returns. *Review of Financial Studies*, 22(11):4493-4529.
- Campbell, J. Y., Lo, A. W., and MacKinlay, A. C. (1997). *The Econometrics of Financial Markets*. Princeton University Press.
- Carhart, M. M. (1997). On persistence in mutual fund performance. *Journal of Finance*, 52(1):57-82.
- Chaudhury, M. (2017). Volatility and expected option returns: A note. *Economics Letters*, 152:14.
- Coval, J. D. and Shumway, T. (2001). Expected option returns. *Journal of Finance*, 56(3):983-1009.
- Dennis, P., Mayhew, S., and Stivers, C. (2006). Stock returns, implied volatility innovations, and the asymmetric volatility phenomenon. *Journal of Financial and Quantitative Analysis*, 41(2):381-406.
- Fu, F. (2009). Idiosyncratic risk and the cross-section of expected stock returns. *Journal of Financial Economics*, 91(1):24-37.
- Guo, H., Kassa, H., and Ferguson, M. F. (2014). On the relation between egarch idiosyncratic volatility and expected stock returns. *Journal of Financial and Quantitative Analysis*, 49(1):271-296.
- Heston, S. L. (1993). A closed-form solution for options with stochastic volatility with applications to bond and currency options. *Review of Financial Studies*, 6(2):327-343.
- Hu, G. and Jacobs, K. (2020). Volatility and expected option returns. *Journal of Financial and Quantitative Analysis*, 55(3):1025-1060.
- Malagon, J., Moreno, D., and Rodríguez, R. (2015). The idiosyncratic volatility anomaly: Corporate investment or investor mispricing? *Journal of Banking & Finance*, 60:224-238.
- Malagon, J., Moreno, D., and Rodríguez, R. (2018). Idiosyncratic volatility, conditional liquidity and stock returns. *International Review of Economics and Finance*, 53:118-132.
- Merton, R. C. (1973). Theory of rational option pricing. *Bell Journal of Economics and Management Science*, 4:141-183.
- Nelson, D. B. (1991). Conditional heteroskedasticity in asset returns: A new approach. *Econometrica: Journal of The Econometric Society*, pages 347-370.
- Rubinstein, M. (1984). A simple formula for the expected rate of return of an option over a finite holding period. *Journal of Finance*, 39(5):1503-1509.

Cross-section of index option rates of return and elasticity dynamics on the EU and US markets

Gunnar Niemann^{†‡} Peter Reichling[†] Anastasiia Zbandut[†]

This draft: October 23, 2024

Abstract

This study explores the dynamics of option trading on the EURO STOXX 50 and NASDAQ 100 indices, focusing on the distinct market behaviors, trading activities, and elasticity characteristics in the EU and US option markets. Utilizing a mixed effects panel regression model combined with the GJR-GARCH framework, we examine the influence of various factors on option pricing and investor strategies. Our findings reveal that the EU market exhibits a more conservative trading approach, with a balanced distribution of call options and a concentration of deep out-of-the-money put options. In contrast, the US market favors more speculative strategies, particularly around at-the-money options. The analysis indicates that US options demonstrate higher elasticity, reflecting a greater sensitivity to changes in the underlying assets, while the EU market shows higher trading activity and open interest. Additionally, we identify significant differences in leverage and open interest coefficients between the two markets, suggesting distinct trading behaviors and underlying market structures. This research enhances the understanding of option market dynamics, shedding light on the varying risk profiles and strategic preferences of investors in the EU and US markets.

JEL Classification: G12, G13, G15

Keywords: Option Markets, Index Options, EU vs. US Markets, GJR-GARCH Model, Option Elasticity

[†]Department of Banking & Finance, Otto-von-Guericke University Magdeburg, Germany

[‡]Corresponding author, email gunnar.niemann@ovgu.de

1 Introduction and literature review

For investors, understanding the varying impacts of key variables and predictors on option markets is crucial for making informed investment decisions. Therefore, it is essential to recognize that these effects might differ in magnitude on different option markets, leading to distinct behaviors. Recent literature in the field of option pricing explores the fields of machine learning and big data (e.g. Bali et al. (2023)), social media and political influence on prices (e.g. Kelly et al. (2016); Heng and Leung (2023)), market microstructure and illiquidity (e.g. Christoffersen et al. (2017)), volatility modeling and jumps (e.g. Cremers et al. (2015); Andersen et al. (2017); Eraker and Yang (2022)), the integration of ESG factors (e.g. Orpiszewski et al. (2023); Hu et al. (2024)), or innovative approaches to valuation (e.g. Carr and Wu (2020)). However, these analyses are solely based on United States (US) market data. Therefore, this paper analyzes whether there are differences in key variables and their influences between the US and the Europe (EU) option markets, and, thus, whether findings can be easily transferred from one market to another.

For this purpose, we analyze American-style call and put index options on the EU and US markets with the time horizon from January 2011 to March 2021. The EURO STOXX 50 (ES50) represents the index for the EU market and the NASDAQ 100 (N100) represents the index for the US market. These indices are chosen due to their high trading volumes of index options and representation of their respective economies. We measure whether the markets differentiate in terms of underlying volatility (VOLA), underlying volatility of volatility (VOV), option elasticity (Omega), delta, moneyness, trading volume, and open interest. Reichling et al. (2023) empirically analyze American-style equity call and put options and find that the relationship between equity option rates of return and changes in systematic and idiosyncratic volatility varies between the EU and the US markets. For moneyness levels, the authors report that, while both the EU and US markets show a positive relationship between moneyness and option rates of return, the direction of this relationship differs between the two markets. The EU market tends to have a stronger influence of moneyness on option rates of return, especially for nonlinear relationship, compared to the US market. For call options on the US market, systematic volatility exhibits a negative impact on at-the-money options; however, it becomes increasingly positive with moneyness. Conversely, on the EU market, systematic volatility shows a positive impact on out-of-the-money options and a negative impact on at-the-money call options; it decreases with moneyness and becomes more negative for higher moneyness levels. A similar pattern is also observed for put options.

Besides Reichling et al. (2023), our methodology and choice of variables as well as their estimation model are based on three publications. Firstly, Hu and Jacobs (2019) examine the relationship between expected option rates of return and the underlying volatility. The study contributes to the literature by highlighting the theoretically expected relationship between stock volatility and option rates of return. The authors emphasize the importance of considering overall volatility when examining the determinants of option rates of return and caution against biased results which may arise from assumptions about underlying volatility. The authors examine the leverage effect in options, suggesting that options with lower volatility are priced more affordably, thereby offering a higher degree of leverage to the investor. Additionally, Hu and Jacobs (2019) derive options elasticity with respect to volatility and show that the expected call (put) returns decrease (increase) with underlying volatility. Secondly, Chaudhury (2017) extends the study of Hu and Jacobs (2019) and analyzes at the relationship between asset volatility and expected option returns with respect to drift and volatility effects and shows that this relationship is not straightforward. The study builds on previous research by simultaneously considering the idiosyncratic and systematic volatility of the underlying on expected option rates of return. The study shows that the direction and strength of the relationship between volatility and expected option rates of return are not uniform, but rather depend on factors such as the asset's beta level, volatility level, the option's

moneyiness and maturity. The results suggest that the source of volatility, whether idiosyncratic or systematic, plays a crucial role in shaping the cross-section of option rates of return. Furthermore, the study emphasizes the importance of understanding not only the underlying volatility levels but also the source of volatility, to capture the dynamics of expected option rates of return. By considering these factors simultaneously, the study sheds light on how the relationship between volatility and expected option rates of return can vary in different scenarios and reveals the complexity of option price dynamics. Thirdly, Aretz et al. (2022) further investigate how fluctuations in the underlying volatility caused by systematic or idiosyncratic factors affect the pricing of European-style call options. The authors derive the expected options rates of return with respect to systematic and idiosyncratic volatility and identify two effects, elasticity and underlying asset effects. They show that idiosyncratic volatility affects option elasticity and systematic volatility affects the option elasticity and has an opposite effect on the expected asset return. Thus, the net effect of the underlying volatility depends on which of those two effects dominates. The study shows that systematic volatility has a positive effect on the prices of in-the-money and at-the-money call options, but a negative effect on the prices of out-of-the-money call options. Conversely, idiosyncratic volatility has a negative effect on the prices of call options. In addition, the study shows that systematic volatility premiums are significantly priced in for at-the-money call options.

In our study, we take a deeper look at the elasticity effect on options rates of return and examine the differences between the US and EU markets. We apply a GJR-GARCH model¹ to capture volatility dynamics for the N100 and the ES50 indexes. The application of GARCH models in our field is a common technique. Oh and Park (2023), for example, find that incorporating volatility derivatives in the estimation of a two-factor GARCH pricing model significantly enhances the pricing accuracy of put options, particularly for long-term options, by capturing realistic volatility and skewness term structures. The finding that GARCH models are superior in pricing options compared to other models is also supported by, e.g., Kannianen et al. (2014); Papantonis (2016). In the field of GARCH models, the GJR-GARCH has proven to be a particularly useful choice for the simulation of option prices, as it allows for asymmetric effects of positive and negative shocks on volatility. This can even be demonstrated in direct tests of individual GARCH models (e.g. Nugroho et al. (2019)). Although the GJR-GARCH model provides a slightly better fit for the US options market, the fitted GJR-GARCH models provide a very good overall representation of realized volatility for both markets. Thereafter, to analyze the influence of option elasticity on option rates of return, as well as the sensitivity of elasticity to changes in option delta and leverage, we employ two separate mixed-effect panel regressions for each sample. We find that, for both call and put options, our model provides a much better fit for the N100 options, than for the ES50 options. Apart from that, we observe the following similarities and differences between the markets, namely (1) we find no effect of underlying volatility on option rates of return which contradicts the literature reviewed earlier. This might be explained by inclusion of options elasticity as the independent variable which absorbs the volatility effect. (2) For VOV, we observe a positive effect for put options and no effect for call options on both markets. This finding might be related to downside protection strategies with put option when the uncertainty in volatility increases. (3) we observe a positive (negative) effect of moneyiness for call (put) option rates of return in the US, we only observe the negative effect for put options on the EU market. (4) Finally, we observe a negative effect of elasticity across all samples which again is a counterintuitive finding. However, options with high elasticity might be deep in-the-money or deep out-of-the-money options with high risk and low return trade-off. Additionally, it also might reflect investors' risk aversion. Based on elasticity surfaces, the EU option market is more sensitive to high elasticity, with more significant changes occurring not only in low volatility conditions but also average and above average volatility bins. In contrast, the elasticity surface for call options on the US market

¹See Glosten et al. (1993).

is rather peaked around low volatility bins, while the EU market shows peaks around average volatility bins. The magnitude of these changes varies between the markets.

It is important to mention, that some of our findings contradict with the findings of other authors. Regarding (1) e.g., Ruan (2020) finds a strict negative relation between equity option rates of return and VOV for call and puts applying US data. In our dataset, the effects observed deviate from and cannot confirm the findings of Ruan (2020). However, it should be noted that the literature does not unanimously agree on the influence of volatility-of-volatility (VOV) on asset returns. Hollstein and Prokopczuk (2017) identify VOV as a systematically priced market factor, demonstrating a significant negative risk premium. Conversely, Baltussen et al. (2018) argue that VOV is not a priced market factor but rather a stock characteristic. Ruan (2020) suggests that these discrepancies in findings may arise from variations in estimation methods. Specifically, Hollstein and Prokopczuk (2017) utilize the VVIX index as a measure of aggregate VOV, while Baltussen et al. (2018) estimate VOV by calculating the individual VOV as proportional to the idiosyncratic volatility of stocks. Alternatively, Ruan (2020) estimates VOV by calculating the individual realized volatility of implied volatility. In our case the VOV was derived by first modeling the index prices with ARIMA and capturing the residual volatility using GJR-GARCH. The forecasted volatilities from GJR-GARCH allow us to measure the change in volatility, which is then used to determine the change in the conditional volatility. This process mirrors the calculation of return volatility, ensuring consistency and robustness in our approach. We selected the GJR-GARCH model after testing various GARCH models, including EGARCH and T-GARCH. The choice was based on the lowest Bayesian Information Criterion (BIC), indicating that it provides the best balance of fit and parsimony for our data.

Following that, our objective is to examine the sensitivity of elasticity to delta and leverage. Therefore, we conduct a mixed-effects panel regression. The model has high explanatory power for both markets and option types. We observe persistence in the elasticity levels throughout the maturity. For both markets, we observe no influence of volatility on elasticity. For delta and leverage, we observe a negative effect for call options, which is stronger for the US market, and a positive effect only for US put options. What is surprising is that we find opposite effects for open interest. Open interest refers to the total number of outstanding or open option contracts held by market participants at the end of each trading day. We find that open interest negatively influences call and put options' elasticity on the US market; however, for the EU market, we observe a positive effect for call options' elasticity.

The paper proceeds as follows. In section 2, we provide details on the applied methodology and, therefore, explain the regression type models. Section 3 gives insights into our dataset, where we describe the call and put index option samples from the EU and US markets. In section 4, we present and discuss our empirical results. Finally, in section 5, we conclude.

2 Methodology

Our analysis is grounded in the Black and Scholes (1973) and Merton (1973) framework, which assumes that the underlying asset's volatility remains constant throughout the option's maturity. To more accurately capture the dynamics of the underlying asset, we estimate its volatility using an ARIMA-GJR-GARCH model. We then use the average volatility derived from this model for each option in our analysis.² To estimate the daily volatility of the underlying, we first fit an ARIMA model to construct the mean behavior of the index rates of return and then apply a GJR-GARCH model to the ARIMA residuals to capture volatility dynamics for the N100 and ES50 indexes separately. The ARIMA (p, d, q) model includes the order of the autoregressive component, indicated as p , the degree of differencing, indicated as d , and the order of the moving average component, indicated as q . At first and before fitting

²See e.g. Duan (1995).

the model, the time series of index returns r_t is differentiated d time as:

$$y_t = \Delta^d \cdot r_t \quad (2.1)$$

where Δ denotes the differencing operator and y_t represents the series obtained after differencing. We test the time series on stationarity with the Augmented Dickey-Fuller test. Then, the ARIMA model is applied to the time series y_t as follows:

$$\hat{y}_t = \mu + \sum_{i=1}^p a_i \cdot y_{t-i} + \sum_{j=1}^q b_j \cdot \varepsilon_{t-j} + \varepsilon_t \quad (2.2)$$

where \hat{y}_t represents the predicted values by the ARIMA model, μ denotes the mean of the series, a_i denotes the coefficients of autoregressive terms, y_{t-i} are the lagged values, b_j denotes the coefficients of the moving average terms, ε_{t-j} are the lagged forecast errors and ε_t are the error terms. To choose the optimal order of the ARIMA model, we estimate different model fittings where each parameter p , d , and q can each take values from 0 to 10. The (p, d, q) combination that shows the lowest Akaike Information Criterion (AIC), which focuses on the goodness of fit, is taken. After fitting the ARIMA model for each index, we analyze the model residuals on autocorrelation with the Ljung-Box test and on normality with the Jarque-Bera test. We also check if heteroskedasticity is present in the model residuals. After model diagnostics, we apply the GJR-GARCH model on the ARIMA residuals to capture the volatility dynamics as follows:

$$\varepsilon_t = \sigma_t \cdot \eta_t \quad (2.3)$$

$$\sigma_t^2 = \omega + \sum_{i=1}^p \alpha_i \cdot \varepsilon_{t-i}^2 + \sum_{h=1}^o \gamma_h \cdot \varepsilon_{t-h}^2 \cdot I_{t-h} + \sum_{j=1}^q \beta_j \cdot \sigma_{t-j}^2 \quad (2.4)$$

where η_t is white noise, σ_t^2 denotes the conditional variance, ω denotes the baseline volatility, α_i is the coefficients of past shocks, γ_h denotes the coefficient of leverage effect,³ I_{t-h} is a dummy variable that equals 1 if $\varepsilon_{t-h} < 0$ and 0 otherwise, β_j denotes the coefficients of volatility persistence over time. We choose the GJR-GARCH model since it extends the standard GARCH model by considering asymmetry in volatility response to positive and negative shocks, i.e., leverage effect. The GJR-GARCH (p, o, q) includes the order of the past shocks' component, indicated as p , the order of asymmetry, indicated as o , and the order of the persistence of volatility over time, indicated as q . To choose the optimal order for the GJR-GARCH model, similar as for the ARIMA model, we estimate different model fittings and take the one with the lowest BIC. Here, we consider BIC since, compared to AIC, it prioritizes model parsimony. Our decision to select the ARIMA model with AIC and the GJR-GARCH model with BIC follows the goal of receiving a detailed mean model and a stable volatility model. By applying this approach in the ARIMA-GJR-GARCH model selection, we leverage the strengths of both criteria. After fitting the GJR-GARCH model, we check the model on stability with the Cumulative Sum control chart (CUSUM) test, on remaining volatility clustering and on conditional heteroscedasticity, i.e., ARCH effects, in squared standardized residuals with the Ljung-Box test and Engle's ARCH test, respectively.

Our goal is to analyze how options elasticity influence option rates of return and the elasticity sensitivity to option delta and leverage changes. For this we employ two separate mixed effect panel regressions for each sample as:

$$r_{it} = \alpha + \beta_{\text{VOLA}} \cdot \text{VOLA}_{it} + \beta_{\text{VOV}} \cdot \text{VOV}_{it} + \beta_{\Omega} \cdot \Omega_{it} + \beta_{\text{M}} \cdot \text{M}_{it} + \beta_{\text{OI}} \cdot \text{OI}_{it} + \beta_{\text{VOL}} \cdot \text{VOL}_{it} + \gamma_t + u_i + \xi_{it} \quad (2.5)$$

³Negative shocks increase volatility more than positive shocks of the same magnitude.

where, for each option i at each point in time t , r_{it} denotes the rate of return, Vol_{it} denotes the underlying volatility estimated with the ARIMA-GJR-GARCH model, VOV_{it} denotes the volatility of underlying volatility, Ω_{it} denotes elasticity, M_{it} denotes moneyness, VOL_{it} denotes volume, OI_{it} denotes open interest, γ_t is the time effect (fixed effect which captures unobserved heterogeneity over time), u_i is the random effect (random effect which captures unobserved heterogeneity across entities), and ξ_{it} denotes the residual. We calculate the elasticity based on the Black and Scholes (1973) and Merton (1973) framework and Kraft (2003) where the elasticity for call Ω_{call} and put Ω_{put} options equal:

$$\Omega_{call} = \frac{dC/C}{dS/S} = \delta_{call} \cdot \frac{S}{C} \quad \Omega_{put} = \frac{dP/P}{dS/S} = \delta_{put} \cdot \frac{S}{P} \quad (2.6)$$

where δ_{call} and δ_{put} equals $N(d_1)$ and $N(-d_1)$, respectively, with $d_1 = \frac{\ln(\frac{S}{K}) + (r_f + \frac{\sigma_S^2}{2}) \cdot T}{\sigma_S \sqrt{T}}$ where S denotes the price of the underlying, K denotes the strike price, r_f denotes the risk-free rate of return, σ_S denotes the volatility of the underlying, T is the time to maturity; S/C and S/P represent the options leverage with C and P denoting the price of call and put option, respectively. To analyze the elasticity sensitivity to delta and leverage, we run the following mixed effects panel regression:

$$\begin{aligned} \Omega_{it} = & \omega + \beta_{\Omega_{t-1}} \cdot \Omega_{it-1} + \beta_{\text{VOL}_{it}} \cdot \text{VOL}_{it} + \beta_{\Delta} \cdot \Delta_{it} + \beta_{\text{LEV}_{it}} \cdot \text{LEV}_{it} \\ & + \beta_{\text{OI}_{it}} \cdot \text{OI}_{it} + \beta_{\text{VOL}} \cdot \text{VOL}_{it} + \chi_t + \lambda_i + \zeta_{it} \end{aligned} \quad (2.7)$$

where, for option i at time t , Δ_{it} denotes option delta, LEV_{it} denotes option leverage and χ_t , λ_i , ζ_{it} represent the time-specific effect, entity-specific effect and error term, respectively. We add the lagged elasticity, which refers to a dynamic panel model, to account for persistence. Since the scales of the independent variables are different, we standardize (normalize) the data before running the regression. This serves not only the numerical stability of our model but also ensures that each independent variable equally contributes to the model. We include the constant in the regression to better capture the mean levels of the data and to have a baseline return, which helps to interpret other effects. Our choice to run a mixed effects panel regression is based on the underlying volatility measure. Since we analyze options written on a single index for each market, for each sample the underlying volatility is constant across options (entities). When running a fixed effects panel regression including either time or entity effects, the underlying volatility is absorbed, indicating a perfect collinearity with these effects. By including time fixed effects in a random effects model, we control for time-specific shocks with random variation across entities. The random effects model assumes that the entity-specific effects are random and uncorrelated with the independent variables, thus it estimates the effect of time-invariant variables such as underlying volatility, which changes over time but is constant across entities within each time period and for options maturity. To take into consideration heteroscedasticity and autocorrelation, we use the covariance estimator according to Newey and West (1987) to calculate the standard errors. We check the independent variables for multicollinearity by calculating the Variance Inflation Factor (VIF) and pairwise correlation coefficients. For the model diagnostics, we use the F-test and the Wald test to check the overall model significance and the significance of the joint effect of independent variables on the dependent variable, and the Durbin-Watson test to check for autocorrelation in residuals.

3 Data

Option data is obtained from IVolatility.com. The sample consists of American-style call and put index options on the EU and US markets with the time horizon from January 2011 to March 2021. The ES50 represents the index for the EU market; it consists of 50 blue-chip companies across 12 Eurozone countries, where each stock is weighted by free-float market capitalization. The N100 represents the index

for the US market; it consists of the 100 largest non-financial companies listed on the N100 stock market also weighted by free-float market capitalization. These indices were chosen because of the large number of options traded on both indices, which leads to continuous observations with little noise compared to other indices. Each option in the dataset is identified by its strike price and its expiration date. In order to increase the data quality, for each point in time, we keep options: (i) with positive bid and ask prices, positive trading volume, and open interest; (ii) that have not reached their expiration date yet; (iii) with bid price lower than the ask price. We leave out options with observations less than five as this leads to low sample sizes for the regression. As for the risk-free rate of return, we obtain the data from Kenneth French's website⁴ for the corresponding time period and for the corresponding market. We calculate the time-to-maturity in business days and later transform it to the yearly term to calculate option elasticity. To compute the option rates of return, we use the underlying close stock price that is adjusted for corporate actions like splits, special cash, and others. We also adjusted the option return to the number of trading days between observations to get the daily option return. Option leverage is calculated as the ratio of the underlying close stock price and option price, and option moneyness is calculated as the ratio of the underlying close stock price and option strike price. We calculate the moneyness in dynamic, i.e., at each point in time, to capture its real-time changes, which reflect the current market state. For call options with moneyness levels $1.025 \geq M \geq 0.975$, we refer to ATM options; options with $M > 1.025$ and $M > 1.1$ represent ITM and DITM options, options with $M < 0.975$ and $M < 0.9$ represent OTM and DOTM options, respectively. The opposite holds for put options. Option volume represents the number of option contracts traded and option open interest is the total number of outstanding option contracts that have not been settled or closed yet.

Table 3.1 depicts the summary statistics for the analyzed samples. The mean daily return for all samples is positive; for call options on the EU market, the daily return shows higher variability (the standard deviation for the EU market is 1.81 and for the US market 0.47) and extreme outliers compared to call options on the US market (the maximum daily return for the EU market is 646.12 and for the US market, it is 29.04). The same holds for put options; however, the level of outliers is smaller compared to call options (the maximum daily return for the EU market is 293.42, and for the US market, it is 73.16). This greater variability emphasizes a more dynamic and riskier trading environment on the EU market. The presence of extreme outliers in returns suggests that EU options may be subject to more sudden price fluctuations. The mean moneyness for call options on the EU and the US market is almost at the same level (0.96 on the EU market and 0.98 on the US market); for put options, the mean is a bit higher (1.21 on the EU market and 1.11 on the US market) but also at the same level. EU call options show a much wider range from 0.43 to 35.75 compared to US call options, with a range from 0.60 to 4.78. EU put options also exhibit higher moneyness, however, at a lower level, ranging from 0.23 to 7.84, compared to US options with a range from 0.56 to 3.92. A wider dispersion in moneyness values and the variability of EU options suggest a broader range of risk exposures and could reflect a more heterogeneous set of market views and hedging strategies.

Figure 3.1 visualizes the distribution of option moneyness categories for all samples. EU call options cover each moneyness category more or less equally, showing a little higher concentration around the OTM category. US call options are less balanced, having a notable peak around the ATM category (over 40 percent). The concentration around ATM options might reflect the speculative trading strategy where investors benefit from immediate sensitivity (short-term price movement) to changes in the underlying. EU and US put options both show a concentration around DOTM options, for EU option, it is more pronounced (over 50 percent). Such a high concentration might reflect the trading strategy where investors hedge their investments against the downside risk of the underlying. For the EU market, the

⁴<https://mba.tuck.dartmouth.edu/pages/faculty/ken.french/data.library.html>

Table 3.1: Summary statistics

This table provides summary statistics of daily return, moneyness, volume, open interest, elasticity, and leverage for all 1,726,772 EU and US call and put options in the dataset. It reports the mean, standard deviation (std), minimum (min), 25th percentile (25%), 50th percentile (50%), 75th percentile (75%), and maximum (max) values for the daily return, moneyness (M), volume (VOL), open interest (OI).

	Daily return	M	VOL	OI
EU call options (n=322,232)				
mean	0.0260	0.9640	3071	46937
std	1.8134	0.2822	7950	60394
min	-0.9994	0.4310	1	1
25%	-0.0909	0.9091	25	4993
50%	-0.0071	0.9632	266	22476
75%	0.0653	1.0066	2300	67219
max	646.1290	35.7541	505110	460154
US call options (n=375,750)				
mean	0.0407	0.9828	47	290
std	0.4776	0.0970	234	807
min	-0.9740	0.6030	1	1
25%	-0.1196	0.9521	2	19
50%	-0.0049	0.9826	6	57
75%	0.1000	1.0052	22	191
max	29.4000	4.7856	12763	14385
EU put options (n=506,083)				
mean	0.0055	1.2158	2817	50975
std	0.6747	0.3129	6999	67549
min	-0.9960	0.2375	1	1
25%	-0.1019	1.0362	45	5079
50%	-0.0190	1.1282	332	23153
75%	0.0478	1.2904	2194	70372
max	293.4282	7.8408	559367	575901
US put options (n=522,707)				
mean	-0.0007	1.1114	54	339
std	0.5344	0.1861	373	1130
min	-0.9790	0.5658	1	1
25%	-0.1638	1.0153	2	21
50%	-0.0458	1.0547	7	64
75%	0.0442	1.1323	23	215
max	73.1667	3.9238	74308	70737

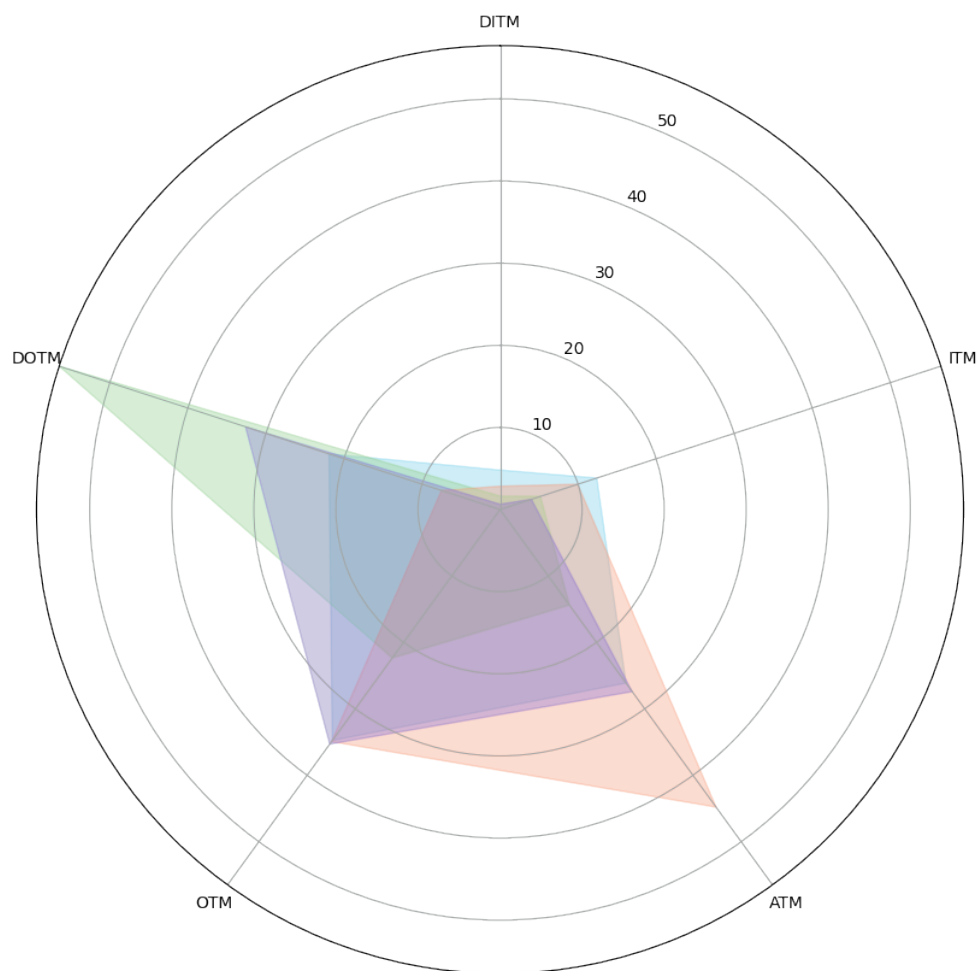


Figure 3.1: Distribution on moneyness categories

The figure shows the distribution of all EU and US call and put options in the sample over the different option moneyness categories DOTM, OTM, ATM, ITM, and DITM in percentage terms.

balanced distribution in call options and the concentrated put options around DOTM options indicate a conservative and hedge-oriented trading behavior, whereas on the US market, the concentration of call options around ATM options signals a preference for speculative strategies with higher risk-taking and more aggressive trading behavior. The volume for EU call and put options with 3,071 and 2,817, respectively, is much higher than for US call and put options with 47 and 54. Similarly, the maximum level of open interest for EU call and put options is 460,154 and 575,901, respectively, which is higher compared to 14,385 and 70,737 for options on the US market. Volume and open interest statistics reveal higher trading activity and greater market participation on the EU market. All samples show extreme elasticity values with US options showing higher elasticity compared to EU options. For call options, the mean elasticity is 55.72 and 73.68 for the EU and the US markets, respectively. For put options, the mean elasticity for the EU market is 8.38, which is way lower than 20.35 for the US market. Higher values for the US market indicate that options on this market are more responsive to changes in the underlying, i.e., the N100 index.

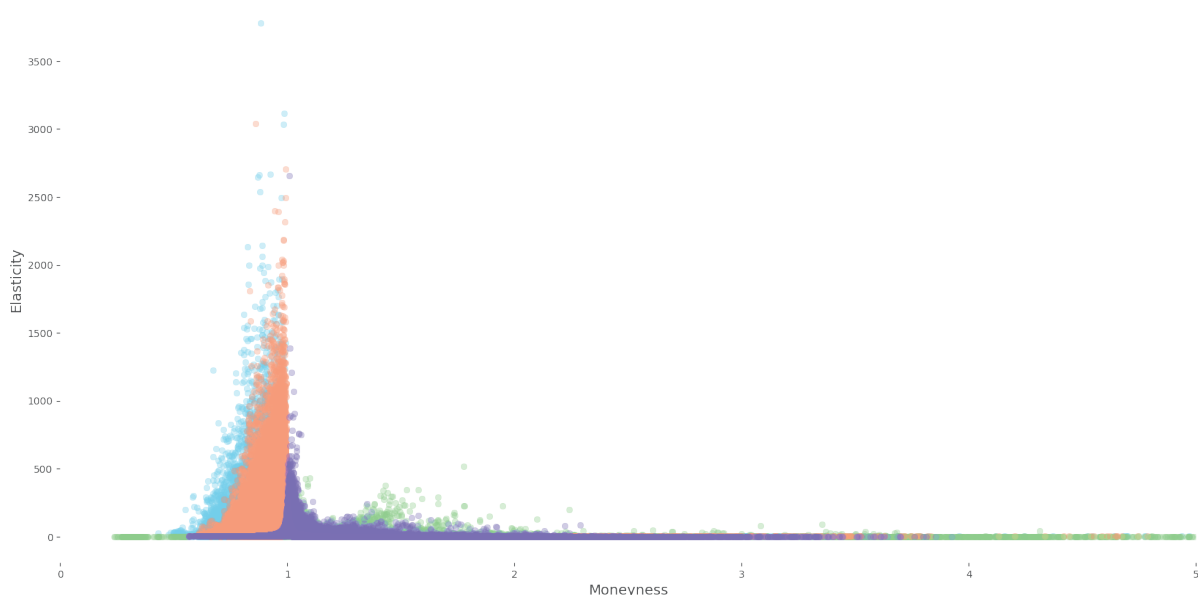


Figure 3.2: Elasticity vs. moneyness

The figure shows the elasticity of the options as a function of their moneyness. For reasons of presentation, observations with moneyness greater than 5 are excluded from this graph.

Figure 3.2 depicts option elasticity against moneyness for all samples with moneyness values smaller than 5 (this range is chosen for a more viewable figure). The elasticity for EU and US call options shows a high concentration around ATM category, whereas EU and US put options disperse across OTM and ITM categories, with EU put options being wider spread in the OTM category. The elasticity for US call options is tight, showing the highest elasticity for ATM options, while EU options are more spread and showing another concentration around OTM options. The same observation holds for put options; on the US market, the elasticity is tight, showing the peak around the ATM category, on the EU market, it is clustered through the OTM category with a strong accent on DOTM options. This figure highlights that the trading behavior on the EU market is risk-averse compared to more risk-loving trading behavior on the US market. Likewise the elasticity, leverage values are also very high, with US options show higher values and EU options exhibit higher means. The greater leverage observed on the US market indicates a more aggressive risk-return tradeoff on the market. The differences in statistics on option characteristics on the EU and US markets reflect varying market dynamics, risk levels, and trading strategies. The more pronounced volatility and higher trading activity on the EU market indicate a tendency towards

frequent trading and greater risk tolerance. On the contrary, the pronounced elasticity and leverage on the US market suggest a possibility of higher returns from small price fluctuations.

4 Results

Table 4.1 represents the summary statistics for N100 and ES50 rates of return. The mean daily return and volatility are at similar levels for both indices, with the ES50 index having a slightly lower mean and higher volatility. The rate of return distribution for both indices is left-skewed, indicating a tendency for negative rates of return (more pronounced for ES50), and exhibits heavy tails, indicating extreme rates of return (more pronounced for N100). The normality test confirms that rates of return for both indices don't follow a Gaussian distribution; the null hypothesis is rejected at the one percent significance level. The Augmented Dickey-Fuller (ADF) test on stationarity shows that both return series are stationary since both ADF statistics are lower than the corresponding ADF critical values.

Table 4.1: Index return statistics

The table provides comprehensive statistics for N100 and ES50 indices. It includes counts of observations, measures of central tendency such as mean and median (50%), variability metrics like standard deviation (Vola), and distribution characteristics such as minimum (Min), maximum (Max), percentiles (25% & 75%) skewness, and kurtosis. Additionally, it presents results from statistical tests: Shapiro-Wilk statistic for normality assessment and ADF statistic for testing unit root presence. *** indicates statistical significance at the 1% level.

	N100	ES50
Count	2571	2599
Mean	0.0762	0.0200
Vola	1.2600	1.3016
Min	-12.1932	-12.4014
25%	-0.4194	-0.5848
50%	0.1174	0.0443
75%	0.6912	0.6307
Max	10.0722	9.2362
Skewness	-0.4448	-0.5133
Kurtosis	12.41	10.51
Shapiro-Wilk statistic	0.909***	0.932***
ADF statistic	-11.558	-18.895
ADF critical value at 1%	-3.4329	-3.4328

Table 4.2 summarizes the results of the ARIMA model fit (ARIMA (5,0,5) for N100 and ARIMA (8,0,2) for ES50), with a slightly better fit for the N100 rates of return series based on Log-Likelihood, AIC, and BIC. Both models show a positive and highly significant constant, which suggests an upward drift over time. The AR part for the indices is different. The N100 model with fewer AR and larger coefficients (showing negative and positive coefficients and all highly significant) indicates a strong autoregressive behavior. The ES50 model includes more AR terms (also with a mix of negative and positive coefficients and almost all highly significant), suggesting a complex autoregressive structure that reflects unique market dynamics. The MA part also shows differences. The N100 model includes more AM terms with larger mixed coefficients, indicating stronger adjustment for past errors, which is typical for volatility clustering or reaction to shocks. The MA structure for the ES50 model is short, which suggests a smoother error correction. The variance of residual being greater for the ES50 model implies a greater level of unexplained volatility. The diagnostics tests show that there is no significant autocorrelation in residuals and that they are not normally distributed and exhibit skewness and heavy tails. The residuals for both models show heteroskedasticity, which approves our next step, i.e., GJR-GARCH model fit. Since ARIMA residuals exhibit skewness and heavy tails, we model the GJR-GARCH process under the Standardized Skewed Student's distribution which includes two parameters, i.e., eta and lambda, which control for tail shape and skewness.⁵

⁵See Hansen (1994).

Table 4.2: ARIMA summary

The table presents the summary of the ARIMA model comparing N100 and ES50. It includes counts of observations, log likelihood, AIC, and BIC, along with coefficient estimates and standard errors for each model parameter alongside the autoregressive (AR) and moving average (MA) terms. Diagnostic tests for model adequacy (stat), including Ljung-Box, Heteroskedasticity, Jarque-Bera statistics, skewness, and kurtosis, with their respective p-values (prob). *, **, and *** indicate significance at the 10%, 5%, and 1% level respectively.

	N100	ES50		
n observations	2571	2599		
Log Likelihood	-4169.70	-4356.41		
AIC	8363.41	8736.81		
BIC	8433.63	8807.17		
const	0.0755*** (0.0150)	0.0207*** (0.0070)		
ar1	-1.7383*** (0.0640)	0.4519*** (0.1350)		
ar2	-0.8493*** (0.1010)	0.5630*** (0.1370)		
ar3	0.9585*** (0.0560)	-0.0141 (0.0150)		
ar4	1.5236*** (0.0810)	-0.0453*** (0.0160)		
ar5	0.7427*** (0.0520)	-0.0177 (0.0180)		
ar6		0.0272* (0.0160)		
ar7		0.0873*** (0.0160)		
ar8		-0.0645*** (0.0150)		
ma1	1.6207*** (0.0680)	-0.4480*** (0.1350)		
ma2	0.6817*** (0.1000)	-0.5500*** (0.1350)		
ma3	-1.0309*** (0.0480)			
ma4	-1.4454*** (0.0880)			
ma5	-0.6391*** (0.0560)			
sigma2	1.5052*** (0.0250)	1.6711*** (0.0240)		
	stat	prob	stat	prob
Ljung Box	0.0200	0.9000	0.0000	0.9900
Heteroskedasticity	1.8500	0.0000	0.8700	0.0500
Jarque-Bera	4559.1800	0.0000	6507.9000	0.0000
Skew	-0.7100		-0.6600	
Kurtosis	9.3700		10.6400	

Table 4.3: GJR-GARCH summary

The table presents a summary of the GJR-GARCH model comparing N100 and ES50. It includes the number of observations, log likelihood, AIC, and BIC. Coefficient estimates and their respective standard errors for model parameters—such as mean (μ), persistence (ω), leverage effect (α_1 , γ_1), volatility persistence (β_1), asymmetric shock (η), and leverage parameter (λ). Diagnostic tests for model adequacy, including Ljung-Box, Engle's ARCH statistic, and CUMSUM statistics, with their respective p-values (prob). *, **, and *** indicate significance at the 10%, 5%, and 1% level respectively.

	N100	ES50		
n observations	2571	2599		
Log Likelihood	-3632.33	-3839.38		
AIC	7278.66	7692.76		
BIC	7319.62	7733.80		
mu	0.0084 (0.0183)	0.0052 (0.0184)		
omega	0.0479*** (0.0094)	0.0349*** (0.0105)		
alpha1	0.0201 (0.0145)	0.0000 (0.0157)		
gamma1	0.2211*** (0.0343)	0.2268*** (0.0431)		
beta1	0.8370*** (0.0180)	0.8702*** (0.0277)		
eta	6.0857*** (0.7000)	6.1054*** (0.7250)		
lambda	-0.1877*** (0.0263)	-0.0950*** (0.0263)		
	stat	prob	stat	prob
Ljung Box	4.3792	0.928618	9.6181	0.4746
Engels ARCH statistic	0.8086	0.9999	0.8595	0.9999
CUMSUM Statistic	0.6552		0.7356	
CUMSUM critical value	0.7837		0.6513	

Table 4.3 summarizes the results for the GJR-GARCH model fit (for both indices GJR-GARCH (1,1,1)), again based on summary metrics, the N100 index show a slightly better fit. The coefficients for the volatility model, i.e., ω , α , γ and β , are highly significant (except for α) for both markets. The level of all volatility coefficients is almost identical for both markets. The insignificant α coefficient indicates that past shocks have no impact on volatility, whereas the highly significant γ coefficient implies the presence of leverage effects, which is slightly higher for the ES50 index. The highly significant β coefficients suggest volatility persistence over time with the ES50 index volatility being a little more persistent. Distribution coefficients for tail and skewness confirm the previous observations. The diagnostic on model adequacy for both indices shows no significant autocorrelation and remaining ARCH effects indicating that fitted processes capture the volatility clustering and heteroscedasticity of rates of return series. The CUMSUM test for the N100 GJR-GARCH process indicates that there is no evidence of significant structural breaks and the model is stable (the test statistic is less than the critical value). The ES50 GJR-GARCH process shows marginal instability with the test statistic exceeding the critical value by a small margin (0.0843). However, this evidence of instability is not pronounced since the difference is not large.



Figure 4.1: GJR-GARCH

The figure shows the GJR-GARCH forecasted volatility versus the realized rolling volatility. The upper graph illustrates the N100, while the lower graph represents the ES50. This comparison highlights the predictive accuracy of the GJR-GARCH model by contrasting its forecasts with the actual observed volatility over time, providing insights into model performance and market behavior.

Figure 4.1 depicts the volatility dynamics forecasted by the GJR-GARCH process and the realized 7-days rolling volatility for the N100 and the ES50 rates of return. Both fitted GJR-GARCH models track the realized volatility very close suggesting a good fit. There are similar notable peaks at years 2011, 2015, and 2020-2021 which mirror European sovereign debt crises, the Chinese stock market crash and the COVID-19 pandemic. For the ES50 there is one more notable peak at the year 2016 likely due to the Brexit referendum. The volatility dynamics for N100 returns show that the market reacts to global macroeconomic events more pronounced compared to steadier volatility in other periods. The volatility for ES50 rates of return is also highly sensitive to market sentiment, however, it also exhibits more frequent spikes in volatility in other periods, indicating increased market instability beyond sentiment-driven fluctuations.

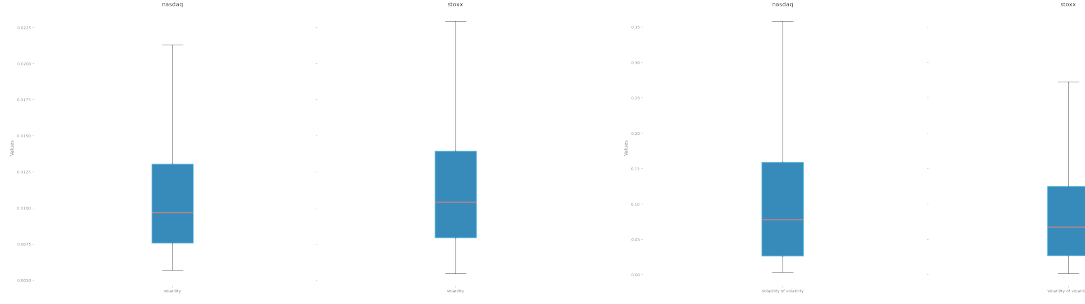


Figure 4.2: Box plots

The figure shows the volatility box plots. The left panel illustrates the distribution for the N100, while the right panel represents the ES50. This visualization presents the distribution of volatility data, highlighting the median, quartiles, and potential outliers, providing a clear summary of the variability and dispersion of volatility across these indices.

Figure 4.2 depicts box plots for the volatility (left-hand side graph) and the volatility of the volatility (right-hand side graph) for the N100 and the ES50 indices. The volatility level and the corresponding upper and lower whiskers are also identical with slightly higher values for the ES50. However, there is a notable difference for indices' VOV levels. For the N100, the dispersion between upper and lower quartiles is greater and the upper whisker is higher than the ones of the ES50. This difference might be explained with respect to the constituents of each index. The N100 excludes companies from the financial sector and is dominated by the tech industry. The ES50 represents blue-chips companies from all industries in the European Union. Compared to the N100, the ES50 represents a more diverse portfolio which might lead to a more stable volatility. However, we note that the ES50 consists of only 50 companies compared to 100 included in the N100 which might weaken the effect of our argumentation above.

To understand the elasticity dynamics, we sort options into seven volatility bins⁶ based on the underlying volatility level of the GJR-GARCH model. Then, we group options based on their volatility bin and moneyness category and calculate the average elasticity for each group. Figures 4.3 and 4.4 illustrate elasticity surfaces for all samples with color gradient yellow-grey-blue indicating the elasticity range from highest to lowest, respectively. Call options' elasticity decreases with moneyness for both the US and the EU market, showing a peak around DOTM option and low volatility bins. From the point of view of volatility bins, the elasticity remains moderately high across all bins for DOTM options, with two peaks observed in BA-L and L-VL bins for the US market and a single notable peak in AA-A bins for the EU market. This might indicate the investors' interest in leveraging their position when the volatility is low and in hedging strategies for unexpected market conditions. The elasticity surface gradient for the US market is steeper with more sharp transitions between moneyness categories and broader peaks compared to softer transitions and more narrow peaks for the EU market. For put options, the elasticity also decreases with moneyness, however having its peak around ATM options for the VL volatility bin, suggesting a high interest in protective put strategies. For the US market, it shows a significant peak at L-VL bins for ATM options and a less remarkable peak at BA-L bins. For the EU market, the surface shows several significant peaks. The most remarkable peak is in the A volatility bin for OTM options, followed by a peak in the VL bin for ATM options, with the least significant peak in the H bin for OTM options. The elasticity exhibits a peak at the VL bin for ATM options for the US market; however, for the EU market, the same magnitude peak is at the H bin for OTM options. The second and third elasticity peaks for the EU market might be due to the more frequent volatility peaks in the underlying. High elasticity values for low volatility bins and ATM and OTM options confirm investors' interest in hedging strategies even when market volatility is low. The elasticity surfaces for both markets show steep gradient transitions across moneyness categories, with broader peaks observed in the EU market.

⁶Very low (VL), low (L), below average (BA), average (A), above average (AA), high (H), very high (VH)

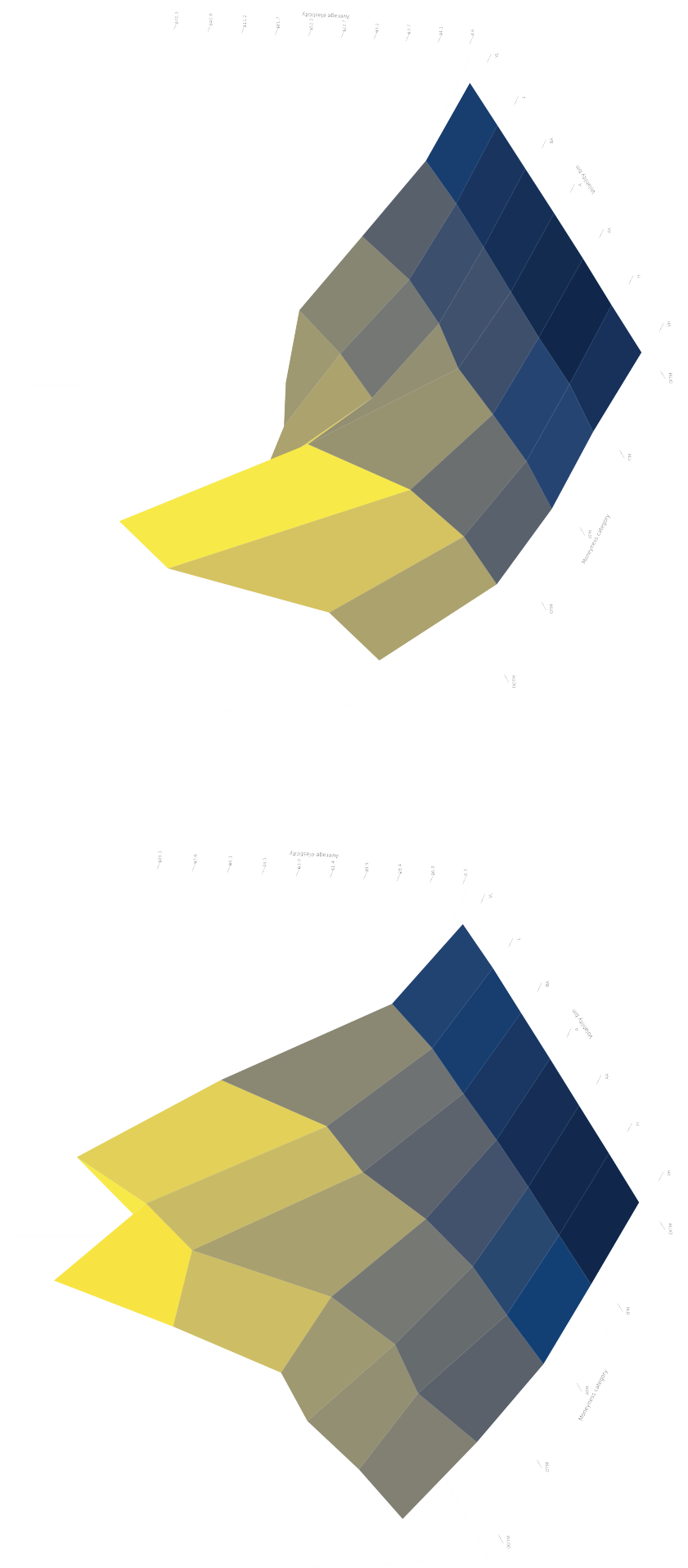


Figure 4.3: Elasticity surfaces for call options

The figure shows the elasticity surfaces, presenting the average elasticity by volatility and moneyness categories. The left panel illustrates the N100 call options, while the right panel represents the ES50 call options. This visualization illustrates how elasticity varies with changes in volatility and moneyness across different market conditions.



Figure 4.4: Elasticity surfaces for put options

The figure shows the elasticity surfaces, presenting the average elasticity by volatility and moneyness categories. The left panel illustrates the N100 put options, while the right panel represents the ES50 put options. This visualization illustrates how elasticity varies with changes in volatility and moneyness across different market conditions.

Table 4.5 represents the mixed effects panel regression outputs according to equation 2.5 for each sample. The levels of R-squared are low for all samples, meaning that the model explains a low part in return variations. The values for overall R-squared are a little bit higher for the US market, showing a slightly better model fit. The negative values for between R-squared for US call and EU put options, alongside the positive within R-squared values, suggest that the model captures time-series variation within entities more effectively than cross-sectional variation across entities. For call options, the volatility coefficients are positive but insignificant, indicating that the rate of return on call options increases with volatility; the coefficients are slightly higher for the EU market. The VOV coefficients differ and are also insignificant. For the US market, it is negative, for the EU market, it is positive. This suggests that rates of return on call options decrease with increasing uncertainty on the US market. The elasticity coefficients for both markets are almost at the same level and are significantly negative, indicating decreasing rates of return with increasing elasticity. The moneyness coefficients differ in significance. For the US market, it is significantly positive, for the EU market, it is insignificantly negative. This suggests that rates of return increase with options being more in the money for the US market. The open interest coefficients are negative for both markets, however, being significant and slightly higher for the EU market. The volume coefficients are significantly positive for both markets. For put options, the volatility coefficients mirror the ones for the call options; they are negative and insignificant, implying that rates of return on put options decrease with increasing volatility. The VOV coefficients are positive and significant for both markets and higher for the EU market. This suggests that the rates of return on put options increase with increasing uncertainty which might indicate the interest in put protection. The elasticity coefficients are significantly negative for both markets, indicating decreasing rates of return with increasing elasticity. Negative and highly significant elasticity coefficients across all samples suggest that index options yield lower rates of return when the sensitivity of option prices to changes in the underlying is high. This, in turn, suggests that these changes lead to lower option prices resulting in a lower rate of return. The moneyness coefficients are significantly negative for both markets, indicating decreasing rates of return when put options become more ITM options. The open interest coefficients are significantly negative and the volume coefficients are significantly positive. The cross-section of option rates of return on the US and the EU markets show overall similar effects with respect to the underlying volatility (except for US put options), the VOV (except for US call options), elasticity, open interest, and volume. However, we find that put options on the EU market are more sensitive to changes in the uncertainty about the volatility. This suggests that the investor in the EU market might be more risk-averse. For the US market, we observe notably higher sensitivities of call and put options with respect to elasticity and moneyness. The model diagnostics confirm the significance and validity of our model.

Table 4.4: Variance inflation factors I

The table presents VIFs for return regressions in the form of equation 2.5 for call and put options on N100 and ES50. VIFs measure multicollinearity among predictor variables, with values close to 1 indicating low multicollinearity. Each row corresponds to a predictor variable, including Intercept, Vola, VOV, M, Elasticity, OI and VOL. Higher VIFs suggest stronger correlations between predictors, potentially affecting the reliability of regression coefficients.

	Call Options		Put Options	
	N100	ES50	N100	ES50
Intercept	1.0000	1.0000	1.0000	1.0000
VOLA	1.3339	1.3816	1.4305	1.5384
VOV	1.3261	1.3808	1.4023	1.4937
M	1.0342	1.0064	1.1421	1.1646
Ω	1.0366	1.0125	1.1364	1.1554
OI	1.1884	1.1467	1.0827	1.1703
VOL	1.1869	1.1446	1.0800	1.1959

Table 4.7 represents the results of the mixed effects panel regression according to equation 2.7 for

Table 4.5: Return regression outputs I

The table presents outputs from return regressions in the form of equation 2.5 for call and put options on N100 and ES50. It includes various statistics such as the number of observations, R-squared values, number of entities and time periods, and coefficient estimates with their corresponding statistical significance. Diagnostic tests include F-test, Wald test, and Durbin-Watson test for autocorrelation, highlighting the model's explanatory power and goodness of fit. The four columns on the left present the coefficients, while the four columns on the right-hand side present the corresponding robust standard errors.

	Call Options		Put Options	
	N100	ES50	N100	ES50
<i>n observations</i>	375750	322232	522707	506083
<i>r-squared</i>	0.0073	0.0003	0.0132	0.0032
<i>r-squared (between)</i>	-0.0412	0.0022	0.0014	-0.0059
<i>r-squared (within)</i>	0.0103	0.0003	0.0148	0.0035
<i>r-squared (overall)</i>	0.0032	0.0003	0.0091	0.0009
<i>entities</i>	25787	8362	35146	11962
<i>time periods</i>	2562	2578	2562	2578
Intercept	0.0461*** (0.0083)	0.0260*** (0.0063)	0.0018 (0.0109)	0.0152 (0.0194)
VOLA	0.0055 (0.0084)	0.0141 (0.0089)	-0.0112 (0.0135)	0.0161 (0.0153)
VOV	-0.0021 (0.0087)	0.0004 (0.0062)	0.0034*** (0.0093)	0.0317*** (0.0071)
Ω	-0.0301*** (0.0029)	-0.0227*** (0.0043)	-0.0699*** (0.0047)	-0.0570*** (0.0050)
M	0.0304*** (0.0033)	-0.0037 (0.0037)	-0.0638*** (0.0058)	-0.0586*** (0.0056)
OI	-0.0008 (0.0019)	-0.0151*** (0.0039)	-0.0048** (0.0018)	-0.0049*** (0.0025)
VOL	0.0143*** (0.0034)	0.0195*** (0.0038)	0.0102*** (0.0025)	0.0098*** (0.0060)
F-test	34.2720	17.1850	30.2820	22.0970
p-value	0.0000	0.0000	0.0000	0.0000
Wald test	319.4600	106.5979	354.0529	209.9075
p-value	0.0000	0.0000	0.0000	0.0000
Durbin-Watson test	2.0712	2.0039	2.0721	2.0749

Table 4.6: Variance inflation factors II

The table presents VIFs for return regressions in the form of equation 2.7 for call and put options on N100 and ES50. VIFs measure with values close to 1 indicate low multicollinearity. Each row corresponds to a predictor variable, including Intercept, Elasticity (lagged), Vola, δ , LEV, OI, and VOL.

	Call Options		Put Options	
	N100	ES50	N100	ES50
Intercept	1.0008	1.0003	1.0009	1.0003
Ω_{t-1}	1.4718	1.4168	1.1195	1.1674
VOLA	1.0113	1.0123	1.0381	1.0045
Δ	1.2777	1.2775	1.1617	1.1735
LEV	1.4376	1.4425	1.0802	1.0944
OI	1.1956	1.1461	1.0870	1.1694
VOL	1.1924	1.1602	1.0803	1.1988

each sample. The values for the overall R-squared are high for all models with the EU market showing slightly higher values. The values of the between R-squared are higher than within R-squared once indicating the model capture differences between entities better. For call options, the lagged elasticity coefficients for all samples are significantly positive and higher for the US market, suggesting persistence in elasticity levels. Since we calculate the moneyiness in dynamic, this result might indicate that elasticity remains consistent throughout options' maturities. The volatility coefficients are insignificant. The delta coefficients are significantly negative on both markets with the stronger effect observed on the US market. This suggests that with increasing option sensitivity to changes in the underlying their elasticity decreases and, according to table 4.5, option rates of return increase. The leverage coefficients are significantly positive, with higher values for the US market, suggesting increasing elasticity for more out of the money options which is also visible in figures 4.3 and 4.4. The open interest coefficient varies. For the US market, it is significantly negative and, for the EU market, significantly positive. This suggest that for the US market, more liquid options show lower elasticity. However, for the EU market, it is other way around; this might imply differences in trading behavior and market structure. The volume

Table 4.7: Return regression outputs II

The table presents outputs from return regressions in the form of equation 2.7 for call and put options on N100 and ES50. It includes various statistics such as the number of observations, R-squared values, number of entities and time periods, and coefficient estimates with their corresponding statistical significance. Diagnostic tests include F-test, Wald test, and Durbin-Watson test for autocorrelation, illustrating the model's explanatory power and goodness of fit. The four columns on the left present the coefficients, while the four columns on the right-hand side present the corresponding robust standard errors.

	Call Options		Put Options	
	N100	ES50	N100	ES50
<i>n observations</i>	375750	322232	522707	506083
<i>r-squared</i>	0.7006	0.7137	0.6273	0.7320
<i>r-squared (between)</i>	0.9031	0.9131	0.8733	0.9440
<i>r-squared (within)</i>	0.5511	0.6649	0.5021	0.6593
<i>r-squared (overall)</i>	0.7468	0.7947	0.7857	0.8620
<i>entities</i>	25787	8362	35146	11962
<i>time periods</i>	2562	2577	2562	2577
Intercept	73.0844*** (0.6503)	53.5050*** (0.8835)	22.4404*** (0.2586)	10.0442*** (0.1908)
Ω_{t-1}	75.7601*** (1.2106)	69.3517*** (1.2927)	23.7731*** (0.4091)	12.2223*** (0.4297)
VOLA	0.9253 (0.7726)	0.9530 (1.2807)	0.2135 (0.3988)	-0.0545 (0.3645)
Δ	-5.6562*** (0.5009)	-2.6348*** (0.3584)	0.4238* (0.2323)	-0.0335 (0.0846)
LEV	9.2868*** (1.3402)	4.2652*** (1.3541)	-0.4895*** (0.0663)	-0.2667*** (0.0447)
OI	-0.5217** (0.2591)	1.2815*** (0.2967)	-0.1549*** (0.0376)	0.0543 (0.0478)
VOL	0.3650** (0.1650)	0.3684*** (0.1198)	0.0940*** (0.0347)	0.2470*** (0.0463)
F-test	2099.2000	1719.3070	1024.4050	2400.6009
p-value	0.0000	0.0000	0.0000	0.0000
Wald test	23065.4194	10374.5691	14199.2659	21173.2285
p-value	0.0000	0.0000	0.0000	0.0000
Durbin-Watson test	2.1400	2.2113	2.1038	2.0708

coefficients are significant for both markets. For put options, the lagged elasticity coefficients are also significantly positive on both markets, however lower than for call options. The volatility coefficients are again insignificant for both market. The delta coefficients show different results. For the US market, we observe a significantly positive effect, however, we do not observe any significance in the delta effect for the EU market. The leverage coefficients mirror the call options results; they are significantly negative with higher values for the US market. This implies that elasticity decreases with leverage; this might occur due to a use of hedging strategies. On the EU market, the leverage effect is less pronounced, suggesting differences in trading and risk management. The open interest coefficients differ, for the US market, it is significantly negative and, for the EU market, it is insignificantly positive. This once again hints at a difference in hedging strategies. The volume coefficients are significantly positive with a stronger effect for the EU market, suggesting increasing elasticity with trading volume. Here, we note that the key difference with respect to lagged elasticity, delta and leverage is that the observed effects are notably stronger for the US market. Additionally, for the EU market, we observe a stronger effect with respect to volume and mixed effects with respect to open interest. The model diagnostics confirm the significance and validity of our model.

5 Conclusion

In option pricing, the literature regularly refers to data from the US option market. This paper takes this as its starting point and examines whether the findings from the US market are transferable to the EU market. Options traded on the N100 serve as a representation of the US option market, while options traded on the ES50 serve as a representation of the EU option market. We find that differences in market behavior and the relationships between common variables for both call and put options exist.

We conduct a battery of additional tests and our results show distinct patterns in option elasticity

across different volatility levels and moneyness categories for the US and EU markets. Call option elasticity generally decreases with moneyness, peaking around DOTM options in low volatility bins. The US market displays sharper transitions and broader peaks in elasticity compared to the EU market, where transitions are softer and peaks are narrower. Put option elasticity also decreases with moneyness but peaks around ATM options in very low volatility environment, reflecting a preference for protective put strategies. Notably, the EU market exhibits three peaks in elasticity for ATM and OTM options in very low and average volatility conditions, respectively, likely due to more frequent volatility spikes. These findings highlight investors' tendencies to leverage positions in low volatility environments and adopt hedging strategies, with the EU market showing broader and more frequent peaks in elasticity.

We evaluate effects regarding rates of return and elasticity of options individually. Regarding rates of return, across all samples we find no effect of the underlying volatility as well as no effect of volatility of volatility for call options. Elasticity negatively affects rates of return in both markets, suggesting that higher sensitivity of option prices to changes in the underlying results in lower overall returns. Moneyness positively affects US call options but does not influence EU call options. For put options, we observe a negative effect on both markets. Open interest negatively impacts rates of return, while trading volume has a positive effect on both markets. For put options, we observe increasing rates of return with higher uncertainty on both markets which a stronger effect on the EU market. These findings suggest that investors in both markets may demand higher returns to compensate for the increased risk due to greater sensitivity to volatility-related uncertainty. The stronger effect on the EU market might indicate a greater reliance on put options for downside protection, reflecting a higher demand for hedging strategies compared to the US market.

Regarding elasticity, we find that it is persistent throughout options moneyness. For call options, underlying volatility shows no effect on elasticity. On the US market, higher liquidity reduces elasticity, whereas on the EU market, it increases elasticity, indicating different trading behaviors. Volume positively impacts elasticity on both markets. For put options, differences in open interest effects suggest varying hedging strategies. These findings highlight distinct trading and risk management practices between the US and EU markets. Taken together, our evidence highlights significant differences in option market behavior between the US and EU markets. This suggests that investors should carefully evaluate their choice of investment model and market to ensure greater precision in their strategies.

References

- Andersen, T. G., Fusari, N., and Todorov, V. (2017). Short-term market risks implied by weekly options. *Journal of Finance*, 72(3):1335-1386.
- Aretz, K., Lin, M.-T., and Poon, S.-H. (2022). Moneyness, underlying asset volatility, and the cross-section of option returns. *Review of Finance*, 27(1):289-323.
- Bali, T. G., Beckmeyer, H., Mörke, M., and Weigert, F. (2023). Option return predictability with machine learning and big data. *Review of Financial Studies*, 36(9):3548-3602.
- Baltussen, G., van Bakkum, S., and van der Grint, B. (2018). Unknown unknowns: Uncertainty about risk and stock returns. *Journal of Financial and Quantitative Analysis*, 53(4):1615-1651.
- Black, F. and Scholes, M. (1973). The pricing of options and corporate liabilities. *Journal of Political Economy*, 81(3):637-654.
- Carr, P. and Wu, L. (2020). Option profit and loss attribution and pricing: A new framework. *Journal of Finance*, 75(4):2271-2316.

- Chaudhury, M. (2017). Volatility and expected option returns: A note. *Economics Letters*, 152:14.
- Christoffersen, P., Goyenko, R., Jacobs, K., and Karoui, M. (2017). Illiquidity premia in the equity options market. *Review of Financial Studies*, 31(3):811851.
- Cremers, M., Halling, M., and Weinbaum, D. (2015). Aggregate jump and volatility risk in the cross-section of stock returns. *The Journal of Finance*, 70(2):577614.
- Duan, J.-C. (1995). The garch option pricing model. *Mathematical Finance*, 5(1):1332.
- Eraker, B. and Yang, A. (2022). The price of higher order catastrophe insurance: The case of vix options. *The Journal of Finance*, 77(6):32893337.
- Glosten, L. R., Jagannathan, R., and Runkle, D. E. (1993). On the relation between the expected value and the volatility of the nominal excess return on stocks. *The Journal of Finance*, 48(5):17791801.
- Hansen, B. E. (1994). Autoregressive conditional density estimation. *International Economic Review*, 35(3):705730.
- Heng, Z. Y. and Leung, H. (2023). The role of option-based information on stocktwits, options trading volume, and stock returns. *Journal of Futures Markets*, 43(8):10911125.
- Hollstein, F. and Prokopczuk, M. (2017). How aggregate volatility-of-volatility affects stock returns. *Review of Asset Pricing Studies*, 8(2):253292.
- Hu, G. and Jacobs, K. (2019). Volatility and expected option returns. *Journal of Financial and Quantitative Analysis*, 55(3):10251060.
- Hu, Y., Lindquist, W. B., and Rachev, S. T. (2024). Sustainability-valued discrete option pricing in complete markets. *Journal of Sustainable Finance & Investment*, 135.
- Kannianen, J., Lin, B., and Yang, H. (2014). Estimating and using garch models with vix data for option valuation. *Journal of Banking & Finance*, 43:200211.
- Kelly, B., Pástor, L., and Veronesi, P. (2016). The price of political uncertainty: Theory and evidence from the option market. *Journal of Finance*, 71(5):24172480.
- Kraft, H. (2003). Elasticity approach to portfolio optimization. *Mathematical Methods of Operations Research (ZOR)*, 58(1):159182.
- Merton, R. C. (1973). Theory of rational option pricing. *Bell Journal of economics and management science*, 4(1):141183.
- Newey, W. and West, K. (1987). A simple, positive semi-definite, heteroskedasticity and autocorrelation consistent covariance matrix. *Econometrica*, 55(3):703708.
- Nugroho, D. B., Kurniawati, D., Panjaitan, L. P., Kholil, Z., Susanto, B., and Sasongko, L. R. (2019). Empirical performance of garch, garch-m, gjr-garch and log-garch models for returns volatility. *Journal of Physics: Conference Series*, 1307(1):17.
- Oh, D. H. and Park, Y.-H. (2023). Garch option pricing with volatility derivatives. *Journal of Banking & Finance*, 146:117.
- Orpiszewski, T., Thompson, M., and Schwendner, P. (2023). The stock and option market response to negative esg news. *SSRN Electronic Journal*.

- Papantonis, I. (2016). Volatility risk premium implications of garch option pricing models. *Economic Modelling*, 58:104-115.
- Reichling, P., Selle, J., and Zbandut, A. (2023). The influence of volatility and moneyness on equity option returns-an empirical analysis. *Working Paper, available from the authors*.
- Ruan, X. (2020). Volatility-of-volatility and the cross-section of option returns. *Journal of Financial Markets*, 48:126.

Pricing of wrapped Bitcoin and Ethereum on-chain options

Anastasiia Zbandut*

This draft: October 22, 2024

Abstract

This paper empirically analyzes mispricing in the Hegic protocol relative to the benchmark prices. It uses the Black Scholes model where the underlying volatility is estimated via the two regimes MS-AR-(GJR)-GARCH model. Options data from the Arbitrum chain indicates stronger market power in wrapped Bitcoin options, while Ethereum options are more balanced. The feasible GLS regression shows that the benchmark price is higher than the Hegic price, especially for call options. Mispricing increases with larger orders, strike price, maturity, and underlying volatility, while higher trading volume reduces it. Ethereum options exhibit greater price alignment, while Bitcoin options show higher mispricing.

JEL Classification: G12, G13, G15, G17

Keywords: decentralized finance, on-chain protocols, automated market maker, options.

*Corresponding author, email anastasiia.zbandut@gmail.com, phone +49 391 67 58412, mailing address Universitätsplatz 2, 39106, Magdeburg.

1 Introduction and literature review

With the emergence of Bitcoin in 2009, one alternative to the classical way of transferring money occurred where users are able to transfer assets in a decentralized way, omitting the intermediary. With the emergence of Ethereum in 2015, a new financial market arised, since the Ethereum ecosystem is a turing-complete programmable blockchain where developers can build decentralized applications managed by smart contracts. From the financial markets point of view, this opportunity enables the creation of decentralized exchanges as self-executing protocols, i.e., on-chain protocols, which completely leaves out the classical intermediary, i.e., they are non-custodial exchanges. However, they introduce a new participant - a liquidity provider who funds protocols with collaterals. With the emergence of tokenization in 2017, it became possible to transfer and trade various assets such as securities and commodities on blockchain platforms, where tokens represent a digital copy, or a fraction, of an asset. Simultaneously, the rise of the initial coin offering made tokens a common means of funding. First on-chain protocols were launched during the period between 2018 to 2020 and became a core component in terms of services they provide in the decentralized finance ecosystem. These protocols are: Uniswap - the on-chain exchange which introduced the automated market maker (AMM) for decentralized trading,¹ MakerDAO launched the on-chain stablecoins pegged to US dollar and Compound provided on-chain lending and borrowing. Mid 2020 was the most significant period for the decentralized finance ecosystem and is colloquially referred to as "DeFi Summer". The launched on-chain lending and borrowing protocol Aave introduced interest rate swaps and together with Compound became very popular for taking loans or earning interest. Synthetix introduced on-chain trading for synthetic assets. Also during this time many other on-chain protocols introduced yield farming for liquidity providers. This was the most crucial event for on-chain protocols since yield farming is an incentive for liquidity providers to give funds and it attracted a significant capital flow to on-chain protocols which is important for their operation and efficiency. Lastly during the "DeFi Summer", on-chain protocols introduced native on-chain tokens which gave a right to participate in protocol governance. Further, the release of the Layer 2 solutions, which provides cross-chain transfer, laid an important milestone in the decentralized network of protocols. Layer 2 solutions address the scalability and high transaction cost issues of Layer 1 blockchains by processing transactions off-chain and settling them in batches. These improvements make decentralized finance more accessible, allowing for faster, lower-cost transactions and enabling broader user participation. In sum, all these events shaped the decentralized finance ecosystem,² which is still growing rapidly.³

This paper is one of the first empirical papers in the field of on-chain protocols, specifically option protocols, and analyzes the options pricing mechanism of the Hegic protocol. It is one of the first on-chain option protocols trading wrapped Bitcoin (wBitcoin) and Ethereum options; it was fist launched in 2020 on the Ethereum blockchain. With the adoption and launch of Arbitrum and Optimism (Layer 2 solutions on the Ethereum chain) in 2021, Lyra and Deri were launched as the first on-chain protocols which use an AMM for options pricing mechanism, along Thales and Vega protocols. In 2022, Hegic protocol was launched on the Arbitrum chain and the paper analyzes options data from this chain.

Among the limited scientific research in the field of on-chain finance and its components, Rahman et al. (2022) provide an extensive overview of existing on-chain derivative protocols and review the difference to classical derivative markets. They stress that decentralized protocols show several advantages which address the limitations of classical markets. Decentralized protocols enable seamless cross-country transactions in real-time around the clock where classical markets face various constraints such as differences in regulatory frameworks, currency exchange rate risk, high transaction costs, etc. By blockchain's

¹See Fu (2023).

²See Werner et al. (2022).

³Detailed statistics of trading volume in the decentralized finance can be found on DeFiLlama.

nature, transactions are securely recorded and always publicly accessible once they are mined on the chain. The transactions' time and process is all time-observable, whereas transactions on the classical market can not be tracked and the process time is unclear. The possibility to acquire a fractional amount of derivatives on-chain attracts the participation of small scale investors which creates a more diverse trading ecosystem. Contrarily, on the classical market, the access to investment opportunities is geographically and economically limited. Rahman et al. (2022) review the structure of Lyra, Deri, Vega and Thales on-chain option protocols with regard to blockchain network, option types, pricing mechanism and governance. They report that the protocols' primary blockchain choice is Ethereum; however, Lyra, Deri and Vega use Layer 2 chains to enhance the protocols' interoperability and flexibility. With respect to the infrastructure, all reviewed protocols use the AMM and oracles to get the real-time price data. The pricing mechanism of the AMM varies among protocols, however, commonly refers to Black and Scholes (1973) and alike frameworks, e.g., Lyra and Deri. Some protocols mix various models with the Black and Scholes (1973) framework, e.g., dynamic supply and demand or auction mechanisms. The protocol governance approach is always based on the native protocol tokens, however, rules, scope and influence in the governance varies among protocols.

The most important part of any on-chain protocol are liquidity providers since they make the trading possible. The rules and opportunities for liquidity providers are similar with differences in incentives and accepted kinds of cryptocurrencies in liquidity pools. Stable coins such as USDT, USDC and DAI⁴ represent the major choice for liquidity pools. Liquidity providers receive rewards based on the premiums paid and, additionally, they also receive an incentive. The latter is different among protocols: Lyra pays rewards in native tokens, Deri offers perpetual futures rates, Vega pays additional fees based on market activity, and Thales rewards with minting fees. The outlined comparison of on-chain protocols highlights the complex nature of decentralized option trading which involves technological aspects, robust financial modeling with integration of real-time data and liquidity management. Smart contracts are responsible for protocol operation, where every single action is embedded in the corresponding smart contract, e.g., market data fetch, liquidity provision, transactions made, option settlement, are approved once the block is mint. Protocols bear costs for every minted block, where the level of these costs depends on the operating chain, cross-chain integration and pricing model choice. Higher data requirements in pricing mechanism results in higher processing costs. To keep costs low, protocols deploy a simplified version of the classical pricing model which, in turn, might lead to difference in prices in the decentralized and centralized exchanges.⁵ Thus, the key components of an on-chain protocol for operating in a cost efficient, transparent and trustless way are: secure smart contracts, an efficient AMM, reliable oracles and a sufficient amount of liquidity providers.

An efficient AMM should represent the specific dynamic nature of the asset. Scientific research in the field of option pricing does not track recent, but rapid development of on-chain protocols. One paper found is Cao and Celik (2021) which does not specify the options' nature, however contributes to the field by deriving the analytical formula for pricing Bitcoin options. It is based on the equilibrium model of Ang et al. (2001) where money supply and aggregated dividend follow jump-diffusion processes. The authors assume Bitcoin as foreign currency in a small open economy and empirically find that the Black and Scholes (1973) model underprices Bitcoin options compared to their model. Although the authors do not differentiate between off-chain and on-chain options, they find that implied volatility is sensitive to jumps in money supply and suggest that additional pricing risk should be considered when valuing cryptocurrency options.

This paper analyzes the pricing mechanism of Hegic protocol to a benchmark, which is the Black and Scholes (1973) model where the underlying volatility estimated using Markov Switching Autoregression

⁴Various stablecoin tracking US dollar might be used based on the protocol's interoperability.

⁵See Qin et al. (2021).

(MS-AR) generalized autoregressive conditional heteroskedasticity (GARCH) processes. It contributes to both the literature on pricing on-chain option protocols and Hegic protocol. The benchmark model follows the Black and Scholes (1973) assumption with respect to constant underlying volatility since Hegic options can only be purchased once and represent single observations. However, this implies that the benchmark price at maturity mirrors the same level of underlying volatility as at the purchase date. Therefore, this method is more reliable for short-time-to-maturity options. Hegic allows options with maturity from 7 to 90 days, where options with low maturity are preferred due to the highly volatile nature of cryptocurrency prices. Thus, the volatility estimation represents sophisticated measures of the underlying market volatility.

A rather large stream of literature, that analyzes cryptocurrency volatility, uses stochastic processes from the GARCH family and find a better fit than classical volatility measures, e.g., historical volatility. Bouri et al. (2017), Katsiampa (2017) and Stavroyiannis (2018) are some examples in this field and argue that GARCH models capture volatility clustering and persistence in cryptocurrency volatility forecasting. Bariviera (2017) analyze Bitcoin returns and volatility from 2011 to 2017 with respect to the efficient market hypothesis and calculates the time-series long-term memory with the Hurst exponent. The author shows that the long memory of Bitcoin volatility is stronger than its returns, which indicates a difference in dynamics. Moreover, Bariviera (2017) observes a regime switch in Bitcoin return which was not caused by returns' long memory and that the volatility persistence in long memory causes volatility clustering. Thies and Molnár (2018) examines the existence of structural breaks in Bitcoin volatility from 2012 to 2018. They apply a Bayesian change point model to detect structural breaks and identify regimes that show similar statistical levels. The authors find 48 structural breaks in Bitcoin return which show different lengths, mean and volatility. To investigate regimes, Thies and Molnár (2018) cluster identified structural breaks based on posterior volatility and specify seven volatility regimes; however, regimes one to four show low volatility and regimes five to seven exhibit high volatility. Ardia et al. (2019), an extension of Katsiampa (2017), empirically study the presence and changes in Bitcoin volatility regimes from 2011 to 2013. The authors compare 18 MS-AR GARCH models using a Bayesian method, the standard GARCH and the GJR-GARCH processes with two and three volatility regimes in MS models.⁶ The results show that Bitcoin volatility exhibits regime changes and proves that two-regime switching models account for structural breaks better than one regime models. The best performing model is the two regimes MS-AR GJR-GARCH model with conditional t-skewed distribution. The authors also confirm inverted leverage, found by Bouri et al. (2017), Stavroyiannis (2018) and Katsiampa (2017), in both regimes.

This paper applies the two regime MS-AR GJR-GARCH model, i.e., the optimal model is chosen upon minimal Bayesian Information Criterion (BIC) among GARCH and GJR-GARCH processes, to estimate the underlying volatility. We confirm the persistence in Bitcoin volatility observed in the aforementioned papers and contributes with the observed persistence in Ethereum; however, in the high volatility regime. In this paper, we show that smoothed probability regimes vary between Ethereum and Bitcoin. Where Bitcoin shows more frequent transition between regimes and Ethereum shows more pronounced peaks. The paper also confirms the observed inverted leverage affect; however only in the Bitcoin low volatility regime, since other models show a better fit in the standard GARCH model. We observe higher low volatility for Ethereum compared to the Bitcoin. Also for Ethereum, significant autoregressive terms and the high probability of staying in the high regime suggest a higher market reaction to news and events.

Andolfatto et al. (2024) is the first empirical paper in the field of on-chain option protocols. The authors describe the AMM pricing mechanism of the Lyra protocol. Their research is focused on the Lyra protocol on the Arbitrum chain where they empirically analyze the implied volatility difference

⁶The single regime MS model represents the benchmark.

of the European-style off-chain, Deribit, and on-chain, Lyra, options written on Bitcoin and Ethereum. They find that, on average, the implied volatility of the on-chain options is higher and increases with moneyness and maturity. They argue that increased implied volatility on-chain may potentially represent the blockchain risk. In their empirical analysis, the authors built the volatility premium trading strategy on various maturities and moneyness levels for put and call options, i.e., a long position in the off-chain options and a short position in the on-chain options. They show that the profitability of the strategy increases with Lyra’s native token LYRA, which measures the expectations of the protocol’s future profits. Their paper also investigates the implied volatility dynamics with the Vector Autoregression model and finds that positive shocks in trading volume lead to persistent increased implied volatility for the on-chain options. In further analysis, the authors show that the net buying pressure of retail investors increases implied volatility since they mostly invest in call options. Moreover, the authors find that the on-chain implied volatility is highly sensitive to market events which cause changes in the underlying asset, whereas this effect is not observed for off-chain options. Although Andolfatto et al. (2024) focus on volatility premium arbitrage, it represents the peer paper in the field of on-chain options protocols. This paper shares Andolfatto et al. (2024) findings about off- and on-chain protocols infrastructure and ecosystem, and confirms a high sensitivity in Ethereum volatility to market events. However, the research of this paper focuses on the asset pricing model for on-chain protocols.

To analyze the sensitivity in price differences between the Hegic pricing model and the benchmark (mispricing), we perform the Feasible Generalized Least Squares (FGLS) regression, which is broadly used in financial quantitative analysis, when the data shows heteroskedasticity and autocorrelation. The on-chain options data represent cross-section data, where several options can be bought at one date. Since these options face the same levels of the underlying, it might lead to a high autocorrelation. The option data was obtained from the Arbitrum chain and includes wBitcoin and Ethereum call and put options from October 24, 2022, to May 21, 2024. The data shows that 40 percent of wBitcoin options, mostly at-the-money calls, were purchased by only two addresses. Andolfatto et al. (2024) also observe that traders take long positions in call options more frequently. The large concentration of Bitcoin options in only two addresses indicates a high market power. The sample for Ethereum options is larger and more diverse, where 40 percent of all options were bought by 18 addresses; options distribution is more balanced than that of wBitcoin ones. A significantly high amount of at-the-money options on both wBitcoin and Ethereum suggests a leverage strategy, which is common in speculative trading. We confirm the participation of small-scale investors and observes a trend toward short-term investments.

When comparing Hegic and benchmark prices, we find positive mispricing for all samples (except for Ethereum puts), which indicates the benchmark price is higher (lower for Ethereum puts) than the Hegic price, which is more pronounced for call options on both wBitcoin and Ethereum. The volatile and scattered mispricing of wBitcoin options suggests a rather inefficient AMM and a somewhat speculative market. On one hand, if the mispricing persists, the Hegic liquidity pool might bear a systematic risk of mispricing, which might lead to persistent losses for liquidity providers. On the other hand, Hegic protocol limits users to only take long positions and, therefore, limits arbitrage opportunities to buying underpriced options. Conversely, mispricing can provide a liquidity pool with an opportunity to earn higher premiums from overpriced options. Ethereum options exhibit a better alignment with benchmark prices, which might reflect a better-calibrated AMM and a more stable market.

The regression results for both Ethereum and wBitcoin options suggest that large option orders increase and the increased trading volume of the underlying decreases mispricing with a lower magnitude for wBitcoin options. Other findings show mixed results, where Ethereum options show a negligible impact; however, for wBitcoin options, the mispricing increases with strike price, maturity and the underlying volatility. wBitcoin call options show lower mispricing than puts, whereas Ethereum calls exhibit more mispriced options than puts. The paper also finds both wBitcoin and Ethereum at-the-

money and out-of-the-money options do not differ in mispricing. In further analysis, the paper calculates the implied volatility of Hegic options in the Black and Scholes (1973) framework and compares it to market volatility. The volatility difference for wBitcoin options shows dispersed clustering for some strike price levels with calls having higher market volatility than the implied volatility and puts showing higher volatility convergence. Ethereum call and put options also show notable clustering for some strike prices but are closer to the volatility convergence than wBitcoin options. The paper observes notable spreading of volatility differences for high strike prices which indicates higher price differences. This finding is partially in line with Andolfatto et al. (2024), where the authors find that on-chain implied volatility increases with moneyness and maturity. Ethereum put options show higher implied volatility than the market volatility compared to Ethereum calls, i.e., overpriced put options. To account for these discrepancies, the Hegic protocol could implement dynamic pricing based on the amount of acquired options and enhance the AMM for higher out-of-the-money options. Also, it would be an advantage to analyze if and which arbitrage strategies are possible at the Hegic protocol.

The rest of the paper is organized as follows: Section 2 outlines differences between centralized and decentralized options trading infrastructure, ecosystem and pricing mechanisms; it compares Lyra, Deri and Hegic on-chain option protocols. Section 3 presents the empirical analysis with subsection 3.1 devoted to the methodology, subsection 3.2 describes the data sample and subsection 3.3 reports the results. The paper concludes with section 4.

2 On-chain option protocols

Trading options at the centralized exchange are also called off-chain,⁷ e.g., Deribit, which is a cryptocurrency futures and options exchange, involves an intermediary between the option’s writer and holder. This intermediary guarantees the option’s clearing and settlement,⁸ manages the users’ funds, and executes trades on the users behalf.⁹ The off-chain exchange infrastructure involves the order book system, which matches the options’ writes and the holders’ bids and provides liquidity. Trading options at the decentralized exchange, i.e., on-chain, do not require an intermediary, i.e., users manage their funds and execute their trades. A decentralized option trading platform represents a protocol deployed on a blockchain, e.g., Ethereum, which defines rules and standards for processing the data, i.e., consensus mechanism, transaction validation, data structure, etc., and refers to the on-chain option protocol. The protocol consists of various smart contracts, i.e., a self-executing program (piece of code) operating on predefined conditions, which manage options clearing, pricing and settlement, liquidity provision and management. In terms of an on-chain option protocol, an AMM is a smart contract which sets option prices, and the choice of the pricing model varies among protocols. To trade, add liquidity, or view the portfolio, users interact with smart contracts via a front-end application. The option execution and settlement happens based on the predefined conditions.¹⁰ On the classical option market, an option contract is an agreement between one writer and one holder with an intermediary executing orders. In option protocols, a liquidity pool represents a collection of funds, usually stablecoins, e.g., USDC, USDT,¹¹ or

⁷Usually off-chain protocols use an order book system for clearing but options settlement happens on-chain, e.g., the dXdY protocol. For more information see Rahman et al. (2022) pp. 18-20.

⁸Compared to classical option exchanges, where an independent clearing institution is responsible for options’ clearing and settlement, centralized exchanges for cryptocurrencies handle the clearing process internally. The option’s settlement happens immediately (also during weekends) after the order is matched, which differs to typically one or two business days (meaning, if the option is exercised on Friday, the settlement can happen on Tuesday) on the classical options exchange. Usually, settlements are in cash, compared to classical options, which might involve physical delivery.

⁹In other words, centralized exchanges provide custodial service

¹⁰The protocol’s governance, i.e., upgrades and changes, is conducted based on the share in protocol native tokens. Users owning protocol tokens can vote on proposed changes. The distribution of protocol tokens and respective amount threshold for voting rights varies among protocols.

¹¹Stablecoins are tokens pegged to the US dollar. For more broad overview on stablecoins see Ante et al. (2023)

DAI,¹² and represent a significant role in the protocol operation. Liquidity providers deposit their funds as collateral to the liquidity pool and, in turn, receive a profit proportional to their supplied funds. The liquidity pool funds are then used to execute and secure orders. Some option protocols use a peer-to-peer model, i.e., one writer and one holder (users), and some use a peer-to-pool model, i.e., the pool is the counterparty to the user. Another important part of the protocol infrastructure is an oracle, e.g., Chainlink, as they provide real-time market data for their AMM. All transactions, options data, and contract details are publicly available and can be retrieved from the blockchain where the option protocol operates.

In the following, the paper adds to the discussion in section 1 and provides a comparison in the infrastructure (blockchain, AMM, and oracles), the ecosystem (liquidity providers and traders), and the pricing mechanism of on-chain option protocols. The discussion ends with the introduction of the analyzed protocol in this paper, the Hegic protocol. All discussed protocols belong to top options protocols based on the total value locked with, in US dollars, 63 million, 42 million, and 12 million for Lyra, Deri, and Hegic, respectively. They represent a peer group of option protocols with significant differences in options pricing mechanism and traded options.

Lyra¹³ is a peer-to-pool protocol built on two blockchains, Ethereum and Optimism (Layer 2 for Ethereum),¹⁴ and offers trading European-style Bitcoin and Ethereum call and put options. The AMM for pricing of options follows the Black and Scholes (1973) and Black (1976) models, and receives the following market data from the Block Scholes oracle: the implied volatility,¹⁵ spot and forward prices of the underlying, risk free rates and perpetual prices. Lyra splits liquidity into two liquidity pools, i.e., the collateral and the delta pools, and accepts funds in USDC and DAI. The collateral pool holds the collateral which is necessary to back options traded in the protocol, i.e., it ensures that there is sufficient liquidity for premium and settlement of traded options. The pool offers options in 28 day period rounds with four discrete maturity possibilities, i.e., 7, 14, 21, and 28 days.¹⁶ The delta pool mitigates the risk of the collateral pool by investing in the underlying assets, i.e., delta hedged strategy based on the Black and Scholes (1973) framework. Liquidity providers earn trading fees proportional to their pool share and the reward in LYRA tokens as an incentive. They can withdraw their collateral at any time if the pool has sufficient liquidity. Users can take both long and short positions, i.e., buy and sell assets. When shorting an option, users deposit a collateral, which is liquidated if it falls below the minimum threshold.

Deri¹⁷ is a peer-to-peer protocol built on Ethereum, Binance and Huobi blockchains,¹⁸ offering trading of everlasting options written on Bitcoin, Ethereum, Solana, and Binance. The AMM for everlasting options¹⁹ is based on the Black and Scholes (1973) framework with the interest rate equal to zero, where option prices are derived for maturity approaching infinity. Oraclum and Pyth are two oracles which obtain the underlying market price and volatility for pricing options. Rahman et al. (2022) explain the price adjusted process with Deri’s proactive market making algorithm which equalize long and short positions in the liquidity pool based on oracles. Deri offers liquidity pools in Ethereum, Binance coin, USDC, and DAI, where liquidity providers earn trading and funding fees, i.e., periodic payments between traders and are based on the difference between the option and the underlying price. These funding fees are also used for the protocol’s risk management. Liquidity providers’ withdrawals are possible upon sufficient liquidity, otherwise liquidity providers must wait until funds are added to the pool. Traders can

¹²A stablecoin on the Ethereum blockchain, backed by a mix of cryptocurrencies to maintain pegging to the US dollar.

¹³See Lyra’s white paper by Dawson et al. (2023) and official website; documents can be found in the *About* section.

¹⁴Layer 2 are bridge contracts built on existing blockchains which enhances scalability and enable cross-chain transactions. For more details see McCorry et al. (2021).

¹⁵The protocol uses stochastic volatility surfaces to estimate the implied volatility.

¹⁶See Rahman et al. (2022) p.22.

¹⁷See Deri’s white paper by 0xAlpha et al. (2023) and official website; documents can be found in the *Docs* section.

¹⁸Deri bridge facilitates the cross-chain trading in a cost-efficient way.

¹⁹See 0xAlpha et al. (2021).

take a continuous position in options since options show no maturity, leverage their position by providing a collateral and, in some cases, receive funding fees.

Hegic²⁰ is a peer-to-pool protocol built on Ethereum and Arbitrum (Layer 2) chains and offers American-style wBitcoin²¹ and Ethereum call and put options (called hedge contracts in the protocol) and their various combinations. Hegic options give a right to sell or buy the underlying at any time during time to maturity and receive DAI. The AMM for pricing options does not follow any classical pricing model and depends on the contract's moneyness and maturity. Hegic allows buying only at-the-money and out-of-the-money options. There are four discrete strike prices possible, with a ten percent variation from the market price of the underlying, i.e., 100, 110, 120 and 130 percent for calls and 100, 90, 80 and 70 for puts. The maturity interval for all options is from 7 to 90 days. The AMM represents a predetermined rate v of each individual option's strike price K and maturity, and defines the option price O as:

$$O = v \cdot K \quad (2.1)$$

For example, the rate of an at-the-money put option with a strike price of \$200 and a maturity of one month is 8 percent. Thus, the price of such a contract is \$16. The same logic is applied to out-of-the-money options.²² In order to activate the option contract, the buyer must pay a settlement fee s that depends on the settlement rate r_s , the amount, and the option's price and is defined as:

$$s = Amount \cdot P \cdot r_s \quad (2.2)$$

For at-the-money options, the settlement rate is one percent, and for out-of-the-money options 0.5 percent.²³ For the example mentioned, the settlement fee for one option is \$0.16. The premium paid by the option holder is the sum of the price and the settlement fee and, in the example mentioned, equals \$16.16. The protocol receives the real-time market prices from the Chainlink and swaps assets to DAI on the decentralized exchange Uniswap. The writer of the Hegic protocol is the liquidity pool and represents the users' counterparty. This implies that the writer's risk is spread among liquidity providers; each liquidity provider bears the counterparty risk proportional to their pool share. Liquidity providers can supply DAI, USDC, and USDT to the liquidity pool and receive writeDAI tokens (ERC20 token), automatically mined, and the corresponding liquidity providers are rewarded with premiums paid by the option holders. The liquidity pool's gained premiums and faced losses are distributed between the liquidity providers proportional to their pool shares. Additionally, the allocated liquidity in the pool in DAI is converted into CHAI²⁴ that earns interest on DAI via the MakerDAO ecosystem through collateralized debt positions. This earned interest is an additional profit for liquidity providers and an incentive to provide funds to the liquidity pool. The portion of liquidity is locked in the pool for the whole maturity of hedge contracts. However, some portion of liquidity stays unlocked so that a liquidity provider can claim their funds in DAI at any time. When the liquidity provider withdraws the funds they supplied, the writeDAI tokens are burned. In case the unlocked liquidity in the pool is

²⁰See Hegic's white paper by Wintermute (2020) and official website; documents can be found in the *Analytics* section.

²¹The Bitcoin is the ERC20 token which enables Bitcoins to operate in the Ethereum ecosystem and holds the 1:1 ratio. ERC20 token represents standards for smart contracts which manage tokens on the Ethereum blockchain in various decentralized applications.

²²Hegic protocol does not trade in-the-money options. However, in their white paper, the price for the in-the-money option, in addition to the predefined rate, also includes the difference between the strike and the underlying market price, which is similar to the funding fee at Deri. For example, the put option has a strike price of \$220, one-month maturity, and a rate of 4 percent; the price is determined as:

$$220 \cdot 0.08 + (220 - 200) = \$37.6$$

The difference in pricing in-the-money options is motivated by its intrinsic value, as exercising such an in-the-money option would result in a profit for the holder and a loss for the writer.

²³As for in-the-money options.

²⁴It is the wrapped DAI in the MakerDAO system and is an ERC20 token.

not enough to withdraw, the liquidity providers wait until a contract matures; however, it is possible to prioritize the liquidity unlock with HEGIC tokens, i.e., native tokens. If several liquidity providers wish to withdraw their funds, their requests are aggregated in the queue. Hegic users can only take a long position in options, i.e., buy options. Upon finding a favorable contract, option holders must activate the contract by paying the total price in Ethereum (primarily cryptocurrency); the payment is accepted once the transaction is mined. When the option is active, the premium paid in Ethereum is automatically swapped to DAI at Uniswap. In order to execute the option, the holder sends Ethereum from the same Ethereum address to the contract and automatically receives DAI.

The comparison of the three on-chain option protocols discussed above highlights a complex and unique approach to trading various kinds of options. Among these protocols, Hegic uses the simplest pricing mechanism²⁵ compared to the more sophisticated and empirically tested models, as in Lyra and Deri. Therefore, the paper investigates if the Hegic AMM prices options similar to the benchmark model. The observed deviations between the Hegic price and the benchmark price are then analyzed with respect to the options' and underlying assets' characteristics. In case of significant mispricing, the paper outlines arbitrage opportunities and liquidity pool exploitation, considering the Hegic infrastructure.

3 Empirical analysis

3.1 Methodology

The paper calculates option benchmark prices in the Black and Scholes (1973) framework since it is a commonly used (or referenced) model in the cryptocurrency market. To introduce notations, the price for call C and put P options with underlying volatility σ are calculated as:²⁶

$$\begin{aligned} C &= S \cdot N(d_1) - K \cdot e^{-r_f \cdot T} \cdot N(d_2) \\ P &= K \cdot e^{-r_f \cdot T} \cdot N(-d_2) - S \cdot N(-d_1) \end{aligned} \quad (3.1)$$

where S denotes the price of the underlying, K denotes the strike price, r_f denotes the risk free rate, T denotes maturity, $d_1 = \frac{\ln(\frac{S}{K}) + (r + \frac{\sigma^2}{2}) \cdot T}{\sigma \cdot \sqrt{T}}$ and $d_2 = d_1 - \sigma \cdot \sqrt{T}$. To capture volatility dynamics in cryptocurrencies, the paper applies two models: to account for structural breaks in volatility, the MS-AR model is applied, and to account for volatility clustering, the Glosten-Jagannathan-Runkle GJR-GARCH model is deployed. This method provides the current level of constant volatility at the purchase date.²⁷ Thus, the estimation of σ is done in two steps: first, the identification of low and high volatility regimes with the MS-AR model is conducted as:²⁸

$$r_t = \mu_{\rho_t} + \sum_{i=1}^a \phi_{\rho_t, i} \cdot r_{t-i} + \varepsilon_{\rho_t, t} \quad (3.2)$$

where $\rho_t \in \{0, 1\}$ denotes the regime at time t . Ardia et al. (2019) apply demeaning to the time series and incorporate an autoregressive term of 1, which simplifies the data structure. However, this approach may not fully capture the complex dynamics of cryptocurrencies. This paper chooses the amount of autoregression terms r_{t-i} based on the partial autocorrelation function. Since there is a significant evidence of volatility persistence²⁹, accounting for higher-order autocorrelation improves the regime predictions. The second step is modelling the volatility process for each regime identified by the MS-AR

²⁵From the white paper, it remains unclear how the predefined rates are set.

²⁶See Black and Scholes (1973)

²⁷Hull (2012) discusses the estimation of the underlying volatility and suggests that GARCH processes are preferable since they consider mean revision and asymmetric shocks.

²⁸See Hamilton (1989).

²⁹See Bouri et al. (2017), Katsiampa (2017), Bariviera (2017) and Stavroyiannis (2018).

model. For this, the paper fits the GJR-GARCH model with conditional skewed T-distribution³⁰ as:³¹

$$\begin{aligned} \varepsilon_{\rho_t,t} &\sim \mathcal{N}(0, \sigma_{\rho_t,t}^2) \\ \sigma_{\rho_t,t}^2 &= \omega_{\rho_t} + \sum_{i=1}^p \alpha_{\rho_t,i} \cdot \varepsilon_{\rho_t,t-i}^2 + \sum_{i=1}^o \gamma_{\rho_t,i} \cdot \varepsilon_{\rho_t,t-i}^2 \cdot I(\varepsilon_{\rho_t,t-i} < 0) + \sum_{j=1}^q \beta_{\rho_t,j} \cdot \sigma_{\rho_t,t-j}^2 \end{aligned} \quad (3.3)$$

The optimal GJR-GARCH model is chosen for each cryptocurrency and regime based on the lowest Bayesian Information Criteria (BIC). The paper estimates the individual GJR-GARCH process for different combinations where p and q vary from 1 to 10 and o varies from 0 to 5. If the best model yields o equals zero, the GJR-GARCH model transforms into the standard GARCH process.

The price difference Δprice_j for an individual option j is calculated as:

$$\Delta\text{price}_j = \frac{C(P)_j - O_j}{O_j} \quad (3.4)$$

with Δprice_j indicating price alignment and mispricing otherwise. In the further regression analysis, Δprice_j represents the dependent variable. The paper performs Feasible Generalized Least Squares (FGLS) regression,³² which is broadly used in financial quantitative analysis, when the data shows issues with heteroskedasticity and autocorrelation. The choice of the regression model is made based on the nature of on-chain options, which can only be purchased once.³³ Thus, the data exhibits a cross-sectional nature. Many options are purchased on the same date; however, they correspond to unique transactions. Such data structures, where different options face the same levels of the underlying on the same date, leads to a high autocorrelation of the error term when applying the Ordinary Least Squares (OLS) regression. FGLS is employed in two steps: first, estimating the variance-covariance matrix of the error terms with explanatory variables and, second, conducting GLS regression. The estimation of the variance-covariance matrix of the error terms involves fitting the OLS regression for each underlying j to obtain residuals as follows:

$$\begin{aligned} \Delta\text{price}_j &= \beta_j + \beta_{\text{amount}} \cdot \text{Amount}_j + \beta_{\text{strike}} \cdot \text{Strike}_j + \beta_{\text{maturity}} \cdot \text{Maturity}_j + \beta_{\text{return}} \cdot \text{Return}_{t,j} \\ &+ \beta_{\text{volume}} \cdot \text{Volume}_{t,j} + \beta_{\text{volatility}} \cdot \text{Volatility}_{t,j} + \beta_{\text{kind}} \cdot \text{Kind}_j + \beta_{\text{type}} \cdot \text{Type}_j + \xi_j \end{aligned} \quad (3.5)$$

where for the underlying j at the purchase date t : Amount_j denotes the amount of options purchased, $r_{t,j}$ denotes the rate of return, $\text{Volume}_{t,j}$ denotes the volume, $\sigma_{t,j}$ denotes the volatility, Kind_j is a dummy variable which takes the value of one if the option is a call option, Type_j is a dummy variable which takes the value of one if the option is an at-the-money option and ξ_j denotes residuals. The variance of the residuals is estimated by fitting an auxiliary regression as:

$$\begin{aligned} \xi_j^2 &= \gamma_j + \gamma_{\text{amount}} \cdot \text{Amount}_j + \gamma_{\text{strike}} \cdot \text{Strike}_j + \gamma_{\text{maturity}} \cdot \text{Maturity}_j + \gamma_{\text{return}} \cdot \text{Return}_{t,j} \\ &+ \gamma_{\text{volume}} \cdot \text{Volume}_j + \gamma_{\text{volatility}} \cdot \text{Volatility}_{t,j} + \gamma_{\text{kind}} \cdot \text{Kind}_j + \gamma_{\text{type}} \cdot \text{Type}_j + \nu_j \end{aligned} \quad (3.6)$$

where ξ_j^2 denotes squared residuals and ν_j is the error term. Both the OLS and the auxiliary regressions use a heteroskedasticity consistent covariance matrix to estimate the robust standard errors and the variance of residuals, respectively.³⁴ This ensures the accurate estimation of the variance-covariance structure. The fitted values from auxiliary regression are used to construct the diagonal elements of the omega matrix Ω , i.e., variance-covariance matrix, which incorporates the heteroskedasticity pattern.

³⁰Also used in Ardia et al. (2019).

³¹See Glosten and R. Jagannathan (1993).

³²See Campbell et al. (1997) pp. 204-210.

³³There is no OTC market for trading.

³⁴See Davidson and MacKinnon (1993) pp. 300-340.

The second step, the FGLS regression is performed using the constructed omega matrix as:

$$\hat{\beta}_{GLS} = (X^T \cdot \Omega^{-1} \cdot X)^{-1} \cdot X^T \cdot \Omega^{-1} \cdot \Delta price \quad (3.7)$$

where X is the matrix of the independent variable used in equations 3.5 and 3.6. Standard errors are estimated with the Newey and West (1987) estimators to correct for heteroskedasticity and autocorrelation in the residuals. To test the significance of the FGLS regression, the Wald test is applied.

3.2 Data

The options data was obtained from the Arbitrum chain and includes wBitcoin and Ethereum call and put options³⁵ for the time horizon from the October 24, 2022, to May 21, 2024. Unlike the traditional option market, it is possible to purchase a fractional number of any option. All data related to the option, which includes not only price, strike, and maturity but also purchaser address, contract address, and transaction hash, can be transparently retrieved.³⁶

Figure 3.1 represents Sankey charts for purchased options per unique address in the sample. The left segment of each chart illustrates the addresses with the width corresponding to the number of options purchased by this address. Each chart's middle and right segments illustrate the division into kinds, i.e., call and put options, and the division into types. A total of 1,315 wBitcoin options were purchased by 275 unique addresses, where 40 percent of all options were traded by two³⁷ addresses. From the total amount of wBitcoin options, 723 are calls and 377 puts, where 377 and 400 are at-the-money calls and puts, respectively. Andolfatto et al. (2024) also observe that traders take long position in call options more frequently. The large concentration of wBitcoin options in only two addresses indicates a high market power. The sample for Ethereum options is larger, with a total of 2,775 options purchased by 728 unique addresses, where 40 percent of all options were bought by 18 unique addresses.³⁸ Compared to the distribution of wBitcoin options, Ethereum options are more balanced since they are distributed among more addresses. From the total amount of Ethereum options, 1,664 are calls with 1,137 at-the-money and 1,111 puts with 621 at-the-money options. Additionally, the presence of addresses which purchase a large amount of wBitcoin and Ethereum options indicates the participation of advanced large-scale investors in the protocol. A significantly high amount of at-the-money options in all samples suggests a leverage strategy, which is common in speculative trading.

Table 3.1 summarizes descriptive statistics for all option samples, with Ethereum call options being the largest sample. The minimum amount of acquired options are tiny since it is possible to purchase a fractional amount of options. Call options values are smaller than four digits, indicating small-scale investors' participation. wBitcoin put options show the lowest mean amount with the lowest standard deviation among all samples, suggesting lower trading volumes. On the contrary, Ethereum put options exhibit the highest mean amount with the highest standard deviation. wBitcoin and Ethereum call options show higher means and standard deviations than put options, which might indicate increased interest in leveraged strategies. The 75 percent quartile of wBitcoin options amounts to 0.5, which

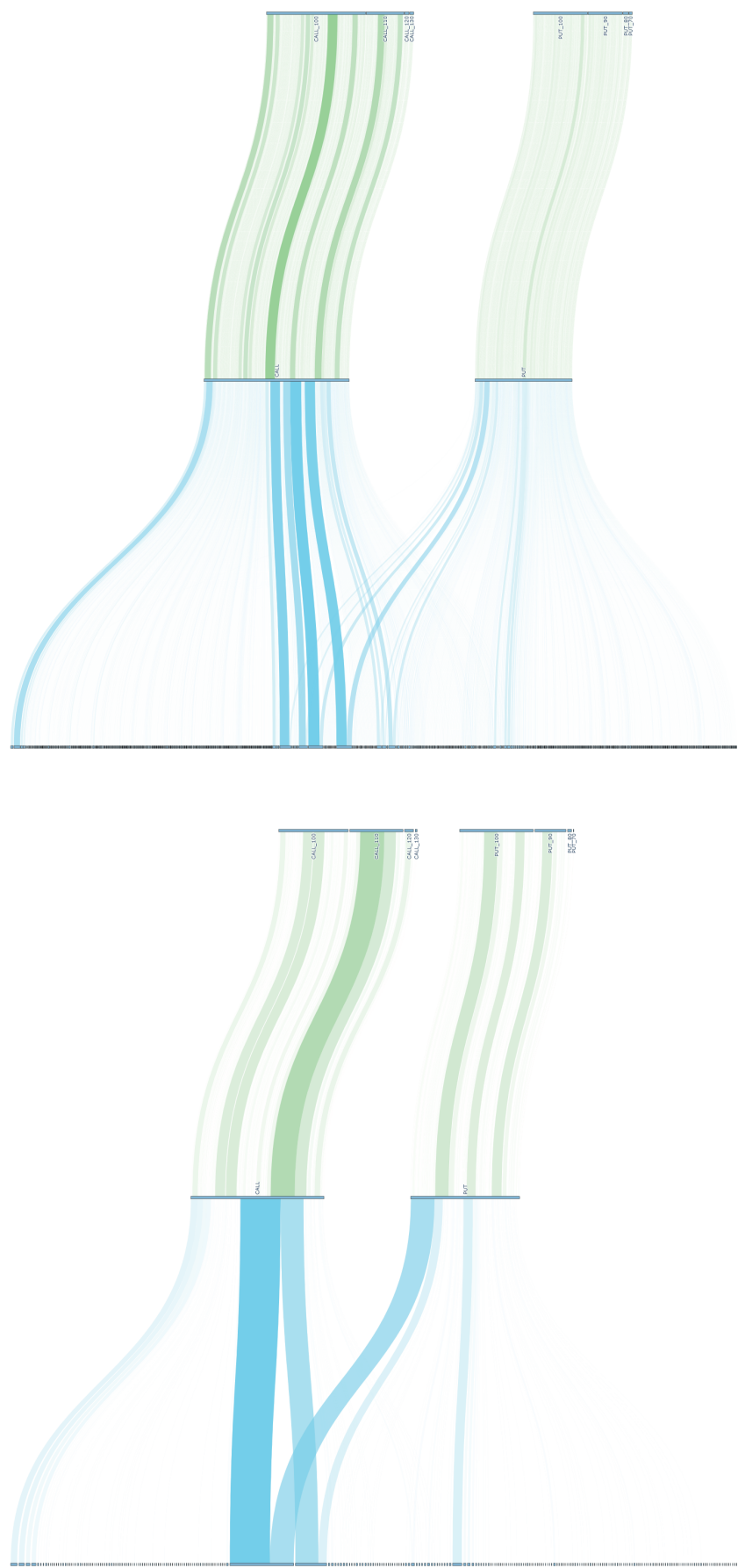
³⁵The data also contains various option trading strategies like bull put spread, straddle, strip, etc.

³⁶Note, such data gives access to large raw data set for research in behavioral finance since knowing the Ethereum address allows extracting the data of other transactions made by the user. Such detailed data can be used to investigate the behavior of options trading addresses and their portfolio holdings. From the point of view of the Hegic protocol, it further gives an important means to make the protocol more efficient and secure by optimizing smart contract parameters and managing risk.

³⁷0x713256418b31dbc8c4da8dc863a345e5f5f6ad3d bought 346 options, and x7a69c8f19879f0400bc9c542700f0ae5839f574c bought 150 options.

³⁸0xed2a45611b967df5647a17dfeaa0dec40806de54 bought 176, 0x713256418b31dbc8c4da8dc863a345e5f5f6ad3d (same address which bought 346 wBitcoin options) 167, 0xb61adeccc0683e7df27d531452e381954891becc bought 130, 0x7a69c8f19879f0400bc9c542700f0ae5839f574c (same address which bought 150 wBitcoin options) 101. Andolfatto et al. (2024) in their sample from the Lyra protocol also observe more Ethereum options traded. The other 15 addresses bought contracts that were less than 80 and bigger than 15 option contracts.

Figure 3.1: Options Sankey charts



(a) wBitcoin

(b) Ethereum

is significantly lower than 8 and 10 for Ethereum call and put options, respectively. Larger amounts of acquired Ethereum options suggest a more liquid market and higher trading interest. Additionally, high maximum amounts of wBitcoin options indicate the participation of large-scale investors, which is also observed in figure 3.1. The premium paid refers to the total amount paid for acquired options. The mean premiums are almost at the same level for all samples, with higher standard deviations for wBitcoin options, reflecting relatively higher wBitcoin prices. The strike price levels are clearly attributed to underlying price levels, with wBitcoin options showing significantly higher strike prices than Ethereum options. Due to the concept of the Hegic protocol, the mean maturity shows similar values across all samples, with the highest value for Ethereum calls, which indicates comparably long-term investments. The minimum maturity is seven days for all samples, which indicates a tendency for short-term investments, with wBitcoin calls filling the 50 percent quartile compared to others showing longer maturity at the same quartile. wBitcoin and Ethereum put options exhibit an increase in maturity from the 25 to 75 percent quartiles which might indicate hedging against downside risk in the long-term. In line with the protocol’s pricing mechanism, all samples show only at-the-money or out-of-the-money options, with slightly more out-of-the-money puts.

Table 3.1: Descriptive statistics of option samples

	Amount	Premium Paid	Strike	Maturity	Moneyness
Call options - wBitcoin ($n = 723$)					
Mean	1.3806	699.5291	29,064.7756	17	0.9495
Std Deviation	4.5786	2253.8008	13,989.1117	21	0.0577
Min	0.0000	0.0186	15,574.2470	7	0.7692
25 %-Quartile	0.0350	15.8999	19,952.6608	7	0.9091
50 %-Quartile	0.1500	47.0000	24,312.8100	7	1.0000
75 %-Quartile	0.5000	366.7770	29,814.1561	15	1.0000
Max	53.5000	28,075.9242	78,565.2299	90	1.0000
Put options - wBitcoin ($n = 592$)					
Mean	0.6232	559.0408	28,933.0447	19	1.0426
Std Deviation	1.5282	2236.6310	13,319.5975	20	0.0696
Min	0.0001	0.1085	11,362.7045	7	1.0000
25 %-Quartile	0.0250	22.7973	20,540.6068	7	1.0000
50 %-Quartile	0.1000	70.3125	25,603.1500	10	1.0000
75 %-Quartile	0.5000	268.8343	30,303.9775	26	1.1111
Max	15.0000	39,551.5471	72,142.1470	90	1.4286
Call options - Ethereum ($n = 1664$)					
Mean	9.3663	673.4381	1943.7615	22	0.9651
Std Deviation	22.2319	1894.1741	617.8966	24	0.0567
Min	0.0000	0.0000	1089.4159	7	0.7692
25 %-Quartile	0.2500	11.7653	1572.7411	7	0.9091
50 %-Quartile	1.1395	83.7159	1790.0698	14	1.0000
75 %-Quartile	8.0000	494.0209	2091.9256	26	1.0000
Max	264.0000	24,372.6270	4457.6131	90	1.0000
Put options - Ethereum ($n = 1111$)					
Mean	12.4002	626.3159	1636.4635	19	1.0672
Std Deviation	33.4195	1963.5321	458.8686	20	0.0969
Min	0.0001	0.0020	811.7060	7	1.0000
25 %-Quartile	1.0000	19.9412	1398.3643	7	1.0000
50 %-Quartile	2.0000	99.4667	1590.4926	10	1.0000
75 %-Quartile	10.0000	474.4329	1801.4949	21	1.1111
Max	516.0000	34,994.2598	4043.2200	90	1.4286

The table reports descriptive statistics for all samples with their sample size n . Amount is a number or a fraction of options purchased, Premium Paid is the paid in US dollar for acquired amount of options, Moneyness is the ratio S/K , Maturity is the time-to-maturity in days.

3.3 Empirical results

The starting point of the analysis is to calculate the underlying volatility for wBitcoin and Ethereum options. For this, the time-series history of daily prices for Bitcoin and Ethereum from December 7, 2018, until May 25, 2024, was downloaded from the CryptoCompare data provider via an API connection. The sample contains different stages of market conditions, i.e., the 2019 market crash due to the COVID-19 pandemic and the bull market in 2020-2021 due to "DeFi Summer", and events concerning regulatory

changes in cryptocurrency trading and mining activities, e.g., MiCa discussions, which are essential for the MS-AR model. Since the paper identifies regime changes in time series, to increase the accuracy of the MS-AR model, it is necessary that the sample includes events which caused regime changes. With the GJR-GARCH model, the paper models volatility dynamics for each regime and provides a more accurate capture of volatility clustering and persistence than a singular regime model, which does not differentiate between regimes.

Table 3.2 summarizes the statistics of Bitcoin and Ethereum rates of return. Mean rates of return for both samples are positive, with around four percentage points higher for Ethereum. This is likely due to the continuously growing decentralized finance ecosystem, where Ethereum is the preferable blockchain and plays a vital role in various on-chain applications. Ethereum rates of return also exhibit higher standard deviation and minimum and maximum values, suggesting significant price variations. This, in turn, again highlights the dominant role of Ethereum in the ecosystem, where an increased amount of projects deployed on its chain and a high transaction flow lead to more frequent price changes. Both Bitcoin and Ethereum time series are left-skewed, suggesting events with a more pronounced price decline. Similarly, high kurtosis values indicate fat tails, which emphasize extreme values in rates of return.

Table 3.2: Descriptive statistics of options' underlying rates of return

	Bitcoin	Ethereum
Mean	0.1491	0.1849
Std Deviation	3.5875	4.6091
Min	-47.9934	-56.9506
25 %-Quartile	-1.3578	-1.8478
50 %-Quartile	0.0778	0.1204
75 %-Quartile	1.7233	2.3479
Max	17.7913	23.3480
Skewness	-1.1730	-1.1068
Kurtosis	21.4857	18.1792

The table reports descriptive statistics of rates of return with sample size $n = 2000$.

Table 3.3 represents the results of fitting the two regime MS-AR models, allowing the autoregressive parameters, trend, and variance to switch between regimes. The paper uses the Limited-memory BroydenFletcherGoldfarbShanno (L-BFGS) algorithm as the optimization method, which fits the model by maximizing the likelihood function to find parameter estimates with a limited amount of computer memory. Compared to the standard BFGS algorithm, the L-BFGS algorithm saves an approximate of the Hessian matrix vectors. Standard errors are calculated using the White (1980) estimator, which are heteroskedasticity robust. The order of the autoregression term is 8 for Bitcoin and 10 for Ethereum. Table 3.3 records MS-AR regimes as regime 0 and regime 1. Based on the values for σ^2 in each regime, for Bitcoin, regime 0 corresponds to a high volatility regime with σ^2 at the level of 28.61, and regime 1 corresponds to a low volatility regime with σ^2 is equal to 2.45. For Ethereum, it is the opposite; regime 0 corresponds to a low volatility regime, and regime 1 corresponds to a high volatility regime, where σ^2 is equal to 51.82 and 6.06, respectively. The autoregressive terms for both Bitcoin and Ethereum show several significant coefficients, with Ethereum's rates of return showing more significant coefficients for high volatility regime, indicating stronger autoregressive behavior. Bitcoin's persistence in a low volatility regime is 77 percent, which is almost the same level as Ethereum's persistence in a high volatility regime at 75 percent. This finding is consistent with Ardia et al. (2019) who report volatility and regime persistence in Bitcoin. For Ethereum, significant autoregressive terms and a high probability of staying in the high regime suggest a higher market reaction to news and events. Additionally, there are relatively low probabilities for regime changes, 36 percent for Bitcoin and 11 percent for Ethereum. This means when entering the regime, returns stay in this regime.

Figure 3.2 depicts the smoothed probabilities of regime 0 (low volatility for Bitcoin and high volatility

Table 3.3: Markov Switching Model Results

	wBitcoin		Ethereum	
	10199.1912		11206.6259	
	10322.3224		11352.1183	
	Regime 0	Regime 1	Regime 0	Regime 1
Constant	0.1208 (0.0823)	0.0712 (0.1870)	0.5293* (0.3153)	0.0924 (0.1378)
Sigma ²	2.4550*** (0.7101)	28.6134*** (7.7156)	51.8320*** (12.8606)	6.0647*** (1.4789)
ar.L1	-0.1311*** (0.0374)	-0.0562 (0.0742)	-0.1359** (0.0543)	-0.1114*** (0.0397)
ar.L2	0.0421 (0.0468)	0.0072 (0.0728)	0.1297** (0.0659)	-0.0398 (0.0423)
ar.L3	0.0539 (0.0459)	-0.0301 (0.0940)	0.0821 (0.1115)	-0.0209 (0.0402)
ar.L4	-0.0794** (0.0368)	0.1206*** (0.0381)	0.0325 (0.2085)	-0.0142 (0.0759)
ar.L5	0.0203 (0.0325)	-0.0581** (0.0294)	-0.0770 (0.0959)	0.0028 (0.0566)
ar.L6	-0.0044 (0.0389)	-0.0515 (0.0826)	0.0807 (0.0717)	-0.0381 (0.0363)
ar.L7	-0.0509 (0.0433)	0.0873 (0.1027)	0.0213 (0.1005)	-0.0071 (0.0442)
ar.L8	-0.0065 (0.0318)	-0.0169 (0.0278)	-0.1571* (0.0917)	0.0199 (0.0304)
ar.L9			-0.0145 (0.0385)	-0.0203 (0.0344)
ar.L10			0.1617* (0.0855)	-0.0151 (0.0601)
Regime transition parameters				
$p(0 \rightarrow 0)$	0.7710*** (0.0556)		0.7502*** (0.0960)	
$p(1 \rightarrow 0)$	0.3659*** (0.1052)		0.1127* (0.0595)	

The table reports results for the two regime MS-AR model described by equation 3.2. The number for autoregressive terms is identified with partial autocorrelation function. The reported standard errors are reported in parentheses and robust to heteroskedasticity and autocorrelation. Statistical significance is judged according to the t-statistic and the 1 percent, 5 percent, 10 percent levels are denoted by ***, **, *.

for Ethereum) in green and regime 1 in purple from the MS-AR model. For Bitcoin, the low volatility regime shows more frequent transitions between low and high volatility states. The interruption in persistence staying in a low volatility regime is observable around early 2020, i.e., the bear market, and late 2020 to early 2021, i.e., the bull market. The high volatility regime shows significant periods around these dates as well, highlighting market reactions. For Ethereum, both regimes show less frequent transitions and show more pronounced peaks, indicating increased market activity. On the contrary, the low volatility regime shows persistence after late 2021, which mirrors the growing adoption and the establishment of the Ethereum chain in the decentralized finance ecosystem.

Figure 3.2: Volatility regimes.

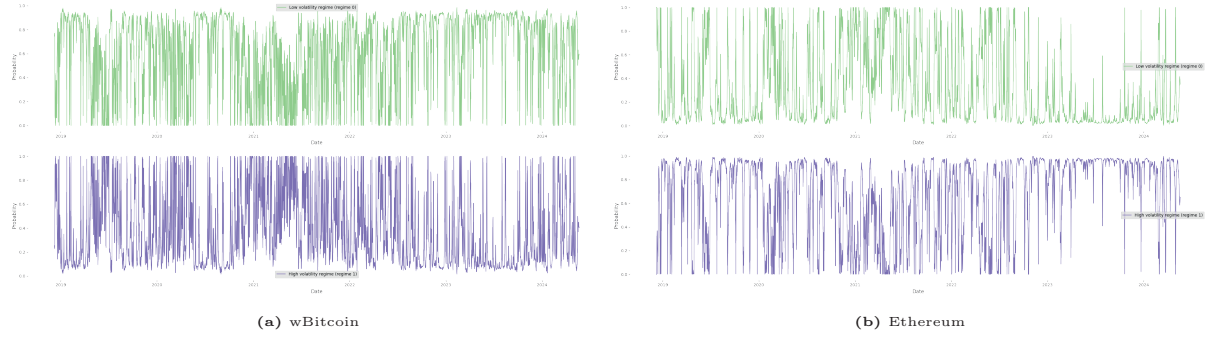


Table 3.4 summarizes the results of fitting the individual GJR-GARCH process for each regime. Only for low volatility, i.e., regime 0 for Bitcoin, the optimal process is GRJ-GARCH (1,1,1). For all the others, the optimal process is the standard GARCH, which is identical to the GRJ-GARCH when the leverage parameter γ equals zero. For Bitcoin, the low volatility regime shows a highly significant inverted leverage effect, i.e., positive shocks increase volatility stronger than negative ones. This finding contradicts typical financial market dynamics; however, is in line with several papers: Bouri et al. (2017) analyzes Bitcoin volatility with GJR-GARCH process from 2011 until 2016 and find an inverted leverage effect. Stavroyiannis (2018) also analyzes Bitcoin with GJR-GARCH for the period from 2013 until 2018 and observes an inverted leverage effect. Katsiampa (2017) explores various GARCH models for Bitcoin prices from 2010 until 2016 and confirms the inverted leverage effect in T-GARCH and AP-ARCH. Ardia et al. (2019) also confirm persistent inverted leverage in Bitcoin from 2011 until 2013 using the MS-GJR-GARCH model. The highly significant β coefficients indicate persistence in low volatility. The high volatility regime with GARCH (1,1) also shows significant ω , α and highly significant β , indicating persistent high volatility (here, the β coefficient is slightly lower than in the low volatility regime). This finding is also in line with Ardia et al. (2019). For Ethereum, the results are similar. The high volatility regime with GARCH (1,1) also shows significant ω , α , and highly significant β , indicating persistent high volatility. However, the β coefficient is lower than for Bitcoin, implying the persistence in volatility is less pronounced for Ethereum. On the contrary, the low volatility regime shows highly significant persistence, which is also slightly higher in magnitude than for Bitcoin. All Ljung-Box statistics show no serial correlation in residuals (p -values > 0.1), and all Engle's ARCH statistics report no significant ARCH effects in residuals (p -values > 0.1).

Figure 3.3 compares volatility dynamics of the market volatility (fitted by the MS-AR-(GRJ)-GARCH model) in blue and 7-days rolling volatility in orange. Both graphs show that market volatility is smoother and has more pronounced peaks around significant market events than rolling volatility, which is rather noisy. The rolling volatility captures short-term volatility and, therefore, is very volatile. By specifying regime changes and volatility clustering, the MS-AR-(GRJ)-GARCH model reduces short-term noise impact on volatility; therefore, the market volatility shows polished dynamics. The peaks for Ethereum are higher, again highlighting a more sensitive response to market events. This finding is in line with

Table 3.4: GARCH Results

Regime	Bitcoin		Ethereum	
	low volatility GJR-GARCH(1,1,1)	high volatility GARCH(1,1)	high volatility GARCH(1,1)	low volatility GARCH(1,1)
AIC	6785.3842	3294.1601	3025.3312	8079.4733
BIC	6822.0511	3320.5530	3050.7008	8111.2821
Mean model				
μ	0.2107** (0.0993)	0.1197 (0.1652)	0.3629 (0.2269)	0.1315 (0.0945)
Volatility model				
ω	0.1620 (0.5642)	3.5636* (2.0924)	8.1344* (4.2226)	0.1500 (0.2621)
α_1	0.1141 (0.0714)	0.1336* (0.0591)	0.1325* (0.0736)	0.0674* (0.0397)
γ_1	-0.0895*** (0.0255)			
β_1	0.9306*** (0.1161)	0.7304*** (0.1029)	0.6330*** (0.1429)	0.9325*** (0.0485)
Distribution				
η	2.9555*** (0.4766)	2.9625*** (0.3934)	3.2018*** (0.5555)	3.5463*** (0.3412)
λ	0.0602 (0.0467)	0.0054 (0.0496)	0.0044 (0.0539)	0.0277 (0.0333)
Ljung-Box statistic	14.2746	1.9784	0.4306	6.5972
p -value	0.1608	0.9965	0.9999	0.7628
Engle's ARCH statistic	0.8115	0.0317	0.0287	1.3423
p -value	0.9999	0.9999	0.9999	0.9993

The table reports results for the optimal GJR-GARCH process defined in equation 3.3. The coefficients displayed correspond to mean (top panel) and variance (middle panel) model, and the corresponding distribution (bottom panel). The respective standard errors reported in parentheses with statistical significance judged according to the t-statistic and the 1 percent, 5 percent, 10 percent levels are denoted by ***, **, *. In addition to AIC and BIC coefficients, the goodness-of-fit is judged by the Ljung-Box and the Engle's ARCH statistics.

Andolfatto et al. (2024) which empirically show that Ethereum on-chain options are more sensitive to market events than Bitcoin options. Despite this, volatility measures are very close to each other and display, in general, the same dynamics. This suggests that the chosen models effectively capture the underlying volatility dynamics by filtering out the noise and specifying volatility trends and persistence.

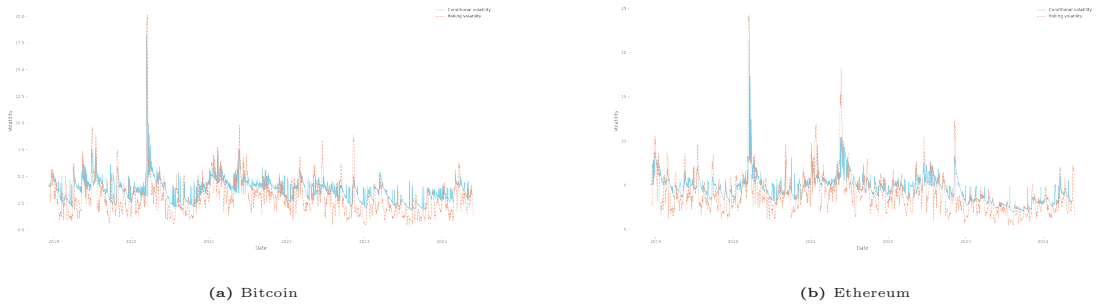
Figure 3.3: Volatility dynamics.

Table 3.5 summarizes statistics for the difference between the benchmark and the Hegic protocol prices. Since it is possible to acquire a fractional number of options, Hegic prices are standardized to one option, so it is the price per option contract. Mispricing mean values for all samples (except for Ethereum put options) are positive, with the highest for wBitcoin calls, which indicates the benchmark price is, on average, higher (lower for Ethereum put options) than the Hegic price. Mean levels for Ethereum options are lower and suggest closer alignment with benchmark prices. Standard deviation values show higher mispricing variation for wBitcoin options, with the highest value for calls. Minimum and maximum values indicate extreme cases of mispricing with comparably same levels for wBitcoin and Ethereum options. The distribution and width of displayed quartiles show slightly more dispersed

mispricing values for wBitcoin options. Mispricing values are right-skewed, suggesting more observations where the benchmark price is higher than the Hegic price which is more pronounced for call options. High kurtosis values suggest extreme price differences, which are again more pronounced for calls.

Table 3.5: Descriptive statistics of options' mispricing

	wBitcoin		Ethereum	
	call options	put options	call options	put options
Mean	0.17505	0.0249	0.0973	-0.0645
Std Deviation	0.67728	0.3962	0.4285	0.3581
Min	-0.99617	-0.9941	-0.9875	-0.9999
25 %-Quartile	-0.1707	-0.2070	-0.1260	-0.2732
50 %-Quartile	0.0520	0.0105	0.0631	-0.0243
75 %-Quartile	0.3112	0.2702	0.2437	0.1389
Max	4.5893	1.4120	4.2998	2.0546
Skewness	2.7762	0.33981	2.23161	0.14577
Kurtosis	13.8208	4.00729	14.9655	5.2434

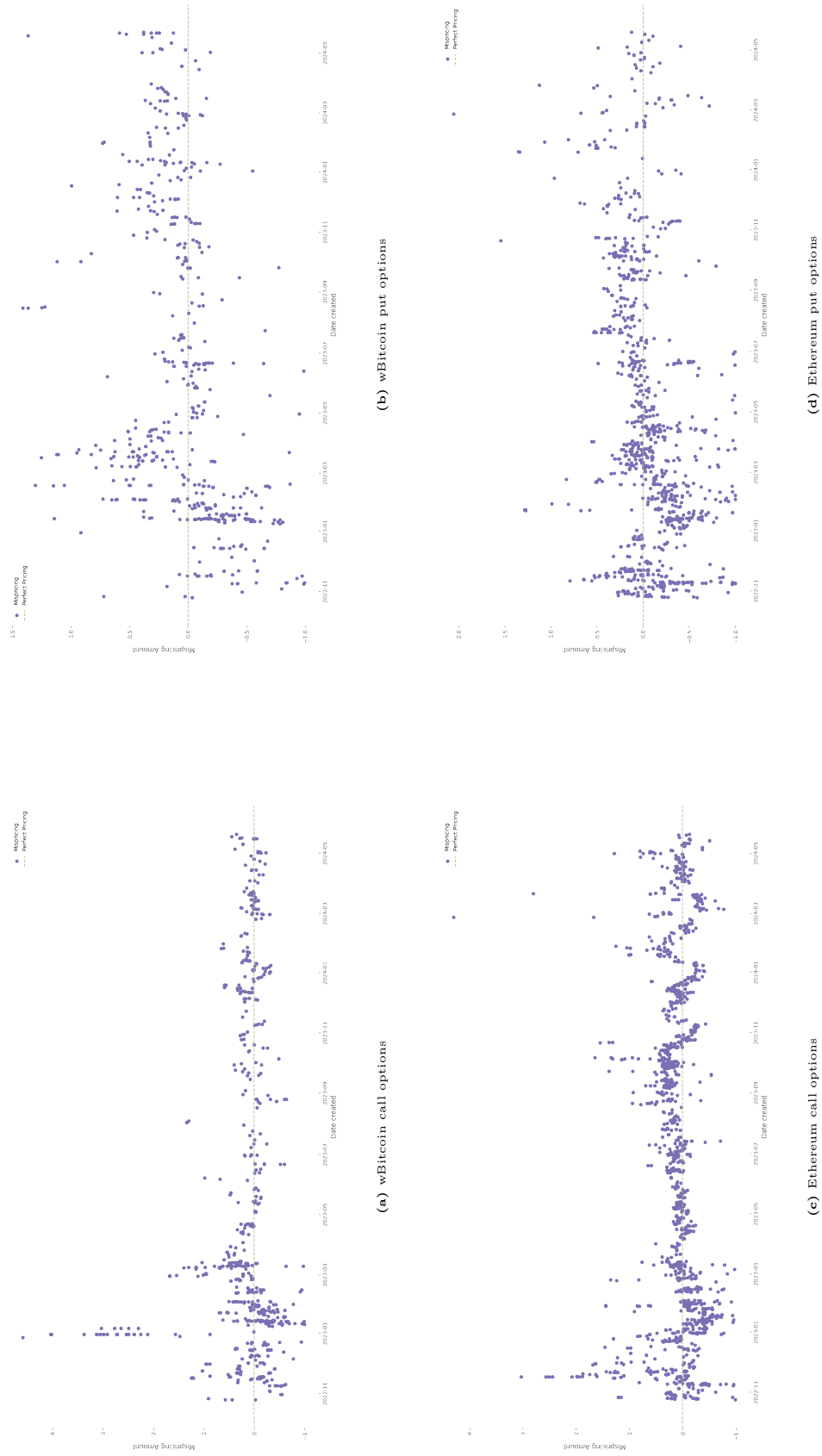
The table reports descriptive statistics for mispricing defined in equation 3.4.

Figure 3.4 visualizes table 3.5 with purple circles indicating mispricing for individual options at specific dates, and the green taped line indicates the equality between Hegic and benchmark prices. The upper graphs correspond to wBitcoin options, and the bottom ones to Ethereum; the left-hand side graphs correspond to calls, and the right-hand side to put, respectively. All samples show mispricing, with higher dispersion from the green line for wBitcoin and Ethereum put options. wBitcoin call options show significant mispricing from November 2022 to late February 2023, whereas put options show a high dispersion at a lower magnitude. The wide and volatile mispricing of Bitcoin options suggests inefficient predefined rates and a somewhat speculative market. Therefore, the Hegic liquidity pool might bear a systematic risk of mispricing, which might lead to persistent losses for liquidity providers. The protocol constraints limit arbitrage opportunities for traders to buying underpriced options; conversely, the mispricing can provide the liquidity pool an opportunity to earn higher premiums from the overpriced options. Ethereum options exhibit a better alignment with benchmark prices, i.e., narrower mispricing spread, with calls closer to the equality line, reflecting better-calibrated pricing by the Hegic protocol and a more stable market.

To investigate the mispricing sensitivity with respect to the options' and underlying assets' characteristics with the FGLS model, first, the paper conducts correlation and variance inflation factors analysis of explanatory variables to ensure no significant pairwise correlation between variables and identify the degree of multicollinearity among them, respectively. To account for differences in the scale and distribution of explanatory variables, second, the paper applies log transformation for amount, strike, maturity and volume variables and to ensures that all explanatory variables equally contribute to the FGLS model. All variables (except for dummies) are standardized by removing mean and scaling to the unit variance. Campbell et al. (1997) reviews log transformation and standardization applications and report improved models performance. Wooldridge (2010) highlights the importance of log transformation for skewed data and subsequent standardization to handle different scale levels. The pairwise correlation analysis (A.2) reveals no severe correlation between explanatory variables. For wBitcoin options, it shows low correlations, expect for some pairs with moderate coefficients, e.g., strike and type. For Ethereum options, a moderate correlations are also observable for some pairs, i.e., volume and volatility, suggesting higher underlying volatility for higher trading volume. Table A.1 reports variance inflation factors for explanatory variables in the FGLS regression. All values are below five which is a common threshold used, indicating no multicollinearity among variables.

Table 3.6 presents the results for the FGLS model according to equation 3.7. The adjusted R^2 for both regressions are high and almost at the same level, with wBitcoin options showing a slightly better fit. The intercept coefficients are negative but not significant, with a coefficient of higher magnitude for Ethereum

Figure 3.4: Mispricing



options. Negative and insignificant intercepts suggest no inherent mispricing bias. Amount coefficients are positive and highly significant, with a slightly higher value for Ethereum options, suggesting that a higher acquired amount, i.e., large orders, leads to higher mispricing. To account for these discrepancies, the Hegic protocol could implement dynamic pricing based on the amount of acquired options. Strike price coefficients are significantly positive for wBitcoin options, indicating that higher strike prices lead to higher mispricing. To increase market efficiency, the Hegic protocol could enhance the pricing for higher out-of-the-money options. The strike price coefficient is negative and insignificant for Ethereum options, suggesting rather unsubstantial impact. The maturity coefficient for wBitcoin is significantly positive, suggesting options with a longer time to maturity exhibit higher price differences. For Ethereum, the maturity coefficient is insignificantly negative, again indicating a negligible impact. The coefficients for the trading volume of the underlying suggest decreasing mispricing with a lower magnitude for wBitcoin options. This substantial but different magnitude impact emphasizes the importance of market activity in aligning prices between the benchmark and the Hegic protocol. Moreover, this, in turn, explains the overall better price congruence for Ethereum options since they are the mostly traded option in the protocol. Underlying volatility coefficients show mixed results, with positive and highly significant for wBitcoin and negative and insignificant for Ethereum options. For wBitcoin, the underlying volatility coefficient indicates mispricing increases with rising volatility; for Ethereum, the underlying volatility has no sophisticated effect. Dummy variables for kind and type, again, show mixed results. For wBitcoin options, a negative and highly significant kind coefficient suggests that calls show lower mispricing than puts. wBitcoin calls show more acquired options than puts, which could lead to better pricing. For Ethereum, the kind coefficient is significant (less than for Bitcoin) and positive, indicating that call options exhibit more mispriced options than puts. This finding contradicts the observation made regarding trading volume; however, it can be interpreted by an imbalance between demand and supply. Since Ethereum is the most preferred blockchain for various on-chain applications,³⁹ excessive demand for call options might produce high mispricing. Positive and insignificant type coefficients indicate that at-the-money and out-of-the-money options do not differ in mispricing.

The observed mispricing might also occur if the Hegic AMM is based on a falsely estimated underlying volatility. In practice, the implied volatility method is widely used in risk management, future market volatility forecasting, and pricing options. The high difference between implied volatility and observed market volatility demonstrates potential mispricing and can create arbitrage opportunities to exploit the liquidity pool of the Hegic protocol. Thus, traders can practice favorable arbitrage opportunities by comparing two volatilities to identify over- and underpriced options. Andolfatto et al. (2024) practically show the volatility premium trading strategies at Lyra protocol. However, depending on the mispricing direction, it can be an additional gain for the liquidity pool. It gets higher premiums for overpriced options; this happens when the implied volatility is higher than the one observed on the market. Moreover, if the market volatility remains low, the probability of exercising an overpriced option decreases, leading to a benefit of the liquidity pool since the probability of keeping the premium increases. The liquidity pool also bears the risk of extra losses due to underpriced options, i.e., when the implied volatility is lower than the market volatility - the liquidity pool collects lower premiums. From the trader's point of view, when options show higher (lower) implied volatility than the market volatility, traders can sell (buy) overpriced (underpriced) options. Thus, traders can perform the volatility premium arbitrage by exploiting volatility discrepancies. Additionally, traders can build delta-neutral strategies, i.e., combining option with underlying, to take advantage of the mispricing and hedge market movements. Note that arbitrage strategies with selling overpriced options can not be practically executed in the Hegic protocol.

³⁹Ethereum is currently the preferred blockchain, but there is growing competition from other blockchains, such as Solana. It offers significantly lower transaction fees and has a more efficient consensus mechanism, making it a strong alternative. As demand for scalable and cost-effective solutions increases, Solana's advancements could potentially challenge Ethereum's dominance in the decentralized finance space.

Table 3.6: Feasible Generalized Least Squares

	wBitcoin options	Ethereum options
Intercept	-0.0213 (0.0512)	-0.2700 (0.1775)
Amount	0.0228*** (0.0086)	0.0334*** (0.0107)
Strike	0.0559*** (0.0204)	-0.0160 (0.0267)
Maturity	0.0166* (0.0094)	-0.0087 (0.0118)
Return (underlying)	0.0005 (0.0082)	-0.0167 (0.0145)
Volume (underlying)	-0.0743*** (0.0140)	-0.1353*** (0.0207)
Volatility (underlying)	0.0789*** (0.0230)	-0.0662 (0.0554)
Kind	-0.0896*** (0.0337)	0.0869** (0.0362)
Type	0.0280 (0.0424)	0.1827 (0.1681)
Adj. R^2	0.5617	0.4961
Cond. number	46.5044	38.8960
F-statistic	39.1036	28.5514
p -value	0.0000	0.0000
Wald-statistic	312.8189	228.3650
p -value	0.0000	0.0000

The table reports results for the FGLS regression according to equation 3.7. The respective Newey-West adjusted standard errors are reported in parentheses. Statistical significance at the 1 %, 5 %, 10 % level is denoted by ***, **, *. The adjusted R^2 value, the F-statistic and the Wald-statistic account for the goodness-of-fit of the applied model.

Moreover, in assumption of the benchmark model, the underlying volatility is constant and might only be appropriate in short-term investments.

Estimating underlying volatility with the MS-AR-(GJR)-GARCH model reflects the sophisticated and appropriate risk measure for a specific date. However, this estimate is assumed to be constant in the Black and Scholes (1973) framework until the option matures. The volatility estimate mirrors the prevailing market volatility for short-time-to-maturity options. However, the estimate might show a bias to real market volatility at maturity for long-time-to-maturity options. To account for these biases, the smoothed probabilities of volatility regime changes can help identify potential future volatility regime switches. The paper uses the Brent (1971) method, i.e., root-finding algorithm, to solve the optimization process where the objective function, i.e., the difference between the Hegic and the benchmark prices, equals zero and calculates the implied volatility.

Figure 3.5 depicts the difference between the implied and the market volatilities (corresponding summary statistics reported in table A.2). Blue circles correspond to the volatility difference for each option at each specific date, and the green line corresponds to the convergence of volatilities. The x-axis shows strike prices, and the y-axis shows the volatility difference level. The volatility difference for wBitcoin options shows dispersed clustering between strike price levels of 15,000 and 30,000. wBitcoin calls exhibit a slightly negative mean, indicating that, on average, the market volatility is higher than the implied volatility, i.e., on average underpriced call options. The skewness and kurtosis slightly differ from normal distribution values, suggesting that observed volatility differences are centered around zero. wBitcoin puts show a more scattered pattern along all strike prices, with the negative mean very close to zero, indicating a higher volatility convergence. Skewness and kurtosis show higher deviations from the normal distribution, which implies extreme positive volatility differences, i.e., overpriced put options. Ethereum options reveal a notable clustering for strike prices between 1,500 and 2,000 and are closer to the volatility convergence line than wBitcoin options. Ethereum call options mean of volatility difference is slightly negative but very close to zero, indicating minor occasions of underpriced options. A notable spreading of volatility differences for high strike prices indicates higher price differences. This finding is partially in line with Andolfatto et al. (2024), where the authors find that on-chain implied volatility

Figure 3.5: Mispricing



increases with moneyness and maturity. Ethereum put options also show high dispersion with observable extreme values of 0.91. The mean is almost zero but positive compared to Ethereum call options, i.e., on average overpriced put options. Ethereum options exhibit higher skewness and kurtosis, which indicate higher extreme differences in volatility. These findings could be used to enhance the market efficiency of the Hegic protocol by recognizing cases of significant mispricing.

4 Conclusion

This paper empirically analyzes differences in the Hegic protocol and the benchmark prices by estimating the sensitivity of mispricing to options' and underlying assets' characteristics. For the benchmark, the paper calculates the option price in the Black and Scholes (1973) framework. To consider the volatile nature of the cryptocurrencies, the paper calculates the underlying volatility with the help of two models: to account for structural breaks in volatility, the Markov Switching Autoregression model is applied, and to capture volatility clustering, the Glosten-Jagannathan-Runkle GARCH model is deployed for each regime. The analysis is conducted with data from the Arbitrum chain and includes wBitcoin and Ethereum call and put options from October 24, 2022, to May 21, 2024. The large concentration of wBitcoin option contracts in only two addresses indicates a high market power, whereas the Ethereum options sample is more diverse and the options' distribution is more balanced. The sample shows a high number of at-the-money options on both wBitcoin and Ethereum suggesting a leverage strategy. The paper confirms the participation of small-scale investors with the largest sample for Ethereum call options and observes a trend in the short-term investments.

With respect to the volatility analysis, this paper confirms the persistence observed in Bitcoin and contributes to the literature by identifying persistence in Ethereum, specifically within the high volatility regime. The paper shows that Bitcoin shows a more frequent transition between volatility regimes and Ethereum shows more pronounced peaks. The paper also confirms the observed inverted leverage affect in Bouri et al. (2017), Katsiampa (2017), Stavroyiannis (2018) and Ardia et al. (2019); however only in the Bitcoin low volatility regime. The paper observes higher low volatility and higher market reaction to news and events for Ethereum compared to Bitcoin; this finding confirms Andolfatto et al. (2024) observations. Additionally, the paper observes relatively low probabilities for regime changes, indicating stable regimes.

The sensitivity analysis of the price difference between the Hegic pricing model and the benchmark (mispricing) is performed using a feasible Generalized Least Squares regression, which accounts for the inherent heteroskedasticity in the error terms. The paper finds positive mispricing for almost all samples, which indicates that the benchmark price is higher than the Hegic price, which is more pronounced for call options. Ethereum options show a closer alignment with benchmark prices and wide and volatile mispricing of Bitcoin options suggests a rather inefficient market; in case of a continuous mispricing, the Hegic liquidity pool might face persistent losses. The regression results suggest that large option orders increase and the increased trading volume of the underlying decreases mispricing with a lower magnitude for wBitcoin options. Additionally, for wBitcoin options: the increase in strike price, maturity and the underlying volatility increases mispricing. The difference between implied and market volatility shows dispersed clustering for some strike price levels for wBitcoin options. Ethereum options also show notable clustering for some strike prices; however, closer to the volatility convergence. The paper also observes notable spreading of volatility difference for high strike prices. Following the findings of this paper, Hegic can improve the efficiency protocol's AMM.

Appendix: Further empirical results

A Additional material

Figure A.1: Partial autocorrelation function.

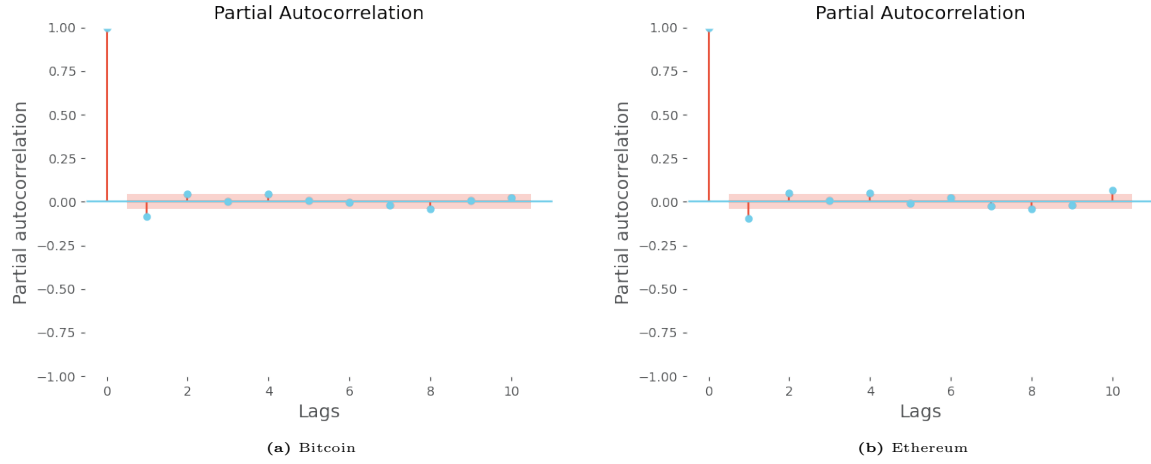


Figure A.2: Correlation matrices.

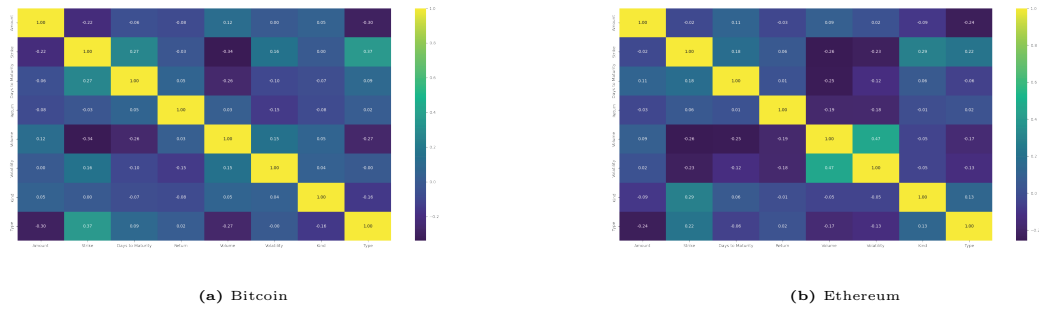


Table A.1: Variance Inflation Factor

	WBTC market	ETH market
Intercept	4.6253	4.4292
Amount	1.1222	1.0892
Strike	1.4042	1.2357
Maturity	1.1429	1.1200
Return	1.0434	1.0505
Volume	1.2593	1.4251
Volatility	1.1175	1.3186
Kind	1.0420	1.1032
Type	1.2932	1.1450

The table reports variance inflation factors for explanatory variables in the FGLS regression according to equation 3.7.

Table A.2: Descriptive statistics of options' mispricing

	Bitcoin		Ethereum	
	call options	put options	call options	put options
Mean	-0.0194	-0.0055	-0.0074	0.0484
Std Deviation	0.1432	0.1542	0.1643	0.1849
Min	-0.5074	-0.4451	-0.6082	-0.5378
25 %-Quartile	-0.1036	-0.1145	-0.0920	-0.0598
50 %-Quartile	-0.0171	-0.0047	-0.0276	0.0084
75 %-Quartile	0.0627	0.0936	0.0604	0.1269
Max	0.4749	0.7154	0.8252	0.9127
Skewness	0.1700	0.3819	0.4054	1.2628
Kurtosis	3.7762	4.4548	5.8807	6.4725

The table reports descriptive statistics for the volatility difference between implied volatility and MS-AR-(GJR)GARCH volatility estimates.

References

- 0xAlpha, Fang, D., and Chen, R. (2021). The exchange protocol of everlasting options. *Working paper*.
- 0xAlpha, Fang, D., and Chen, R. (2023). Deri v4: A cross-chain decentralized protocol of derivatives. *Working paper*.
- Andolfatto, A., Naik, S., and Schoenleber, L. (2024). Decentralized and centralized options trading: A risk premia perspective. *Working paper*.
- Ang, A., Hodrick, R. J., Xing, Y., and Zhang, X. (2001). Systematic jump risks in a small open economy: simultaneous equilibrium valuation of options on the market portfolio and the exchange rate. *Journal of International Money and Finance*, 2:191218.
- Ante, L., Fiedler, I., Willruth, J. M., and Steinmetz, F. (2023). A systematic literature review of empirical research on stablecoins. *FinTec*, 2:3447.
- Ardia, D., Bluteau, K., and R  de, M. (2019). Regime changes in bitcoin garch volatility dynamics. *Finance Research Letters*, 29:266271.
- Bariviera, A. F. (2017). The inefficiency of bitcoin revisited: A dynamic approach. *Economic Letters*, 161:14.
- Black, F. and Scholes, M. (1973). The pricing of options and corporate liabilities. *Journal of Political Economy*, 81(3):637654.
- Bouri, E., Azzi, G., and Dyhrberg, A. H. (2017). On the return-volatility relationship in the bitcoin market around the price crash of 2013. *Economics*, 11(1).
- Brent, R. P. (1971). An algorithm with guaranteed convergence for finding a zero of a function. *The Computer Journal*, 14(4):422425.
- Campbell, J. Y., Lo, A. W., and MacKinlay, A. C. (1997). *The Econometrics of Financial Markets*. Princeton University Press.
- Cao, M. and Celik, B. (2021). Valuation of bitcoin options. *Journal of Futures Markets*, 41(7):10074026.
- Davidson, R. and MacKinnon, J. G. (1993). *Estimation and inference in econometrics*. Oxford University Press.
- Dawson, S., Romanowski, D., Cheng, A., Abramov, V., Kim, J., Fitzgerald, J., Forster, N., Gorham, T., and Ksett (2023). Lyra v2. *Working paper*.

- Fu, F. (2023). Sok: Decentralized exchanges (dex) with automated market maker (amm) protocols. *ACM Computing Surveys*, 55(11):150.
- Glosten, L. R. and R. Jagannathan, D. E. R. (1993). On the relation between the expected value and the volatility of the nominal excess return on stocks. *Journal of Finance*, 48(5):1779-1801.
- Hamilton, J. D. (1989). A new approach to the economic analysis of nonstationary time series and the business cycle. *Econometrica*, 57(2):357-384.
- Hull, J. C. (2012). *Options, Futures, and Other Derivatives*. Prentice Hall, 8 edition.
- Katsiampa, P. (2017). Volatility estimation for bitcoin: A comparison of garch models. *Economics Letters*, 158:36.
- McCorry, P., Buckland, C., Yee, B., and Song, D. (2021). Sok: Validating bridges as a scaling solution for blockchains. *Cryptology ePrint Archive*, pages 146.
- Newey, W. and West, K. (1987). A simple, positive semi-definite, heteroskedasticity and autocorrelation consistent covariance matrix. *Econometrica*, 55(3):703-708.
- Qin, K., Zhou, L., Afonin, Y., Lazzaretti, L., and Gervais, A. (2021). Cefi vs. defi -comparing centralized to decentralized finance. *arXiv: Quantitative Finance*.
- Rahman, A., Shi, V., Ding, M., and Choi, E. (2022). Sok: Synthetic assests, derivatives, and on-chain portfolio management. *arXiv: Quantitative Finance*, 55(3):11.
- Stavroyiannis, S. (2018). Value-at-risk and related measures for the bitcoin. *Journal of Risk Finance*, 19:127-136.
- Thies, S. and Molnár, P. (2018). Bayesian change point analysis of bitcoin returns. *Finance Research Letters*, 27:223-227.
- Werner, S., Perez, D., Gudgeona, L., Klages-Mundt, A., Harz, D., and Knottenbelt, W. (2022). Sok: Decentralized finance (defi). In *Proceedings of the 4th ACM Conference on Advances in Financial Technologies*, 127:30-46.
- White, H. (1980). A heteroskedasticity-consistent covariance matrix estimator and a direct test for heteroskedasticity. *Econometrica*, 48(4):817-838.
- Wintermute, M. (2020). Hegic: On-chain options trading protocol on ethereum powered by hedge contracts and liquidity pools. *Working paper*.
- Wooldridge, J. Y. (2010). *Econometric Analysis of Cross Section and Panel Data*. The MIT Press.